

Formation of molecules in ultra-cold atomic gazes via quasi-resonant fields

Ruzan Sokhoyan

▶ **To cite this version:**

Ruzan Sokhoyan. Formation of molecules in ultra-cold atomic gazes via quasi-resonant fields. Other [cond-mat.other]. Université de Bourgogne; Institute for Physical Research (Ashtarak), 2010. English. ⟨NNT : 2010DIJOS083⟩. ⟨tel-00689121⟩

HAL Id: tel-00689121

https://theses.hal.science/tel-00689121v1

Submitted on 19 Apr 2012

HAL is a multi-disciplinary open access archive for the deposit and dissemination of scientific research documents, whether they are published or not. The documents may come from teaching and research institutions in France or abroad, or from public or private research centers.

L'archive ouverte pluridisciplinaire **HAL**, est destinée au dépôt et à la diffusion de documents scientifiques de niveau recherche, publiés ou non, émanant des établissements d'enseignement et de recherche français ou étrangers, des laboratoires publics ou privés.



HAL Authorization

UNIVERSITÉ DE BOURGOGNE
Laboratoire Interdisciplinaire Carnot de Bourgogne UMR CNRS 5209

NATIONAL ACADEMY OF SCIENCES OF ARMENIA
Institute for Physical Research

FORMATION OF MOLECULES IN ULTRACOLD ATOMIC GASES VIA QUASI-RESONANT FIELDS

by
RUZAN SOKHOYAN

A Thesis in Physics
Submitted for the Degree of
Doctor of Philosophy

Date of Defense: June 7, 2010

The Jury:

Artur ISHKHANYAN	Professor Institute for Physical Research, NAS, Ashtarak	*Supervisor*
Hans-Rudolf JAUSLIN	Professor ICB, Université de Bourgogne, Dijon	*Supervisor*
Claude LEROY	Maître de Conférences ICB, Université de Bourgogne, Dijon	*Supervisor*
Armen MELIKYAN	Professor Russian-Armenian (Slavonic) University, Erevan	*Examiner*
Atom MURADYAN	Professor Yerevan State University, Erevan	*Referee*
Hrachya NERSISYAN	Professor Institute of Radiophysics and Electronics, NAS, Ashtarak	*Referee*

LABORATOIRE INTERDISCIPLINAIRE CARNOT DE BOURGOGNE-UMR CNRS 5209
UNIVERSITE DE BOURGOGNE, 9 AVENUE A. SAVARY - 21078 DIJON - FRANCE

INSTITUTE FOR PHYSICAL RESEARCH, NATIONAL ACADEMY OF SCIENCES OF ARMENIA
ASHTARAK-2, 0203 ARMENIA

Formation de molécules dans des gaz atomiques ultra froids par des champs quasi résonnants.

Nous montrons que dans le cas d'une forte interaction non linéaire entre un système atome-molécule ultra froid et un champ électromagnétique quasi résonnant, le processus de formation moléculaire peut évoluer suivant deux scénarios en fonction des caractéristiques du champ électromagnétique : champ : régime faiblement oscillatoire ou régime fortement oscillatoire. Dans le cas du régime faiblement oscillatoire, le nombre de molécules augmente sans oscillations prononcées des populations atomiques et moléculaires alors que de fortes oscillations de Rabi apparaissent dans le second cas.

Une solution approchée « d'ordre zéro » est présentée. Elle décrit la dynamique temporelle du régime faiblement oscillatoire dans le cas limite d'une forte non linéarité d'un problème à deux états couplés. Cette solution approchée est obtenue essentiellement en tant que solution d'une équation différentielle non linéaire d'ordre 1 et contient un paramètre libre qui dépend des caractéristiques du champ électromagnétique. Plusieurs interprétations quantitatives et significatives peuvent être alors déduites à partir de cette solution analytique. En particulier, nous montrons que l'application d'un champ laser intense à des condensats de Bose-Einstein atomiques n'est pas le procédé le plus favorable à l'obtention de condensats moléculaires. Toujours dans le même régime, nous montrons qu'on peut au plus convertir 1/3 des atomes initiaux en molécules si le champ extérieur appliqué est sans croisement.

Nous avons aussi déterminé une solution générale, extrêmement précise, rendant compte de la dynamique temporelle de l'interaction non linéaire entre un système atome-molécule et le champ appliqué dans le cas du régime fortement oscillatoire. La solution s'exprime à l'aide de la fonction sinus elliptique de Jacobi et contient un paramètre libre. En fonction de la configuration du champ externe, seul l'argument de la fonction change et la dépendance fonctionnelle du paramètre libre varie.

Une analyse approfondie, dans la limite fortement non linéaire, pour le problème à deux états couplés est présentée dans le cas d'un champ extérieur représenté par le modèle sans croisement

de Rosen-Zener. Des relations analytiques décrivant la dynamique temporelle du système sont construites pour tous les deux régimes oscillatoires, faible et fort, dans la limite de la très forte non linéarité.

Une étude précise de l'influence de la diffusion élastique entre particules, atome-atome, atome-molécule et molécule-molécule, sur la dynamique de formation cohérente de molécules molécules sous l'action d'un champ extérieur représenté par le modèle de Landau-Zener, montre que, dans la limite de la très forte non linéarité, le processus de formation moléculaire est principalement décrit par une équation différentielle non linéaire. Cependant les oscillations de population atome-molécule, qui apparaissent immédiatement après que le système soit passé par la résonance, sont essentiellement gouvernées par une équation linéaire.

Remerciements

J'aimerais exprimer ma sincère reconnaissance à mes Directeurs de thèse, les Professeurs A. Ishkhanyan, H.-R. Jauslin, C. Leroy et K.-A. Suominen pour leur aide et leur patience. Je remercie l'Ambassade de France en Arménie pour son aide financière, notamment la bourse No. 2006-4638 en tant que Boursière du Gouvernement Français et INTAS pour son support financier Jeune Chercheur Ref. No. 06-1000014-6484.

Acknowledgments

I would like to express sincere gratitude to my supervisors Profs. A. Ishkhanyan, H.-R. Jauslin, C. Leroy, and K.-A. Suominen for their help and patience. I acknowledge the support of French Embassy in Armenia for Grant No. 2006-4638 as Boursière du Gouvernement Français and INTAS for Young Scientist Fellowship Ref. No. 06-1000014-6484.

CONTENTS

Introduction, 4

Chapter 1. Statement of the problem and basic mathematical tools, 11

1.1. The physical model and governing set of equations, 11

1.2. Exact equation for the molecular state probability, 13

1.3. The linear two-state problem associated with the nonlinear one and the class property theorem of exactly solvable models, 15

1.4. Polar coordinates, 18

1.5. Discussion of different models and their relevance to physical experiments, 19

1.6. Summary, 25

Chapter 2. Change in the adiabatic invariant in a nonlinear Landau-Zener problem, 27

2.1. Introduction, 27

2.2. The basic notions and equations, 30

2.3. The example of the Landau-Zener model and the phase space of the Hamiltonian, 33

2.4. Adiabatic invariance and the nonlinear Landau-Zener problem, 41

2.5. Super-adiabatic sequence and the nonlinear Landau-Zener problem, 44

2.6. Modification of the adiabatic approximation, 46

2.7. Review of the previous results on the Landau-Zener model, 48

2.8. Interrelation between the new and previous approaches, 51

2.9. Summary, 54

Chapter 3. Two strong nonlinearity regimes in cold molecule formation, 56

3.1. Introductiom, 56

3.2. General overview of the Rosen-Zener model, 58

3.3. Weak coupling limit for the Rosen-Zener model, 63

3.3. Strong coupling limit for the Rosen-Zener model, 68

3.4. Two strongly nonlinear distinct scenarios of cold molecule formation, 78

3.5. Improvement of the approximation (3.50) for the weakly oscillatory regime of the strong nonlinearity limit, 85

3.6. Summary, 88

Chapter 4. Quadratic-nonlinear Landau-Zener Problem for Association of an Atomic Bose-Einstein Condensate with Inter-Particle Elastic Interactions Included, 92

4.1 Introduction, 92

4.2 General observations, 93

4.3 Mathematical treatment, 98

4.4 Summary, 108

Conclusion, 111

References, 116

Introduction

Atom trapping and cooling [1-3] paved the way for the observation of Bose-Einstein condensation of dilute atomic gases [4-5]. Nowadays, physics of ultracold gases, in general, and Bose-Einstein condensates (BEC), in particular, has developed into a very exciting field of research at the boundary between atomic physics and condensed-matter physics allowing one to observe a whole series of unusual quantum phenomena (for reviews see, e.g., [6-8]). Previously, it was recognized that Bose-Einstein condensation lies at the heart of such phenomena as superfluidity and superconductivity. But since these phenomena had been observed in systems in which the interactions between the constituent particles play an important role, it was of considerable interest to realize Bose-Einstein condensation in an "ideal gas."

The signature of a Bose-Einstein condensation is a macroscopic occupation of a single quantum mechanical state which describes the atomic motion. Using a method applied by Satyendra Nath Bose to derive the black-body spectrum [9], Albert Einstein predicted the phenomenon of Bose-Einstein condensation in 1925 [10]. When a gas of bosonic atoms is cooled below a critical temperature T_c, a large fraction of the atoms condenses in the lowest quantum state. Atoms at temperature T and with mass m can be regarded as quantum-mechanical wave packets that have a spatial extent of the order of a thermal de Broglie wavelength $\lambda_{dB} = \sqrt{2\pi\hbar^2/(mk_BT)}$. The value of λ_{dB} is the position uncertainty associated with the thermal momentum distribution and increases with decreasing temperature. When atoms are cooled to the point where λ_{dB} is comparable to the interatomic separation, the atomic wave packets "overlap" and the gas starts to become a "quantum soup" of indistinguishable particles. Bosonic atoms undergo a quantum-mechanical phase transition and form a BEC, a cloud of atoms all occupying the same quantum-mechanical state at a precise temperature (which, for an ideal gas, is related to the peak atomic density n by $n\lambda_{dB}^3 = 2.612$).

Bose-Einstein condensation was observed in 1995 in a remarkable series of experiments on vapors of rubidium [5] and sodium [4] in which the atoms were confined in magnetic traps and cooled down to extremely low temperatures, of the order of fractions of microkelvins. The first

evidence for condensation emerged from time-of-flight measurements. The atoms were left to expand by switching off the confining trap and then imaged with optical methods. A sharp peak in the velocity distribution was then observed below a certain critical temperature, providing a clear signature for Bose-Einstein condensation.

After the realization of the atomic BECs, the next challenge was to create a BEC of molecules [11-13]. This prospect was perhaps even more appealing since molecules due to their complex internal structure offer a vast range of properties not available to atoms. For example, ultracold molecules are of vast interest due to important applications, such as ultra-precise molecular spectroscopy and low Doppler width studies of collision processes [14-15], "superchemical" reactions [16], precision measurements of an electron's electric dipole moment (with certain polar molecules) [17-18], and quantum computing [19-20]. Another important application that ultracold molecules could suggest is a molecular clock which would complement the existing atomic clocks in the quest for constraints on time variation of fundamental constants [21].

But standard laser cooling techniques [1-3] that had been developed and realized for atoms are unsuitable for molecules due to their rich and complex level structure. Hence, in order to obtain ultracold molecules, different approaches should be applied. Two major techniques currently widely used for molecule production from cold atoms are the magnetic Feshbach resonance [22-26] and optical laser photoassociation [27-29].

A Feshbach resonance is a scattering resonance for which the total energy of two colliding atoms is equal to the energy of a bound molecular state, and atom-molecule transitions can occur during a collision. The energy difference of the free atoms and bound molecules can be controlled via a magnetic field when the corresponding magnetic moments are different. To describe a magnetically tuned Feshbach resonance, a simple expression for the *s*-wave scattering length has been introduced [24]:

$$a = a_{bg}\left(1-\frac{\Delta B}{B-B_0}\right). \qquad \text{(I.1)}$$

The parameter B_0 indicates the Feshbach resonance position, where the scattering length a becomes infinite. The value of the magnetic field $B = B_0 + \Delta B$ corresponds to the zero scattering length, and the parameter ΔB is referred to as the resonance width. If we tend $B \to \infty$ then $a = a_{bg}$, hence, the background scattering length a_{bg} represents the off-resonat value of a. The parameter a_{bg} can be both negative and positive, that corresponds to off-resonant attractive and repulsive interactions, respectively.

Nowadays, Feshbach resonances are a routinely used tool to control the interaction between atoms in ultracold quantum gases. In the experiment [30], due to coherent Feshbach resonance in a BEC of ^{85}Rb atoms, a mixture of atomic and molecular states has been created and probed by sudden changes in the magnetic field in the vicinity but not across the Feshbach resonance. In this experiment, the variation of the magnetic field gave a rise to oscillations in the number of atoms that remain in the condensate. By measuring the oscillation frequency, for a large range of magnetic fields, it has first been proved that a quantum superposition of atoms and diatomic molecules has been created. In further experiments, ultracold molecules have been formed in degenerate Fermi gases of **Li** atoms [31-32] and afterwards a Bose-Einstein condensation has been realized in the obtained ensemble of molecules [11-13]. For comprehensive reviews, covering various aspects and applications of Feshbach resonances in ultracold gases, see Refs. [33-34].

As it has been mentioned above, another technique applied for cold molecule production is photoassociation. Photoassociation is the process in which two colliding atoms interact with a laser field to form an excited molecule. Photoassociation has been used to produce ultracold molecules (not in a BEC state) from atomic BECs [35-36]. While Feshbach resonances have been efficient for realization of molecular condensates, photoassociation has been widely used to study long range molecular interactions and to probe ultracold gases [37]. Finally, we would like to mention that both Feshbach-resonance and photoassociation usually lead to molecules in highly excited states, and one of the hot topics of the field is formation of “real” ultracold molecules, i.e. those in deeply bound levels. To stabilize the molecules in their ground potentials several schemes have been

suggested, such as two-colour photoassociation [38-39] and a Feshbach optimized photoassociation [40].

The theoretical basis to describe the presented experimental advance was first developed by Juha Javanainen and coworkers [41-44], who proposed a simple one-color photoassociation scheme based on a two-state phenomenological Hamiltonian, and Peter Drummond et al. [45], who introduced a quantum field theory, describing coherent dynamics of coupled atomic and molecular BECs, produced either through one-color photoassociation or Feshbach resonance.

For what follows, it is important that, basically speaking, the coherent photoassociation and coherent Feshbach resonance theories are mathematically rather similar. Under certain conditions (justified for most of the current experiments), these two theories are described by the same system of nonlinear differential equations of first order [41-45] obtained within the framework of the semiclassical mean-field Gross-Pitaevskii theory [46-49]. This system of equations is of fundamental importance for all classical and bosonic field theories with a generic cubic nonlinearity: generally, it comes up in the theories where the interaction terms of the Hamiltonian are of the form $b^{+}aa$. The same system can be used for the description of bosonic molecule formation in degenerate Fermi gases. Indeed, in Ref. [50] it has been noted that, within the mean-field approximation, ***association*** of diatomic molecules from degenerate ***Fermi*** gases is mathematically equivalent to ***dissociation*** of a molecular condensate into ***bosonic*** atoms, and vice versa, ***dissociation*** of a molecular condensate into degenerate ***Fermi*** atoms is equivalent to ***association*** of diatomic molecules starting from ultracold ***bosonic*** atoms. Moreover, the same set of equations comes up when analyzing the second-harmonic generation in a lossless quadratic medium [51-54].

It should be noted that the model considered here takes into account neither spatial structure of the condensate and laser field nor trapping potential effects so that it is applicable, strictly speaking, to the infinite homogeneous condensates only. However, it has been previously shown that this zero-dimensional model can be considered as an approximation to a one-dimensional condensate in the limit where the kinetic-energy term in the Hamiltonian can be ignored. By comparison with a full numerical treatment, it has been shown that this turns out to be a good

approximation as long as the applied fields are of short duration [55-57]. Under the Thomas-Fermi approximation of large enough particle numbers [58], the spatial inhomogeneity caused by the trapping potential may then be approximated by averaging over the density distribution [41-45, 55-57].

In the present work we both qualitatively and quantitatively study temporal dynamics of diatomic molecule formation at coherent photo- and magneto-association (Feshbach-association) of ultracold atoms. Our mathematical analysis is based on the mentioned nonlinear system of two coupled equations which defines a nonlinear two-state problem. The nonlinear two-state problem has been discussed in numerous papers and elucidated from different points of view (see, e.g., Refs. [59-71]). Most of the present developments are devoted to the analysis of the case when the external field configuration is given by the resonance-crossing Landau-Zener model [72]. This particular choice of the external field configuration is justified by the fact that the Landau-Zener model serves as a prototype of all level-crossing models; hence, deep understanding of the Landau-Zener model will be an essential step towards intuitive perception of all level-crossing processes in general. However, previously it has already been observed that Landau-Zener-based predictions may be substantially altered when more realistic models are discussed [71]. Hence, in the present work we examine the level crossing as well as non-crossing processes in general, i.e., we assume arbitrary external field configurations and compare the derived results with those for the basic Landau-Zener model. Here we mainly focus at an analytical description of the temporal dynamics of cold molecule formation.

In ***Chapter 1*** we discuss general properties of the governing set of equations and discuss various external field configurations. We derive an exact nonlinear differential equation of third order for the molecular state probability; this equation will play a central role in our analysis. We show that the phases of the condensates are explicitly expressed in terms of the molecular state probability and explicitly write the corresponding equations. We define a linear two-state problem associated with the nonlinear one under consideration. And finally, we present various external field configurations and discuss their relevance to contemporary physical experiments.

In ***Chapter 2*** we analyze the system's dynamics by using the Hamiltonian formulation of the

nonlinear two-state problem under consideration. We consider the case when the external field configuration is defined by the Landau-Zener model. Due to the structure of the corresponding classical phase space, the adiabatic theorem breaks down even at very small sweep rates, and the adiabatic approximation diverges because of the crossing of a separatrix. First, by introducing a complex term into the Hamiltonian of the system, we eliminate this divergence and construct a valid zero-order approximation. Further, taking into account that the molecular conversion efficiency and the change of the classical adiabatic invariant at the separatrix crossing are related quantities, we calculate the change of the action for the situation when the system starts from the all-atomic state that corresponds to the case of zero initial action. The absolute error of the presented formula for the change in the action is of the order of or less than 10^{-4}.

In ***Chapter 3*** we show that two distinct strongly nonlinear scenarios of molecule formation in an atomic Bose-Einstein condensate are available: the association process in the first case is almost non-oscillatory in time while in the second case the evolution of the system displays strongly pronounced Rabi-type oscillations. By analyzing the exact differential equation for the molecular state probability, we construct highly accurate approximate solutions for both interaction regimes. Investigation of the constructed analytical solutions leads to several qualitative conclusions of practical significance. In particular, we show that in the almost non-oscillatory regime of the strong nonlinearity limit, the non-crossing models are able to provide conversion of no more than one third of the initial atomic population.

In ***Chapter 4*** we study the strong coupling limit of the nonlinear Landau-Zener problem for coherent photo- and magneto-association of cold atoms taking into account the atom-atom, atom-molecule, and molecule-molecule elastic scattering. Using an exact third-order nonlinear differential equation for the molecular state probability in this generalized case, we develop a variational approach which enables us to construct a highly accurate and simple analytic approximation describing the temporal dynamics of the coupled atom-molecule system. We show that the approximation describing the time evolution of the molecular state probability can be written as a sum of two distinct terms; the first one, being a solution of a limit first-order nonlinear equation, effectively describes the process of the molecule formation while the second one, being a

scaled solution to the linear Landau-Zener problem [72] [but now with negative effective Landau-Zener parameter (see below) as long as the strong coupling regime is considered], corresponds to the remaining oscillations which come up when the process of molecule formation is over.

The main results of this dissertation have been published as 6 articles in peer reviewed journals, 4 conference proceedings and 2 conference abstract books **[73-78]**.

Chapter 1

Basic Mathematical Formulations and Tools

In the present chapter we discuss general properties of the governing set of equations and present various external field configurations. First, we derive an exact equation for the molecular state probability and define the linear two-state problem associated with the nonlinear one under consideration. Further, we present the class property theorem of the exactly solvable models to indicate that the set of exactly solvable models can be split into a number of independent classes. We show that the phases of the condensates are explicitly expressed in terms of the molecular state probability. Finally, we discuss various external field configurations and show their relevance to contemporary physical experiments.

1.1. The physical model and governing set of equations

Under the assumption that all the atoms and molecules existing in the system belong to condensates of zero-momentum atoms and molecules, respectively, the coherent conversion of bosonic atoms into diatomic molecules can be described by the following phenomenological momentum-representation two-mode Hamiltonian [43]:

$$\frac{\hat{H}}{\hbar} = \delta_t\, b_0^+ b_0 + \frac{U}{2\sqrt{N}}(b_0^+ a_0\, a_0 + a_0^+ a_0^+ b_0)\,, \tag{1.1}$$

where $\hbar$ is Planck's constant devided by 2π, $a_0(a_0^+)$ and $b_0(b_0^+)$ are boson annihilation (creation) operators for zero-momentum atoms and molecules, respectively. The detuning δ_t defines the difference in energy between a stationary molecule and two stationary atoms dressed by the field which can be adjusted by tuning the laser field frequency in the case of photoassociation or by variation of the magnetic field in the case of Feshbach resonance. In the case of photoassociation

the atom-molecule coupling U can be controlled by variation of the laser field intensity, while in the case of Feshbach resonance it is a fixed constant (if the particle density is supposed not to vary). The commutativity of the Hamiltonian (1.1) with the operator $\hat{N} = a_0^+ a_0 + 2b_0^+ b_0$, $[\hat{H}, \hat{N}] = 0$, reflects the conservation of the total number of particles N, that is, the number of atoms plus twice the number of molecules.

In the case of Feshbach association of utracold bosonic atoms the atom-molecule coupling is given as $U = \sqrt{n} g / \hbar$, where $g = \hbar \sqrt{8\pi \tilde{a}_1 \Delta B \Delta\mu / m_1}$ [79-80] [recall Eq. (I.1)]. In this expression ΔB is the width of the resonance, $\Delta\mu$ is the difference in magnetic momentum between the atomic and the bound molecular states. The parameter n denotes the mean density of particles: $n = N/V$, where V is the volume of trapped particles. The detuning δ_t is given as $\delta_t = \Delta\mu [B(t) - B_0] / \hbar$, where $B(t)$ is the external magnetic field, B_0 denotes the position of the Feshbach resonance.

A possible way to derive the mean-field equations of motion for the system defined by the Hamiltonian (1.1) is to write the Heisenberg equations of motion for the operators $a = a_0 / \sqrt{N}$ and $b = b_0 / \sqrt{N}$ and then replace them by their expectation values. It has been proven that many-body calculations converge to the mean field theory as the number of the constituent particles is increased: for short enough interaction times the mean-filed theory is already applicable at $N = 10$ [65]. Thus, application of the mean-field approximation results in the following coupled set of equations [41-45]:

$$\begin{aligned} i a_t &= U(t) b \bar{a}, \\ i b_t &= \frac{U(t)}{2} a^2 + \delta_t(t) b. \end{aligned} \tag{1.2}$$

Hereafter the lower-case alphabetical subscript denotes differentiation with respect to corresponding variable. The first integral is fixed as $J = |a|^2 + 2|b|^2 = 1$. The function a is interpreted as the atomic state probability amplitude and the function b is, conventionally, interpreted as the molecular state probability amplitude. The quantities $|a|^2$ and $2|b|^2$ are the fractions of atoms and

molecules, respectively, with respect to the total number of "atomic particles" N (each molecule is considered as two "atomic particles"). Hence, we refer to $p_1 = |a|^2$ as the atomic state probability and to $p = |b|^2$, conventionally, as the molecular state probability (note that $p_1 \in [0,1]$ whereas $p \in [0,1/2]$). We will consider a condensate being initially in all-atomic state: $|a(-\infty)| = 1$, $b(-\infty) = 0$.

Further, we apply a unitary transformation to the basic set of equations (1.2) and represent the atomic and molecular probability amplitudes as

$$a = a_1, \quad b = a_2 e^{-i\int \delta_t dt} \tag{1.3}$$

that reduces the system (1.2) to the following canonic form:

$$\begin{aligned} i\frac{da_1}{dt} &= U(t)e^{-i\delta(t)}\bar{a}_1 a_2, \\ i\frac{da_2}{dt} &= \frac{U(t)}{2}e^{i\delta(t)}a_1 a_1, \end{aligned} \tag{1.4}$$

that will be further used in the present chapter. Taking account the value of the first integral J, it can be readily seen that a_1 and a_2 that satisfy the normalization condition

$$|a_1|^2 + 2|a_2|^2 = J = 1. \tag{1.5}$$

Nevertheless the transformation (1.3) has been applied, the functions a_1 and a_2 will be referred to as the atomic and molecular states' probability amplitudes, respectively.

1.2. Exact equation for the molecular state probability

In the present section we discuss general properties of the initial system (1.4) and derive equations which will play an essential role in subsequent developments. First, by eliminating from the initial system (1.4) one of the dependent variables, we obtain the following nonlinear differential equations of second order for the atomic and molecular states' probability amplitudes a_1 and a_2:

$$a_{1tt} + \left(i\delta_t - \frac{U_t}{U}\right)a_{1t} - \frac{U^2}{2}(1 - 2|a_1|^2)a_1 = 0, \tag{1.6}$$

$$a_{2tt}+\left(-i\delta_t-\frac{U_t}{U}\right)a_{2t}+U^2(1-2\,|\,a_2\,|^2)a_2=0\,. \tag{1.7}$$

Hence, instead of dealing with two coupled first-order equations (1.4) one may work with one second-order equation, either Eq. (1.6) or Eq. (1.7). Note that the normalization condition (1.5) is incorporated in these equations.

However, it is not convenient to deal with complex amplitudes since, as numerical simulations show, they differ from their linear analogs (see below) stronger than the modules of amplitudes do. On the other hand, the exact equation for the molecular state probability $p=|a_2|^2$ has been successfully used for the analytical treatment of the problem under consideration (see e.g. [81,70-71,60-62]). Since this equation also plays a central role in the present development, we describe its derivation. First, by direct differentiation we show that the molecular state probability p satisfies the following relations:

$$p_t=\bar{a}_{2t}a_2+\bar{a}_2a_{2t}=-i\frac{U}{2}(a_1^2\bar{a}_2e^{i\delta(t)}-\bar{a}_1{}^2a_2e^{-i\delta(t)})\,, \tag{1.8}$$

$$p_{tt}=\frac{U_t}{U}p_t+\frac{U^2}{2}(1-8p+12p^2)+\frac{U}{2}\delta_t(a_1^2\bar{a}_2e^{i\delta(t)}+\bar{a}_1^2a_2e^{-i\delta(t)})\,. \tag{1.9}$$

Further, again by straightforward differentiation it can be checked that the quantity

$$Z=a_1^2\bar{a}_2e^{i\delta(t)}+\bar{a}_1^2a_2e^{-i\delta(t)}\,, \tag{1.10}$$

which comes up in Eq. (1.9), satisfies the relation

$$Z_t=-\delta_t\frac{2p_t}{U}\,. \tag{1.11}$$

Finally, the differentiation of equation (1.9) followed by some algebra yields the following nonlinear ordinary differential equation of third order for the molecular state probability p:

$$\begin{gathered}p_{ttt}-\left(\frac{\delta_{tt}}{\delta_t}+2\frac{U_t}{U}\right)p_{tt}+\left[\delta_t{}^2+4U^2(1-3p)-\left(\frac{U_t}{U}\right)_t+\frac{U_t}{U}\left(\frac{\delta_{tt}}{\delta_t}+\frac{U_t}{U}\right)\right]p_t+\\ \frac{U^2}{2}\left(\frac{\delta_{tt}}{\delta_t}-\frac{U_t}{U}\right)(1-8p+12p^2)=0\,.\end{gathered} \tag{1.12}$$

Similarly to the case of equations for the probability amplitudes a_1 and a_2, the normalization condition (1.5) is also incorporated in this equation.

The derived equation for the molecular state probability is considerably simplified for the models with constant field amplitude: $U(t) = U_0$. In this case we arrive at the equation

$$p_{ttt} - \frac{\delta_{tt}}{\delta_t} p_{tt} + \left[\delta_t^2 + 4U_0^2(1-3p) \right] p_t + \frac{U_0^2}{2} \frac{\delta_{tt}}{\delta_t}(1-8p+12p^2) = 0 \,. \tag{1.13}$$

An important observation is that for any external field configuration with time dependent coupling $U(t)$ the basic set of equations (1.4) can be reduced to an equivalent system with constant coupling. This is achieved via the following transformation of the independent variable

$$z(t) = \int_{t_0}^{t} \frac{U(t')}{U_0} dt' \tag{1.14}$$

(usually we make the choice $U_0 = \mathrm{Max}[U(t)]$). Note that this transformation changes equation (1.12) to the following much simpler form:

$$p_{zzz} - \frac{\delta_{zz}^*}{\delta_z^*} p_{zz} + \left[\delta_z^{*2} + 4U_0^2(1-3p) \right] p_z + \frac{U_0^2}{2} \frac{\delta_{zz}^*}{\delta_z^*} \left(1-8p+12p^2\right) = 0 \,, \tag{1.15}$$

where the effective detuning δ_z^* is defined as

$$\delta_z^*(z(t)) = \delta_t(t) \frac{U_0}{U(t)} \,. \tag{1.16}$$

The transformed equation for the molecular state probability (1.15) can be represented in the following factorized form:

$$\left(\frac{d}{dz} - \frac{\delta_{zz}^*}{\delta_z^*} \right) \left(p_{zz} - \frac{U_0^2}{2} \left(1-8p+12p^2\right) \right) + \delta_z^{*2} p_z = 0 \,. \tag{1.17}$$

This equation will be used in the developments presented below.

1.3. The linear two-state problem associated with the nonlinear one and the class property theorem of exactly solvable models

Usually, when trying to construct approximate solutions of nonlinear equations, it is important to know the solutions of the corresponding linear equations. In the present case even the

identification of a linear set associated with the nonlinear one (1.4) is not a trivial task since the Hamiltonian (1.1) is essentially nonlinear. To resolve this issue, we address the equation for the molecular state probability (1.12) [or (1.15)]. First, by removing the nonlinear terms from this equation and denoting p_L the new dependent variable we arrive at a linear one:

$$p_{Lttt}-\left(\frac{\delta_{tt}}{\delta_t}+2\frac{U_t}{U}\right)p_{Ltt}+\left[\delta_t^{\,2}+4U^2-\left(\frac{U_t}{U}\right)_t+\frac{U_t}{U}\left(\frac{\delta_{tt}}{\delta_t}+\frac{U_t}{U}\right)\right]p_{Lt}+ \\ \frac{U^2}{2}\left(\frac{\delta_{tt}}{\delta_t}-\frac{U_t}{U}\right)(1-8p_L)=0. \tag{1.18}$$

Further, we directly verify that the obtained linear equation is obeyed by the function $p_L=\left|a_{2L}\right|^2$, where a_{2L} is a solution of the linear set

$$i\frac{da_{1L}}{dt}=U(t)e^{-i\delta(t)}a_{2L}, \\ i\frac{da_{2L}}{dt}=U(t)e^{i\delta(t)}a_{1L}, \tag{1.19}$$

with the following normalization constraint:

$$\left|a_{1L}\right|^2+\left|a_{2L}\right|^2=J_L^{(1/4)}=1/4. \tag{1.20}$$

Hence, the linear set of equations (1.19) can be considered as a linear system associated with the nonlinear system (1.4). From the quantum optics point of view this linear system describes coherent interaction of an isolated atom with optical laser radiation [82]. Note that, within the context of quantum optics, the normalization constraint

$$\left|a_{1L}\right|^2+\left|a_{2L}\right|^2=J_L^{(1)}=1 \tag{1.21}$$

is usually applied, since in this case the quantities $\left|a_{1L}\right|^2$ and $\left|a_{2L}\right|^2$ are interpreted as the first and second states' probabilities, respectively. If instead of applying specific normalizations (1.20) and (1.21), we choose an arbitrary normalization for the functions a_{1L} and a_{2L}, namely,

$$\left|a_{1L}\right|^2+\left|a_{2L}\right|^2=J_L, \tag{1.22}$$

then the function $p_L=\left|a_{2L}\right|^2$ will satisfy the following equation:

$$p_{Lttt}-\left(\frac{\delta_{tt}}{\delta_t}+2\frac{U_t}{U}\right)p_{Ltt}+\left[\delta_t{}^2+4U^2-\left(\frac{U_t}{U}\right)_t+\frac{U_t}{U}\left(\frac{\delta_{tt}}{\delta_t}+\frac{U_t}{U}\right)\right]p_{Lt}+$$
$$\frac{U^2}{2}\left(\frac{\delta_{tt}}{\delta_t}-\frac{U_t}{U}\right)(4J_L-8p_L)=0. \qquad (1.23)$$

Denote the solutions of the linear set of equations (1.19) normalized to unity ($J_L=1$) and $1/4$ ($J_L=1/4$) by $\{a_{1L}^{(1)},a_{2L}^{(1)}\}$ and $\{a_{1L}^{(1/4)},a_{2L}^{(1/4)}\}$, respectively. From Eq. (1.23) it can easily be seen that the functions $p_L^{(1)}=|a_{2L}^{(1)}|^2$ and $p_L^{(1/4)}=|a_{2L}^{(1/4)}|^2$ are related as follows:

$$p_L^{(1/4)}=\frac{p_L^{(1)}}{4}. \qquad (1.24)$$

From here it follows that up to a phase factor the following relations hold:

$$a_{1L}^{(1/4)}=\frac{a_{1L}^{(1)}}{2},\quad a_{2L}^{(1/4)}=\frac{a_{2L}^{(1)}}{2}. \qquad (1.25)$$

These relations are of use for future developments.

Now, we would like to point out an interesting property of the basic set of equations (1.4), the class property theorem of exactly solvable models. Consider the formal solution of the system (1.4) depending on, generally speaking, the complex variable x, i.e. we make the formal change $t\to x$ in the system (1.4) and rewrite it as follows:

$$\begin{cases} i\dfrac{da_1^*(x)}{dx}=U^*(x)e^{-i\delta^*(x)}\bar{a}_1^*(x)\,a_2^*(x), \\ i\dfrac{da_2^*(x)}{dx}=\dfrac{U^*(x)}{2}e^{i\delta^*(x)}a_1^*(x)a_1^*(x). \end{cases} \qquad (1.26)$$

Assume that we managed to find a solution $a_{1,2}^*(x)$ of this system for some functions $U^*(x)$ and $\delta^*(x)$. Then *for the external field configuration characterized by the Rabi frequency*

$$U(t)=U^*(x)\frac{dx}{dt}, \qquad (1.27)$$

and detuning

$$\delta_t(t)=\delta_x^*(x)\frac{dx}{dt}, \qquad (1.28)$$

the solution of the system (1.4) can be written as $a_{1,2}^*(x(t))$, *where* $x(t)$ *is an* ***arbitrary*** *complex-*

valued function. We refer to this statement as to the class property theorem of exactly solvable models [83,59]. It can easily be proved by direct substitution. The only constraint imposed on the function $x(t)$, when considering physical models, is that the coupling $U(t)$ and the detuning $\delta_t(t)$ must be real functions. Thus the class property permits one to split the set of exactly solvable models $\{U(t),\delta_t(t)\}$ into a number of independent classes. Each of these classes will contain an infinite number of exactly solvable models. This theorem was first proven for the linear set of equations (1.19) in Ref. [83] and later on generalized to the case of nonlinear system (1.4) [59].

1.4. Polar coordinates

In sections 1.3 and 1.4 it has been pointed out that the exact equation for the molecular state probability (1.12) [or, equivalently, (1.15)] is a helpful tool for tackling the problem under consideration. If we succeed in finding an exact or approximate solution of this equation then we will be able to indicate the number of molecules existing in the system at arbitrary points of time. However, within the framework of the considered approach, the state of the system is characterized by complex-valued functions a_1 and a_2. If an approximate solution of the equation for the molecular state probability (1.12) is found, then one easily can define the absolute values of these functions: $|a_2| = \sqrt{p}$ and, due to the normalization condition (1.5), $|a_1| = \sqrt{1-2p}$. However, the phases of the complex-valued functions a_1 and a_2 still will be unknown.

In the present section we show that the phases of the condensates can be explicitly expressed in terms of the molecular state probability p. To this end, in the initial set of equations for the probability amplitudes (1.4) we pass to polar coordinates:

$$\begin{aligned} a_1 &= r_1(t)e^{i\theta_1(t)}, \\ a_2 &= r_2(t)e^{i\theta_2(t)}. \end{aligned} \tag{1.29}$$

In polar coordinates the set of equations (1.4) takes the following form:

$$\begin{aligned} -\theta_{1t}r_1 + ir_{1t} &= Ur_1r_2e^{-i(\delta(t)+2\theta_1-\theta_2)}, \\ -\theta_{2t}r_2 + ir_{2t} &= \frac{U}{2}r_1^2e^{i(\delta(t)+2\theta_1-\theta_2)}. \end{aligned} \tag{1.30}$$

By separating real and imaginary parts in this system we arrive at the following set of four equations for the real functions r_1, r_2, θ_1, and θ_2:

$$\begin{aligned} -\theta_{1t} r_1 &= U r_1 r_2 \cos(\theta), \quad r_{1t} = -U r_1 r_2 \sin(\theta), \\ -\theta_{2t} r_2 &= \frac{U}{2} r_1^2 \cos(\theta), \quad r_{2t} = \frac{U}{2} r_1^2 \sin(\theta), \end{aligned} \tag{1.31}$$

where the following notation has been introduced:

$$\theta = \delta(t) + 2\theta_1 - \theta_2 . \tag{1.32}$$

The first and third equations of (1.31) and the normalization constraint (1.5) yield the following equation for the function θ:

$$\theta_t = \frac{U}{2}\left(\frac{1}{r_2} - 6r_2\right)\cos(\theta) . \tag{1.33}$$

Further, from the first equation of the system (1.31), we obtain

$$\theta_1 = -\int_{t_0}^{t} U r_2 \cos(\theta) \mathrm{d}t . \tag{1.34}$$

Finally, from the normalization condition (1.5) and definition $p = r_2^2$, it immediately follows that $r_1^2 = 1 - 2p$. Taking into account these relations and the equations for the phases (1.32)-(1.34), we conclude that the phases θ_1 and θ_2 are unambiguously defined by the function p. Thus, summarizing the results of the present section, we conclude that the initial problem for the determination of the four real functions θ_1, θ_2, r_1 and r_2 is effectively reduced to the problem of determination of the single function r_2 or, equivalently, the molecular state probability $p = r_2^2$.

1.5. Discussion of different models and their relevance to physical experiments

The main goal of the present work is to analyze the dynamics of coherent molecule formation for different external field configurations. The choice of these specific external field configurations is not accidental: they represent essentially different physical situations which are of practical and fundamental interest. In what follows we list the models which will be discussed in the present work and describe their main characteristics. A unifying feature of the listed models is that

for them the linear set of equations (1.19) is ***exactly*** solvable. Hence, in the present work we extend some of the standard, well-developed, linear two-state level-crossing and avoided-crossing models to the nonlinear case.

The simplest possible model is the Rabi model [84] (Fig. 2.1) for which the Rabi frequency and detuning are constant:

$$U = U_0, \quad \delta_t = \delta_0. \tag{1.35}$$

The Rabi model can be exactly solved both in the linear and nonlinear cases. That's why by analyzing the Rabi model one can explicitly examine the qualitative changes that the nonlinearity introduces in the behavior of the system [70]. It can be easily verified that in the case of the linear Rabi problem the probability to occupy a certain state is an oscillatory periodic function of time.

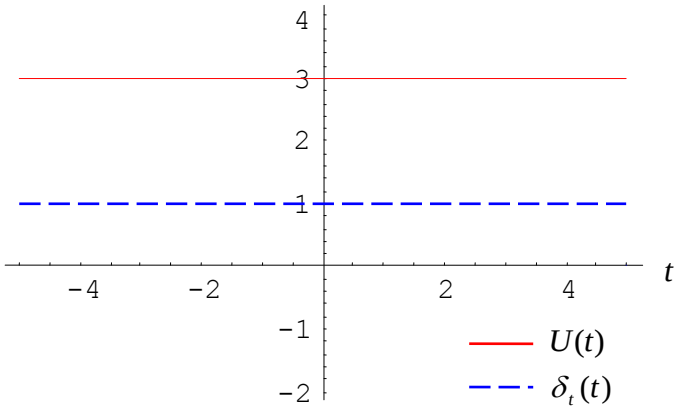


Fig. 2.1. The Rabi model. Solid line - the Rabi frequency, dashed line - the detuning.

But in the nonlinear case the situation drastically changes: for certain initial conditions this probability increases monotonically.

One of the most important models, which also has numerous practical applications, is the Landau-Zener model [72] (Fig. 2.2):

$$U(t) = U_0, \quad \delta_t = 2\delta_0 t. \tag{1.36}$$

This particular model is one of the most used approximations in resonance physics due to its specific features. First of all, the detuning is a linear function of time, which is a realistic assumption near a resonance crossing. Second, the coupling is constant; near the crossing this is a relatively good approximation if the actual coupling changes slowly in time compared to the detuning, which is the usual situation. The Landau-Zener model is considered as the prototype of all the level-crossing models applied so far in the theory of quantum non-adiabatic transitions, thus being a basic tool for understanding the physics underlying such processes. For this reason, it serves as a standard reference to be compared with while discussing all other models.

Further, we notice that one of the parameters involved in the definition of the Landau-Zener model can be eliminated from the equations of motion (1.4) via rescaling of time. This can be achieved, e.g., by applying the transformation

$$t' = \sqrt{\delta_0}\, t \tag{1.37}$$

and introducing the Landau-Zener parameter as

$$\lambda = U_0^2 / \delta_0 . \tag{1.38}$$

Due to this transformation the sweep rate through the resonance is scaled to $\delta_{tt}\,|_{t=0} = 2$ and the effective coupling is given as $\sqrt{\lambda}$. However, in the case of the Feshbach resonance the coupling is constant hence it would be convenient to scale the coupling to unity. This can be achieved via the scaling transformation

$$t' = U_0\, t . \tag{1.39}$$

In this case the effective sweep rate through the resonance will be given as $2/\lambda$. Both the scaling (1.37) and (1.39) will be used in what follows.

Note that the Landau-Zener parameter λ is inversely proportional to the sweep rate through the resonance $2\delta_0$. Taking into account that the equations of motion contain only one combined parameter λ to characterize the external field, one can make an important conclusion: e.g., in the case of photoassociation, applying high laser field intensities U_0^2 and large sweep rates $2\delta_0$ or

applying small laser field intensities U_0^2 and small sweep rates $2\delta_0$ will result in the same final (for $t \to \infty$) molecular population if the ratio $\lambda = U_0 / \delta_0^2$ remains unchanged.

It should be noted, however, that the Landau-Zener model suffers from a substantial shortcoming: the adopted assumption of a detuning diverging at infinity and, hence, a diverging energy, is unphysical. Mathematically, this also leads to considerable complications compared with other models. Nevertheless, for the cases when the transitions take place in a narrow time interval around the resonance point, the time dependence of the actual coupling and detuning far from the

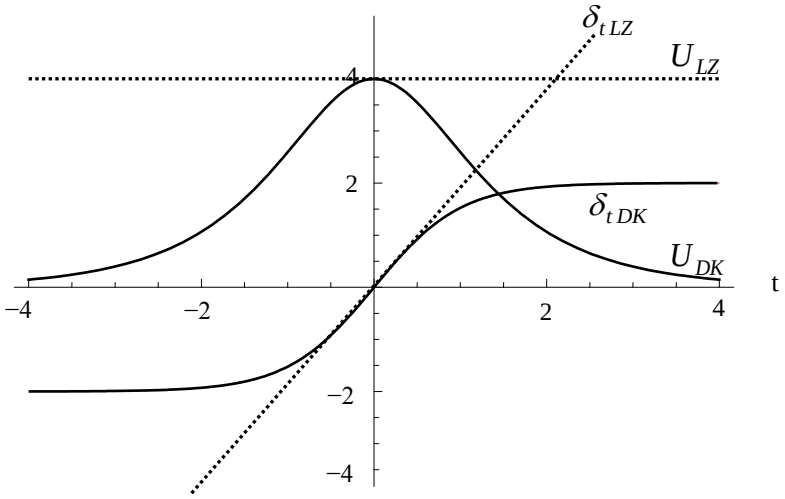


Fig. 2.2. Solid curves - the first Demkov-Kunike model: $U = U_0 \mathrm{sech}(t)$, $\delta_t = 2\delta_0 \tanh(t)$, dotted lines - the Landau-Zener model: $U = U_0$, $\delta_t = 2\delta_0 t$.

crossing does not considerably affect the dynamics of the system and thus the model provides an accurate description of physical processes. The exact solution of the linear system (1.19) for the Landau-Zener model is given in terms of confluent hypergeometric functions ${}_1F_1$ [85].

There exists a model that has all the virtues of the Landau-Zener model and is free from its shortcomings. Such a model is the first Demkov-Kunike quasi-linear level-crossing model of a bell-shaped coupling [86] (Fig. 2.2):

$$U = U_0 \mathrm{sech}(t/\tau), \quad \delta_t = 2\delta_0 \tanh(t/\tau), \quad (\tau > 0). \tag{1.40}$$

The first Demkov-Kunike model is a straightforward generalization of the Landau-Zener model. For seeing this we fix t, take $\delta_0 = \tilde{\delta}_0 \tau$ and let the parameter τ go to infinity; as a result, the Demkov-Kunike model (1.40) is reduced to the Landau-Zener model (1.36).

Another model we would like to address here is the Rosen-Zener model [87] (Fig. 2.4) for which the amplitude and detuning are defined as

$$U = U_0 \mathrm{sech}(t/\tau), \quad \delta_t = 2\delta_0 \quad (\tau > 0). \tag{1.41}$$

In the case of photoassociation, this model can be considered as a physical generalization of the Rabi model. This can be seen by considering the limit of τ going to infinity. The Rosen-Zener model serves as a prototype for all the non-crossing models.

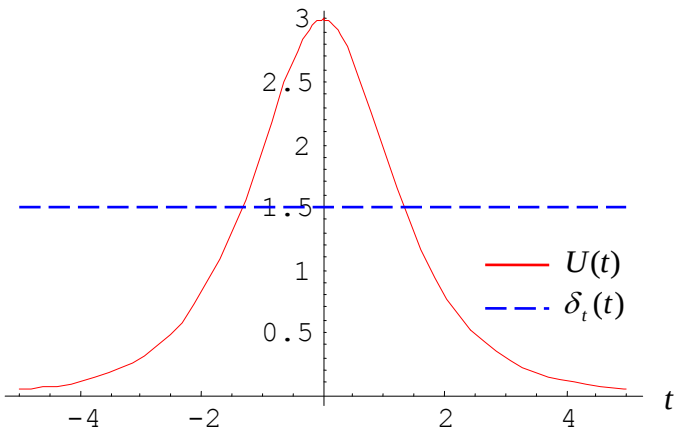


Fig. 2.4. The Rosen-Zener model. Solid line - Rabi frequency, dashed line - detuning.

For the Demkov-Kunike and Rosen-Zener models the exact solution of the linear system (1.19) is given in terms of the Gauss hypergeometric functions ${}_2F_1$ [85]. These two models are unified by the circumstance that they originate from the same integrable class [88].

Another model that we are interested in is the exponential level-crossing model by Nikitin [89] (sometimes referred to as "anti Demkov" model) defined as follows:

$$U(t) = U_0, \quad \delta_t = \Delta(1 - e^{-at}). \tag{1.42}$$

One should also distinguish this model from the well-known second Nikitin-exponential model [90] since in that model the field amplitude is also an exponential function: $U = U_0 e^{-at}$. Obviously, two different cases should be distinguished: the so-called positive Nikitin model (Fig. 2.5) when $a > 0$ and the negative Nikitin model (Fig. 2.6) when $a < 0$. In Eq. (1.42) the crossing point is adjusted to coincide with the origin. In the vicinity of this point the detuning modulation function behaves as the Landau-Zener linear detuning, $\delta_t \approx \Delta a t$ [see (1.42)]. On the other hand, at $t \gg 1/a$ when $a > 0$ (the positive Nikitin model) and at $t \ll 1/a$ when $a < 0$ (the negative Nikitin model) the detuning is practically constant. Hence, it is expected that this model will incorporate the

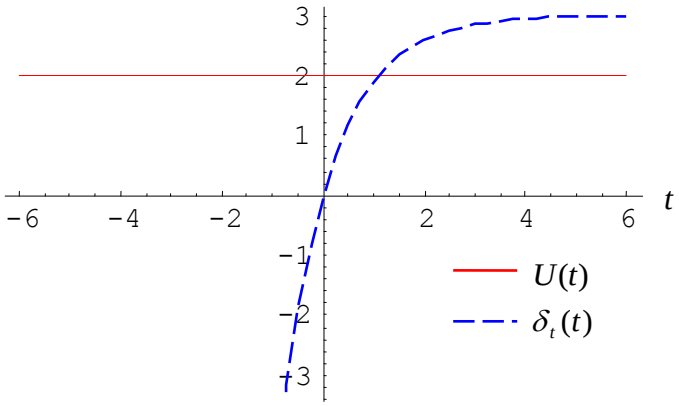


Fig. 2.5. The positive Nikitin model. Solid line - the Rabi frequency, dashed line - the detuning.

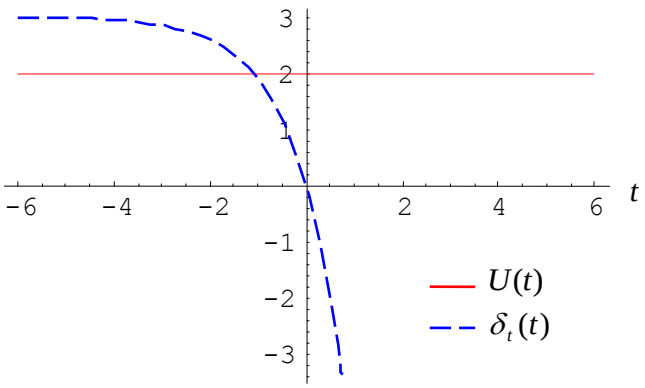


Fig. 2.6. The negative Nikitin model. Solid line - the Rabi frequency, dashed line - the detuning.

characteristics of both Landau-Zener and Rabi models.

To conclude this section, we discuss the relation of the described external field configurations to contemporary physical experiments. Recall that in the case of photoassociation both coupling U and detuning δ_t can vary in time while in the case of magneto-association the coupling is constant. However, generally speaking, this does not imply that the models with coupling varying in time, such as the Rosen-Zener and Demkov-Kunike models, are not applicable to the description of the experiments on Feshbach association of atoms. Indeed, one can reduce these models to a constant-amplitude one via transformation of the independent variable (1.14) and consider the variable z as time. In what follows we demonstrate such an example.

As it has been mentioned above, the ramping of an external magnetic field across a Feshbach resonance is the most commonly adopted scheme to form Feshbach molecules. A typical example is the ^{85}Rb experiment performed by Hodby and co-workers in JILA [91], where coherent formation of Rb_2 molecules via sweep of the magnetic field across the Feshbach resonance is realized. The magnetic field is changed at a given linear sweep rate $\dot{B}$, and the molecule conversion efficiency is measured as a function of the inverse sweep rate. Thus, the external field configuration applied in this experiment corresponds to the Landau-Zener model.

1.7. Summary

In the present chapter we have presented basic mathematical tools and important notions which will play a central role in what follows. We have shown that the molecular state probability p obeys a nonlinear differential equation of third order (1.12). Moreover, we have proven that atomic and molecular condensates' phases, θ_1 and θ_2, respectively, are unambiguously defined by the molecular state probability p [see Eqs. (1.32)-(1.34)]. Hence, the problem of the definition of complex-valued probability amplitudes a_1 and a_2 has been reduced to a problem of determination of the real function p. We have defined a linear set of equations (1.19) associated to the governing nonlinear system (1.4). Further, we have described various external field configurations and presented a preliminary qualitative analysis of the system's behavior for each of them. Importantly,

we have shown that for any model with varying in time coupling $U(t)$, the basic set of equations (1.4) can be reduced to an equivalent system with constant coupling; this is achieved by applying the transformation of independent variable (1.14). Finally, we have discussed the relevance of the described external field configurations to contemporary physical experiments.

Chapter 2

Change in the adiabatic invariant in a nonlinear Landau-Zener problem

In the present chapter we analyze the system's dynamcis by using the Hamiltonian formulation of the nonlinear two-state problem under consideration. Due to the structure of the corresponding classical phase space, the adiabatic theorem breaks down even at very small sweep rates, and the adiabatic approximation diverges because of the crossing of a separatrix. First, by introducing a complex term into the Hamiltonian of the system, we eliminate this divergence and construct a valid zero-order approximation. Further, taking into account that the molecular conversion efficiency and the change of the classical adiabatic invariant at the separatrix crossing are related quantities, we calculate the change of the action for the situation when the system starts from the all-atomic state that corresponds to the case of zero initial action. The absolute error of the presented formula for the change in the action is of the order of or less than 10^{-4}.

2.1. Introduction

The theory of approximate conservation of adiabatic invariants [92] plays an important role in many domains of physics. According to this theory, the action is an approximately conserved quantity of Hamiltonian systems that contain a slowly varying parameter. This result is based on averaging over the fast motion of a time-independent version of the system (i.e., the same system for which the varying parameter is taken as a constant). The theory states that the change in the action during a time-dependent process is usually on the order of the variation rate of the mentioned slow varying parameter. Moreover, there exists an adiabatic invariant, which is conserved to all orders of the parameter variation rate within time periods no longer than the inverse value of this rate. However, the theory also says that this situation can drastically change if the time-independent

version of the system contains separatrices in its phase portrait. In this case the exact phase trajectory of the system may cross the separatrix of the time-independent version of the system. Since the period of the motion along the separatrix is equal to infinity one cannot consider the motion of the time-independent version of the system as a fast one. This results in a breakdown of the averaging method. To describe this case, a rigorous separatrix crossing theory [93-96] has been developed. It has been shown that at the separatrix crossing a jump in the value of the adiabatic invariant occurs, and an asymptotic expression for the value of this jump has been obtained. The separatrix crossing theory has proven to be useful in various problems of plasma physics, hydrodynamics, classical and celestial mechanics, cold molecule formation, etc. (e.g., see Refs. [93-100]).

In the present paper we discuss the coherent formation of ultracold molecules (in particular, molecular condensates) by laser photoassociation or magnetic Feshbach resonance. The situation we discuss in detail is the coherent association of ultracold bosonic atoms for the case when the external field configuration is defined by the resonance-crossing Landau-Zener model.

In the present chapter we consider a nonlinear Landau-Zener problem, defined by Eqs. (1.4) and (1.36) to describe the coherent formation of ultracold molecules (in particular, molecular condensates) by laser photoassociation or magnetic Feshbach resonance. Long ago, the Landau-Zener model which is well known from the linear theory of nonadiabatic transitions became a standard tool in quantum physics. It describes a situation when two quantum states are coupled by an external field of constant amplitude and a variable frequency, the latter being linearly changed in time. When generalizing the Landau-Zener process to those associated with the mean-field dynamics of interacting many-body systems one obtains nonlinear Landau-Zener processes for which the simple physical intuition based on the linear Landau-Zener model may no longer be valid. The nonlinear version of the Landau-Zener crossing problem under consideration has been analyzed in numerous papers (see, e.g., Refs. [59-69,99-100]). In particular, it has been shown that, within the framework of the considered model, the change in the action at the resonance passage is a power-law function of the sweep rate through the resonance, as opposed to the exponential law of the linear Landau-Zener problem.

Landau-Zener dynamics of diatomic molecule formation from degenerate Fermi-gases has been discussed in Refs. [63-68,99-100]. In particular, in Refs. [99-100] the separatrix crossing theory has been employed. One of the main outcomes of Refs. [99-100] is a formula giving the value of the action jump at the separatrix crossing. This formula contains a parameter referred to as the pseudophase, which strongly depends on the initial conditions. Supposing that the pseudophase is a random variable equally distributed over the open segment $]0, 1[$, the authors have succeeded in presenting the dispersion law of the action jump at separatrix crossing.

However, it should be noted that the separatrix crossing theory is not applicable in the case of small initial actions. This kind of situation comes up, e.g., when one considers mean-field dynamics of diatomic molecules formation from ultracold bosonic atoms, if the initial number of molecules is very small or equal to zero. In this case, for the calculation of the action change at a separatrix crossing, a different method has been developed [69] which is based on mapping of the governing equations to a Painlevé equation. Using this method, an asymptotic expression for the action change at the separatrix crossing has been calculated for very slow sweep rates. The mentioned method is also fruitful for the description of diatomic molecules formation from degenerate Fermi-gases [68]; it allows one to generalize and improve the results of Refs. [99-100].

In the present chapter we first discuss the classical phase space of the time-independent version of the problem (for analogous discussions, see, e.g., Refs. [67-68]) and show that the phase trajectory of the time-dependent system will necessarily cross the separatrix of the "frozen" system resulting in the divergence of the adiabatic approximation. Further, we show that it is possible to eliminate this divergence by introducing a complex term into the Hamiltonian of the system, constructing in such a way a valid zero-order approximation. Finally, taking into account that the molecular conversion efficiency is coupled with the change of the action during the whole interaction process we calculate this change in the case when the system starts from the all-atoms state. For arbitrary rates of sweep through the resonance, the absolute error of the presented formula is of the order of or less than 10^{-4}.

2.2. The basic notions and starting equations

In the present chapter, the starting point is the momentum-representation two-mode Hamiltonian (1.1):

$$\frac{\hat{H}}{\hbar} = \delta_t\, b_0^+ b_0 + \frac{U}{2\sqrt{N}}(b_0^+ a_0\, a_0 + a_0^+ a_0^+ b_0)\,. \tag{2.1}$$

As it has been mentioned in Section 1.1, the mean-field equations of motion could be derived by writing the Heisenberg equations of motion for the operators involved and then replacing them by their expectation values. From this approach one can reconstruct the classical Hamiltonian corresponding to the derived set of equations. However, in what follows we apply a different approach: first we define a classical Hamiltonian, corresponding to the second quantization Hamiltonian (1.1), construct the Poisson brackets for the variables involved and then write the classical equations of motion.

Rescaling the boson operators as $a_0 = a\sqrt{N}$ and $b_0 = b\sqrt{N}$, we rewrite the Hamiltonian in new notations:

$$\frac{\hat{H}}{N\hbar} = \delta_t\, b^+ b + \frac{U}{2}(b^+ a\, a + a^+ a^+ b)\,. \tag{2.2}$$

It can easily be seen that the rescaled boson operators a and b obey the following commutation relations:

$$[a,\, a^+] = [b,\, b^+] = 1/N\,, \qquad [a,b] = [a,b^+] = 0\,. \tag{2.3}$$

For large N $(N >> 1)$ our problem approaches a well-defined classical limit in which the operators can be treated as classical objects. Thus, we replace the operators a, a^+, b, and b^+ by c-numbers, and the commutators by classical Poisson brackets. This procedure leads to the classical Hamiltonian

$$H = \delta_t\, \bar{b}\, b + \frac{U}{2}[\bar{b}\, a^2 + (\bar{a})^2 b] \tag{2.4}$$

and the following expressions for the classical Poisson brackets of the functions a and b:

$$\{a, \overline{(ia)}\} = 1, \quad \{b, \overline{(ib)}\} = 1, \quad \{a, b\} = \{a, \bar{b}\} = 0. \tag{2.5}$$

(the asterisk denotes the complex conjugation). The particle conservation property of the Hamiltonian is now expressed by the following relation:

$$\{H, J\} = 0, \tag{2.6}$$

where $J = |a|^2 + 2|b|^2$. Equations (2.5) indicate that the variables a and $\overline{(ia)}$ are canonically conjugate, hence, the Hamiltonian equations of motion in the complex notations are readily written as [101]

$$i\frac{d\bar{a}}{dt} = -\partial H / \partial a, \ \frac{da}{dt} = -i\partial H / \partial \bar{a} \quad \text{and} \quad i\frac{d\bar{b}}{dt} = -\partial H / \partial b, \ \frac{db}{dt} = -i\partial H / \partial \bar{b} \tag{2.7}$$

(t is time). As it can easily be seen, only two of these four equations are independent. Substituting the Hamiltonian (2.4) into (2.7), we arrive at the equations of motion within the framework of the mean field approximation (1.2):

$$\begin{aligned} i\,a_t &= U(t) b \bar{a}, \\ i\,b_t &= \frac{U(t)}{2} a^2 + \delta_t(t) b. \end{aligned} \tag{2.8}$$

with the first integral J which is fixed as $|a|^2 + 2|b|^2 = J = 1$. Recall that we consider a condensate being initially in all-atoms state: $|a(-\infty)| = 1, \ b(-\infty) = 0$.

The Hamiltonian (2.4) is defined in a four-dimensional phase space. However, the dimensionality of the phase space can be reduced. To this end, we take into account that $p_1 = 1 - 2p$ and pass to the polar coordinates, thus, representing the probability amplitudes a and b as

$$a = (1-2p)^{1/2} e^{i\theta_1}, \quad b = p^{1/2} e^{i\theta_2}, \tag{2.9}$$

where θ_1 and θ_2 are the corresponding phases. Further, we rewrite the Hamiltonian (2.4) as follows:

$$H(t,q,p)=\sqrt{p}(1-2p)U(t)\cos q+\delta_t(t)p\ , \tag{2.10}$$

where $q=2\theta_1-\theta_2$. It can be shown by direct verification that the introduced transformation is canonical, with q and p being the generalized coordinate and the generalized momentum, respectively. Thus, Hamilton's canonical equations,

$$\frac{dq}{dt}=\frac{\partial}{\partial p}H(t,q,p),\quad \frac{dp}{dt}=-\frac{\partial}{\partial q}H(t,q,p), \tag{2.11}$$

take the following form:

$$\begin{aligned}\frac{dq}{dt}&=p^{-1/2}\left(\frac{1}{2}-3p\right)\cdot U(t)\cos q+\delta_t(t),\\ \frac{dp}{dt}&=p^{1/2}(1-2p)\cdot U(t)\sin q.\end{aligned} \tag{2.12}$$

In Refs. [67,68] variables analogous to the pair of canonically conjugate variables $\{q,p\}$ have been used for the description of the system's dynamics. However, these variables are not well-defined at $p=0$ and $p=1/2$. Since the imposed initial conditions imply that in the beginning of the process $(t\to-\infty)$ should be $p=0$, it would be more convenient to work with coordinates free of this shortcoming. To this end, we define the following pair of canonically conjugate variables:

$$q'=\frac{1}{\sqrt{2}i}\left(\frac{a}{\bar{a}}\bar{b}-\frac{\bar{a}}{a}b\right),\qquad p'=\frac{1}{\sqrt{2}}\left(\frac{a}{\bar{a}}\bar{b}+\frac{\bar{a}}{a}b\right). \tag{2.13}$$

Note that the variables $\{q',p'\}$ are related to $\{q,p\}$ as follows:

$$q'=\sqrt{2p}\,\sin q,\quad p'=\sqrt{2p}\,\cos q\,, \tag{2.14}$$

hence,

$$p=\frac{1}{2}\left((p')^2+(q')^2\right)\quad \sin q=\frac{q'}{\sqrt{(p')^2+(q')^2}},\quad \cos q=\frac{p'}{\sqrt{(p')^2+(q')^2}}. \tag{2.15}$$

The variables $\{q', p'\}$ are equal to zero at $p=0$ but they are not defined at $p=1/2$ [see Eq. (2.9)]. In the new coordinates the Hamiltonian is written as

$$H(t,q',p')=\frac{1}{\sqrt{2}}U(t)\,p'[1-(p')^2-(q')^2]+\frac{\delta_t(t)}{2}[(p')^2+(q')^2] \tag{2.16}$$

leading to the following equations of motion for the generalized coordinate q' and generalized momentum p':

$$\begin{aligned}\frac{dq'}{dt}&=\frac{1}{\sqrt{2}}U(t)[1-3(p')^2-(q')^2]+\delta_t(t)p',\\ \frac{dp'}{dt}&=\sqrt{2}\,U(t)\cdot p'q'-\delta_t(t)q'.\end{aligned} \tag{2.17}$$

As we see, the new Hamiltonian (2.16) is a polynomial in terms of q' and p'. Note that the function p' satisfies the following nonlinear differential equation of the ***second*** order:

$$\begin{aligned}&\left(p'-\frac{\delta_t}{\sqrt{2}U}\right)\frac{d^2p'}{dt^2}+\left(\frac{\delta_{tt}}{\sqrt{2}U}-p'\frac{U_t}{U}\right)\frac{dp'}{dt}-\frac{1}{2}\left(\frac{dp'}{dt}\right)^2+\\ &3U^2\left(p'-\frac{\delta_t-\sqrt{6U^2+\delta_t^2}}{3\sqrt{2}U}\right)\left(p'-\frac{\delta_t+\sqrt{6U^2+\delta_t^2}}{3\sqrt{2}U}\right)\left(p'-\frac{\delta_t}{\sqrt{2}U}\right)^2=0.\end{aligned} \tag{2.18}$$

As it is immediately seen, the times for which

$$p'-\frac{\delta_t}{\sqrt{2}U}=0 \tag{2.19}$$

are singular points for this equation. By analyzing the initial set of equations (1.2) it can be shown that this condition is equivalent to the following one: $2\theta_1+\delta=C$, where C is a constant.

2.3. The example of the Landau-Zener model and the phase space of the Hamiltonian

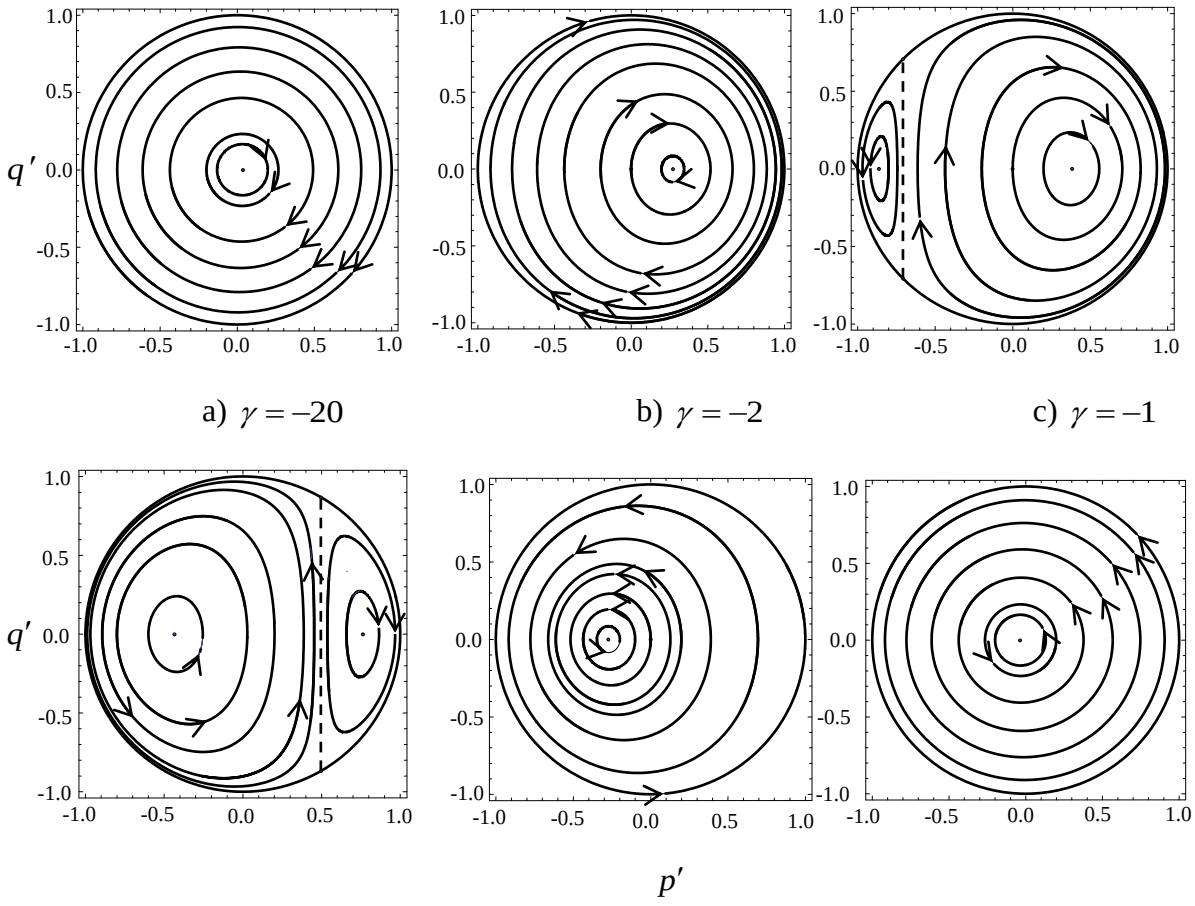
As a fundamentally important example of the external field configuration we choose the Landau-Zener model which is defined by Eq. (1.36):

$$U=U_0,\quad \delta_t=2\delta_0\,t. \tag{2.20}$$

Recall that one of the parameters involved in the definition of the model can be eliminated from the

equations of motion via rescaling of time (see Section 1.5). This can be achieved, e.g., by applying the transformation $\tilde{t} = U_0 t$ to the set of equations (2.17) and introducing the Landau-Zener parameter $\lambda = U_0^2 / \delta_0$. In what follows for simplicity of notations we omit the tilde over $\tilde{t}$. The corresponding Hamiltonian is written as follows:

$$H = \frac{1}{\sqrt{2}} p' \left[1 - (p')^2 - (q')^2\right] + \frac{\gamma}{2}\left[(p')^2 + (q')^2\right], \ \gamma = \varepsilon t, \text{ and } \varepsilon = 2/\lambda. \qquad (2.21)$$



a) $\gamma = -20$ b) $\gamma = -2$ c) $\gamma = -1$

d) $\gamma = 0.7$ e) $\gamma = 2$ f) $\gamma = 20$

Fig 2.1. The level lines of the Hamiltonian (2.21) for different values of the parameter γ. The dots situated within the phase space represent the two elliptic fixed points (2.24). The bounding circle of the phase space and the vertical dashed lines of Figs. c) and d) represent the separatrices (2.27). The vertical dashed line passes through the two saddle fixed points (2.25) which are situated on the

limiting circle of the phase space. The arrows placed along the phase trajectories represent the direction of motion in time.

Note that the Hamiltonian (2.21) contains only one combined parameter λ to characterize the external field.

Considering γ as a constant, in Fig. 2.1 we plot the level lines of the Hamiltonian $H = \text{const}$. The level lines represent the phase trajectories of the system for the case when the parameter γ is fixed. If the Landau-Zener parameter λ is large (i.e. the parameter ε is small), the parameter γ changes slowly in time. In this case we can expect that the system for some time follows a phase trajectory and then slowly passes to another one. Thus, one can imagine that with time the system slowly drifts from one trajectory to another.

To understand the structure of the phase space, we analyze the fixed points of the Hamiltonian system under consideration which are defined by equations

$$\frac{\partial H}{\partial q'} = 0, \quad \frac{\partial H}{\partial p'} = 0, \tag{2.22}$$

that is,

$$\begin{aligned} &\frac{1}{\sqrt{2}}[1-3(p')^2-(q')^2]+\gamma\, p' = 0, \\ &q'(\sqrt{2}p'-\gamma) = 0. \end{aligned} \tag{2.23}$$

Solving this set of equations we obtain the following four fixed points:

$$q'_{01,02} = 0, \quad p'_{01,02} = \frac{\gamma \pm \sqrt{6+\gamma^2}}{3\sqrt{2}}, \tag{2.24}$$

$$q'_{03,04} = \pm\sqrt{1-\gamma^2/2}, \quad p'_{03,04} = \gamma/\sqrt{2}. \tag{2.25}$$

The two points $\{q'_{01}, p'_{01}\}$ and $\{q'_{02}, p'_{02}\}$ are elliptic, while $\{q'_{03}, p'_{03}\}$ and $\{q'_{04}, p'_{04}\}$ are saddle points. The molecular state probability values taken at the considered four fixed points, $p_i = ({q'_{0i}}^2 + {p'_{0i}}^2)/2 \;\; (i = 1...4)$,

$$p_{1,2} = \frac{1}{18}[\gamma^2+3 \pm \gamma\sqrt{\gamma^2+6}] \quad \text{and} \quad p_{3,4} = 1/2, \tag{2.26}$$

are shown in Fig. 2.2 as functions of γ.

Since $p \in [0, 1/2]$, the phase space domain for the variables p' and q' is a disc of

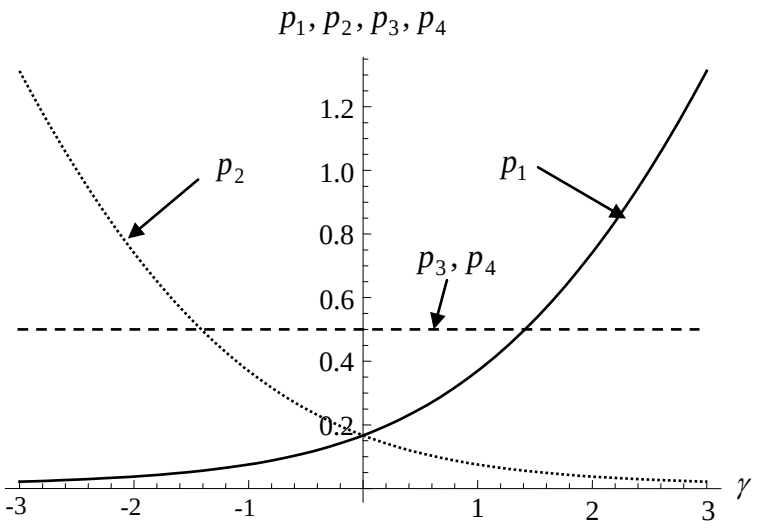


Fig. 2.2. The values of the transition probabilities (2.26) at the fixed points (2.24) $\{q_{1,2},\ p_{1,2}\}$ and (2.25) $\{q_{3,4},\ p_{3,4}\}$.

radius 1. The bounding circle with unit radius of unity corresponds to the all-molecules states, and the center of the circle, $(p', q') = (0,0)$, to the initial all-atoms state (see Fig. 2.1). For $\gamma \to -\infty$, the fixed point $\{q'_{01}, p'_{01}\}$ is situated in the centre of the phase space circle; it moves to the right with increasing γ to stay within the phase space when $\gamma \le \sqrt{2}$. The fixed point $\{q'_{02}, p'_{02}\}$ appears in the phase space at $\gamma = -\sqrt{2}$ to asymptotically approach the center of the phase space when $\gamma \to +\infty$. As to the saddle points, $\{q'_{03}, p'_{03}\}$ and $\{q'_{04}, p'_{04}\}$, they also appear in the phase space at $\gamma = -\sqrt{2}$ and leave the phase space at $\gamma = \sqrt{2}$. Hence, the points $\gamma = \pm\sqrt{2}$ are bifurcation points of the equations of motion corresponding to the Hamiltonian (2.21).

We remark that the coordinate transformation (2.13) is singular for $a = 0$. However, the set $\{a, b \mid a = 0, |b| = 1/\sqrt{2}\}$ can be identified by continuity with the circle $\{q'^2 + p'^2 = 1\}$, since (2.13) implies $q'^2 + p'^2 = 2|b|^2$. One can check directly that $\left(a \equiv 0,\ b = (1/\sqrt{2})e^{i\int \delta_t dt}\right)$ is a solution of the

equations of motion (1.2), for any choice of the time dependent functions $U(t)$ and $\delta_t(t)$. Thus $\{a,b|\ a=0,|b|=1/\sqrt{2}\}$ is an invariant set of the dynamics. The circle $\{q'^2+p'^2=1\}$ is in turn invariant with respect to the time evolution of the variables q', p'.

The trajectory connecting the two saddle points $\{q'_{03},p'_{03}\}$ and $\{q'_{04},p'_{04}\}$ separates the types of motion and is called a separatrix. Taking into account the value of the Hamiltonian at the saddle points, we see that the separatrices correspond to the following trajectories:

$$p'=\gamma/\sqrt{2} \quad \text{and} \quad p'^2+q'^2=1. \tag{2.27}$$

An important property of the separatrix is that the period along it is equal to infinity. In Figs. 1 c) and d) the separatrices correspond to the vertical dashed line and the phase space limiting circle $p=1/2$. An interesting observation is that the singular point of the exact equation for p' (2.18) coincides with the separatrix.

Properties of the constant-amplitude and constant-detuning Rabi model

The phase portraits of Fig. 2.1 describe the dynamics of the system in the case when the external field is defined by the constant-amplitude and constant-detuning Rabi model (1.35):

$$U=U_0, \quad \delta_t=2\delta_0. \tag{2.28}$$

The nonlinear Rabi problem has been discussed in detail in Ref. [70]. Considering the case when the system starts from the all-atoms state, an exact solution to the problem has been obtained. It has been shown that the molecular state probability p is given in terms of the Jacobi elliptic functions which are periodic in time for arbitrary finite U_0 and δ_0, except the case of exact resonance $\delta_0=0$. In this case, the Jacobi elliptic function becomes the hyperbolic tangent, and the molecule formation dynamics displays a non-oscillatory behavior approaching the all-molecule state at $t\to+\infty$. By analyzing the phase portraits of the system (see Fig. 2.1), we can generalize this result to the case of arbitrary initial conditions. Indeed, if the initial conditions are on the separatrix, [i.e., if they satisfy one of the relations (2.27)] then the exact solution to the problem will not be a

periodic function of time, and the molecular state probability will asymptotically go to $1/2$ at $t \to +\infty$.

Finally, we find the exact shape of the phase trajectories at $\gamma \to \pm\infty$ (γ is still time-independent). To this end, we consider the asymptotic behavior of the Hamiltonian (2.21) at $\gamma \to \pm\infty$. The Hamiltonian is then approximated by $H \approx \gamma(p'^2 + q'^2)/2$. Solving Hamilton's equations for this asymptotic Hamiltonian we obtain that for $\gamma \to \pm\infty$

$$p' = \sqrt{2p(\gamma = \pm\infty)}\cos(\gamma t), \quad q' = \sqrt{2p(\gamma = \pm\infty)}\sin(\gamma t). \tag{2.29}$$

Note that the exact phase trajectories of the system at $t \to \pm\infty$ in the case of the Landau-Zener model ($\gamma = \varepsilon t$) are written as follows:

$$p' = \sqrt{2p(t = \pm\infty)}\cos(\gamma t/2 + \varphi_0), \; q' = \sqrt{2p(t = \pm\infty)}\sin(\gamma t/2 + \varphi_0), \tag{2.30}$$

where φ_0 is an integration constant. Interestingly, the phase trajectories (2.29) and (2.30) bound the same area in the phase space (we imply the area inside the phase trajectory circle). Note that in the case of constant γ the directions of rotation for $\gamma > 0$ and $\gamma < 0$ are opposite. In the case of the Landau-Zener model, the directions of rotation for $t \to -\infty$ and $t \to +\infty$ are also opposite.

Properties of the linear two-state problem

To understand how the nonlinearity affects the dynamics of the system, we analyze the phase space of the linear system

$$\begin{aligned} i\,a_{L_t} &= U(t)b_L, \\ i\,b_{L_t} &= U(t)a_L + \delta_t(t)b_L \end{aligned} \tag{2.31}$$

associated with the nonlinear one under consideration (the question how Eqs. (2.31) and (1.2) are related is discussed in detail in Ref. [102]). From the quantum optics point of view this linear system describes coherent interaction of an isolated atom with optical laser radiation [82].

This system has the following first integral:

$$|a_L|^2 + |b_L|^2 = \text{const} = J_L \tag{2.32}$$

which we normalize to unity: $J_L = 1$. Reconstructing the classical Hamiltonian corresponding to

the set of equations (2.31), we arrive at the following result:

$$H_L = \delta_t b_L^* b_L + U[b_L^* a_L + a_L^* b_L] \tag{2.33}$$

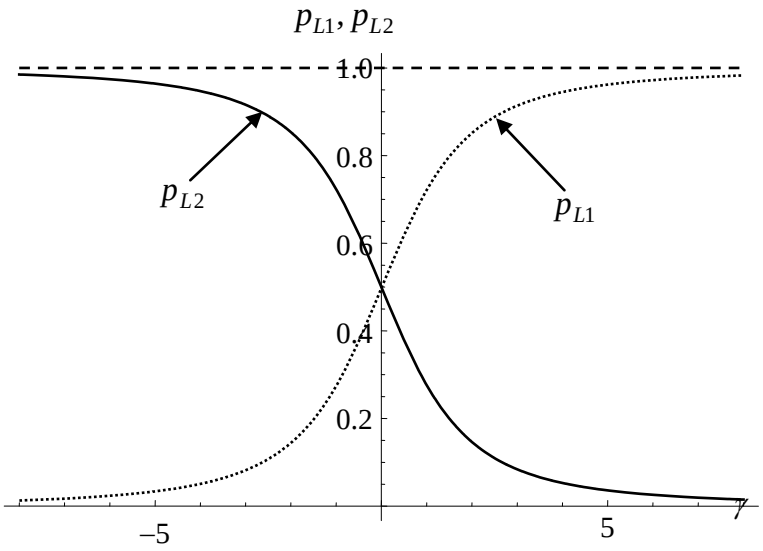


Fig. 2.3. The values of the transition probability at the fixed points (2.37) $\{q_{L1},\ p_{L1}\}$ and $\{q_{L2},\ p_{L2}\}$.

with

$$\{a_L, (ia_L)^*\} = 1,\ \ \{b_L, (ib_L)^*\} = 1,\ \ \{a_L, b_L\} = \{a_L, b_L^*\} = 0. \tag{2.34}$$

In this case, the representation of Hamilton's equations of motion in complex notation (2.7) results in the set of equations (2.31). Further, representing a_L and b_L as

$$a_L = \sqrt{1 - |\, b_L \,|^2}\, e^{i\theta_{1L}} \text{ and } b_L = |\, b_L \,| e^{i\theta_{2L}} \tag{2.35}$$

we rewrite the Hamiltonian (2.33) as follows:

$$H_L(t, q_L, p_L) = 2U(t)\sqrt{p_L(1 - p_L)}\ \cos q_L + \delta_t(t) p_L, \tag{2.36}$$

where $p_L = |\, b_L \,|^2$ and $q_L = \theta_{1L} - \theta_{2L}$. Further, we write corresponding Hamilton's equations of motion, pass to dimensionless parameters via application of the transformation $\tilde{t} = U_0 t$ to this set of equation, and find the fixed points of the obtained equations. This results in the following two elliptic fixed points:

$$q_{L1,2} = 0, \pi\,, \qquad p_{L1,2} = \frac{1}{2}\left(1 \pm \frac{\gamma}{\sqrt{4+\gamma^2}}\right), \tag{2.37}$$

where, as before, $\gamma = \varepsilon t$, $\varepsilon = 2/\lambda$, and for simplicity of notations the tilde over $\tilde{t}$ is omitted. The fixed points (2.37) stay within the phase space for arbitrary values of γ (see Fig. 2.3). Note that the phase space of the time-independent version of the linear system does not contain separatrices. From the set of equations (2.31) it can be easily seen that in the case of the Rabi model the exact solution to the problem is given in terms of harmonic functions. Hence, non-oscillatory behavior of the second state probability, observed under certain initial conditions in the nonlinear case, is excluded in the linear case.

The non-linear Landau-Zener problem

Now, we again address the nonlinear Landau-Zener problem [see Eqs. (2.20)-(2.21)]. Consider that γ slowly changes in time. In this case the phase portrait of the system evolves as it is shown in Fig. 2.1. In the beginning of the process $(t = -\infty)$ the phase portrait contains only one elliptic fixed point $\{q'_{01}, p'_{01}\}$ situated in the center of the phase space. At $\gamma = -\sqrt{2}$ bifurcation takes place: another elliptic and two saddle points, $\{q'_{02}, p'_{02}\}$ and $\{q'_{03,\,04}, p'_{03,\,04}\}$, respectively, enter the phase space at the point $(q', p') = (0, -1)$. The separatrix moves across the phase space from the left to the right while the elliptic fixed point moves towards the center of the phase space. At $\gamma = \sqrt{2}$ another bifurcation takes place: the elliptic fixed point $\{q'_{01}, p'_{01}\}$ and the two saddle points $\{q'_{03,\,04}, p'_{03,\,04}\}$ reach the edge of the phase space and merge at the point $(q', p') = (0, 1)$. When $\gamma > \sqrt{2}$ the phase space again contains only one elliptic fixed point which asymptotically approaches the center of the phase space with $t \to +\infty$. The presented analysis shows that, irrespective of the imposed initial conditions, in the case of the Landau-Zener model the exact phase trajectory will cross the separatrix at a value of $\gamma \in [-\sqrt{2}, \sqrt{2}]$.

2.4. Adiabatic invariance and the nonlinear Landau-Zener problem

In the present section, we construct an approximate solution to the problem using the theory of adiabatic invariants. First, consider the Hamiltonian (2.21), assuming that γ does not vary in time. In this case the action variable, generally defined as

$$I = \frac{1}{2\pi}\oint p'\,dq', \tag{2.38}$$

where the integral is taken over a closed trajectory is a conserved quantity of the Hamiltonian system (e.g., see Ref. [92]). Now, suppose that the parameter γ slowly varies in time: $\gamma = \varepsilon t$, where ε is a small parameter. In this case, according to the adiabatic theorem [92], the action (2.38) is an adiabatic invariant of the system unless the characteristic period of the system is infinity anywhere. Adiabatic invariance implies that for every $\kappa > 0$ there exists $\varepsilon_0(\kappa) > 0$ such that if $0 < \varepsilon < \varepsilon_0$ and $0 < t < 1/\varepsilon$, then

$$|\, I(t) - I(0)\,| < \kappa\,. \tag{2.39}$$

The proof of the adiabatic theorem is based on an averaging over the fast motion a time-independent version of the system (i.e., the same system but with $\gamma = \text{const}$). Hence, it is intuitively clear that the parameter γ should not change noticeably during a characteristic period of system's motion:

$$T d\gamma / dt << \gamma\,. \tag{2.40}$$

On the separatrix the characteristic period goes to infinity $(T = \infty)$; as a result, when the phase trajectory of the exact system moves across the separatrix of the "frozen" system, the adiabatic theorem is not valid any more, and the action changes its initial value. However, once the system's exact phase trajectory has crossed the separatrix, the adiabatic theorem becomes applicable again and the action again becomes an adiabatic invariant of the system.

If the phase trajectory is closed then the action (2.38) is nothing else than the area of the phase space region bounded by the phase trajectory divided by 2π. But this geometrical definition is not unambiguous. A closed trajectory divides the phase space into two domains and one should specify which domain area should be taken. We define the action as the area such that the domain

(whether outer or inner) should always be observed to the right from the path-tracing direction. The action defined in this way will be a continuous function of the parameter γ. Taking into account that in the case of the Landau-Zener model the exact phase trajectories at $t \to \pm\infty$ are given by Eq. (2.30), we can easily calculate the exact value of the action I at $t \to \pm\infty$. Indeed, we notice that at $t \to -\infty$ the exact phase trajectory of the system is a circle with an area equal to $2\pi\, p(t=-\infty)$. Hence, $I(t=-\infty) = p(t=-\infty)$. Further, taking into account the direction of the phase trajectory motion we obtain $I(t=+\infty) = 1/2 - p(t=+\infty)$. Thus, we conclude that the change in the action during the whole interaction process, $I(t=+\infty) - I(t=-\infty)$, can be expressed in terms of the initial $(t=-\infty)$ and final $(t=+\infty)$ molecular state probabilities:

$$I(t=+\infty) - I(t=-\infty) = 1/2 - p(t=+\infty) - p(t=-\infty). \tag{2.41}$$

Taking into account the imposed initial condition, $p(t=-\infty)=0$, we have $I(t=-\infty)=0$ and thus

$$I(t=+\infty) = 1/2 - p(t=+\infty). \tag{2.42}$$

If in the phase space domains, where the exact phase trajectory is away from the separatrix, the action change is neglected then Eq. (2.41) can be interpreted as *the action change at the separatrix crossing* written in terms of the initial $(t=-\infty)$ and final $(t=+\infty)$ molecular state probabilities.

Now, we construct the solution to the problem within the adiabatic approximation and determine its applicability range: this will enable us to find an analytical estimate for the time when the exact phase trajectory crosses the separatrix of the "frozen" system. Recall, that in the beginning of the process $(t=-\infty)$ we have $I(t=-\infty)=0$. Since for $\gamma < -\sqrt{2}$ the phase portrait of the "frozen" system does not contain separatrices, the action variable I is an adiabatic invariant of motion, $I(t) = I(t=-\infty) = 0$. The action of a trajectory is zero if the trajectory is a fixed point of the system. Hence, in our case the phase trajectory of the system within the adiabatic approximation coincides with the first fixed point of Eq. (2.24). Thus, Eq. (2.24) defines a solution of the problem within adiabatic approximation while the exact phase trajectory approaches the separatrix.

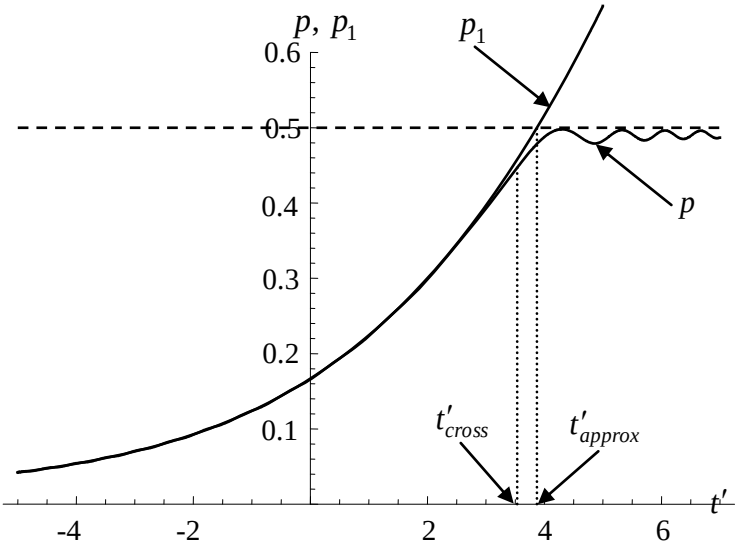


Fig. 2.4. Numerical graph of the molecular state probability p and adiabatic approximation (2.26) p_1 versus time t' for $\lambda = 30$ [where $t' = \sqrt{\delta_0}\, t$ with t being time used in the initial set of equations (1.2)]. Two vertical lines mark the points where the exact phase trajectory and the adiabatic approximation cross the separatrix, $t'_{cross} \approx 3.535$ and $t'_{approx} = \sqrt{\lambda/2} \approx 3.873$, respectively.

It can be seen that the adiabatic trajectory (2.24) and the separatrix (2.27) intersect when $\gamma = \sqrt{2}$. This gives an analytical estimate for the crossing time of the exact phase trajectory and the separatrix of the "frozen" system. In fact, this crossing takes place at a value of γ which is smaller than $\sqrt{2}$. This statement is well confirmed by numerical simulations. In Fig. 2.4 we plot the numerical graph of the molecular state probability p and the adiabatic approximation (2.26) as functions of time; two vertical lines mark the points where the numerical solution and the adiabatic approximation cross the separatrix of the "frozen" system. As was expected, the adiabatic approximation starts deviating from the numerical solution in the vicinity of the separatrix crossing point. Note that at $\gamma = \sqrt{2}$, $p_1 = 1/2$.

Finally, for comparison, we apply the presented approach to the linear set of equations (2.31). In the case when the system starts from the first state, $a_L(t = -\infty) = 1$, $b_L(t = -\infty) = 0$, the

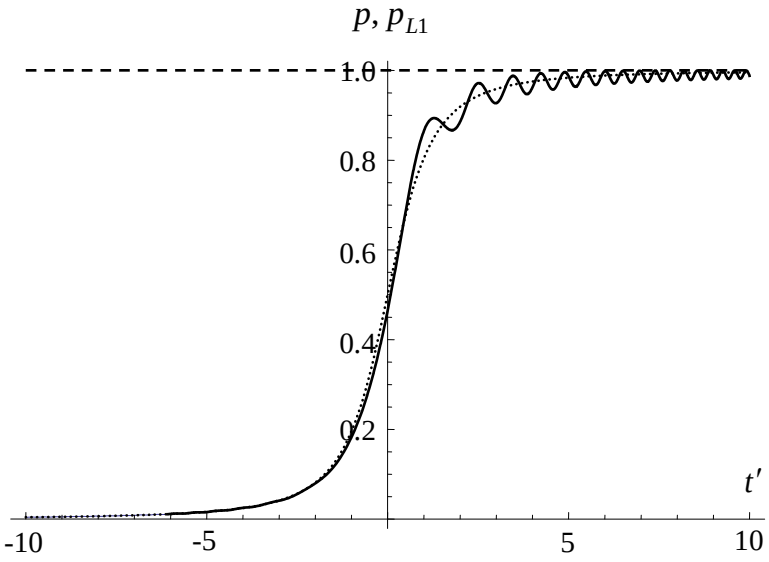


Fig. 2.5. The numerical solutions to the linear problem (2.31) p_L (the solid curve) and the adiabatic approximation (2.37) (the dotted curve) as functions of time t' for $\lambda = 1.7$ [where $t' = \sqrt{\delta_0}\, t$ with t being time used in the linear set of equations (2.31)].

phase trajectory of the system in the adiabatic approximation is given by the fixed point $\{q_{L1}, p_{L1}\}$ [see Eq. (2.37)]. The numerical solutions to the linear problem p_L and the adiabatic approximation (2.37) are shown in Fig. 2.5. As we see, in the linear case the application of the adiabatic approximation does not lead to a divergent result. The small-amplitude oscillations emerging after the system has passed through the resonance considerably diminish at larger values of the Landau-Zener parameter λ; for $\lambda > 3.5$ these oscillations are negligibly small, and the whole temporal dynamics of the system is well described by the adiabatic approximation. In the case of the Landau-Zener model the nonadiabatic corrections for the final transitions probability are exponentially small.

2.5. Super-adiabatic sequence and the nonlinear Landau-Zener problem

The adiabatic approximation can be improved by using a general scheme referred to as super-adiabatic approximations [103]. According to this scheme the *n*-th order adiabatic

approximation is defined by the recurrence relations

$$\begin{aligned}\frac{dq'_{n-1}}{dt} &= \frac{1}{\sqrt{2}}\left[1-3(p'_n)^2-(q'_n)^2\right]+\gamma\, p'_n,\\ \frac{dp'_{n-1}}{dt} &= \sqrt{2}\,p'_n q'_n-\gamma\, q'_n.\end{aligned} \tag{2.43}$$

Consider, e.g., the functions $\{p'_{01}, q'_{01}\}$ as a zero-order approximation and, according to the recurrence relations (2.43), construct the first adiabatic approximation:

$$\begin{aligned}0 &= \frac{1}{\sqrt{2}}[1-3(p'_1)^2-(q'_1)^2]+\gamma\, p'_1,\\ \frac{dp'_{01}}{dt} &= \sqrt{2}\,p'_1 q'_1-\gamma\, q'_1.\end{aligned} \tag{2.44}$$

Elimination of q'_1 from this system shows that the function p'_1 satisfies a polynomial equation of the fourth order:

$$3\left(p'_1-\frac{\gamma+\sqrt{6+\gamma^2}}{3\sqrt{2}}\right)\left(p'_1-\frac{\gamma-\sqrt{6+\gamma^2}}{3\sqrt{2}}\right)\left(p'_1-\gamma/\sqrt{2}\right)^2+\frac{1}{2}\left(\frac{dp'_{01}}{dt}\right)^2=0. \tag{2.45}$$

Studying now the asymptotic behavior of variables $\{q'_1, p'_1\}$ at $t\to+\infty$ ($\gamma\to+\infty$) for the Landau-Zener model, we see that, at large time values, the roots of equation (2.45) behave as

$$\left|p'_{1a,1b}\right|\sim\frac{\gamma}{\sqrt{2}},\quad \left|p'_{1c}\right|\sim\frac{\sqrt{2}}{3}\gamma,\quad \text{and}\quad \left|p'_{1d}\right|\sim\frac{1}{\sqrt{2}\gamma}, \tag{2.46}$$

while the function q'_1 always tends to zero at $t\to+\infty$ as $\left|q'_1\right|\sim C/\gamma$, where C is a constant, depending on choice of the root of (2.45). Besides, by taking the derivative of Eq. (2.45) with respect to time it can be shown that there are points of time at which the derivative of p'_1 becomes infinite. Finally, as can be seen from Fig. 2.6, the transition probability in the first adiabatic approximation is not a single-valued function.

As we see, application of the super-adiabatic sequence improves the adiabatic approximation but does not avoid the divergence at the crossing of the separatrix. Hence, alternative approaches are needed. We will show below that introduction of an imaginary

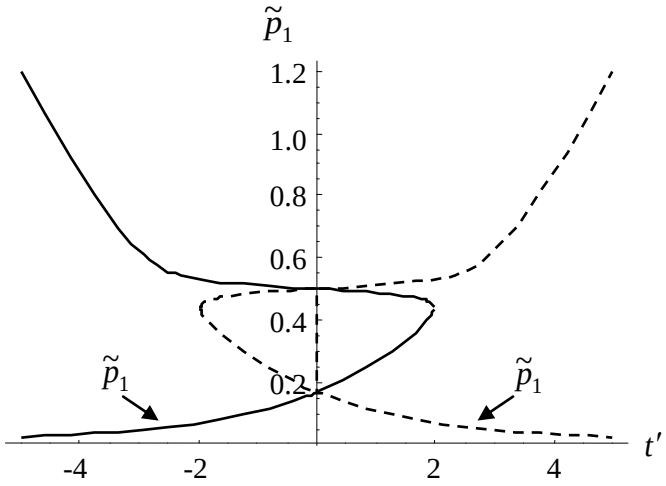


Fig. 2.6. The transition probability given by the first adiabatic approximation, $\tilde{p}_1 = (q_1'^2 + p_1'^2)/2$, versus time t' $(t' = \sqrt{\delta_0}\, t)$.

term in the Hamiltonian (2.16) suggests a possibility to construct a zero-order approximation valid for all time.

2.6. Modification of the adiabatic approximation

In the present section we describe a method which allows us to construct a zero-order approximation valid in the whole time domain. To do this, we analyze the divergence of the adiabatic approximation from the point of view of the theory of ordinary differential equations. From this point of view, when constructing an approximate solution to the set of equations (2.17), we have neglected the two higher order derivative terms. Thus, the divergence of the approximate solution is due to the singular procedure we have applied to construct it. From this we conclude that, when constructing a zero-order approximation, the higher order derivatives cannot be simply neglected: they should necessarily be taken into account, at least to some extent. We present an approach in which instead of neglecting the derivative dp'/dt in (2.17), we replace it by some constant $\tilde{A}$, and define a zero-order approximation to the problem under consideration as a function

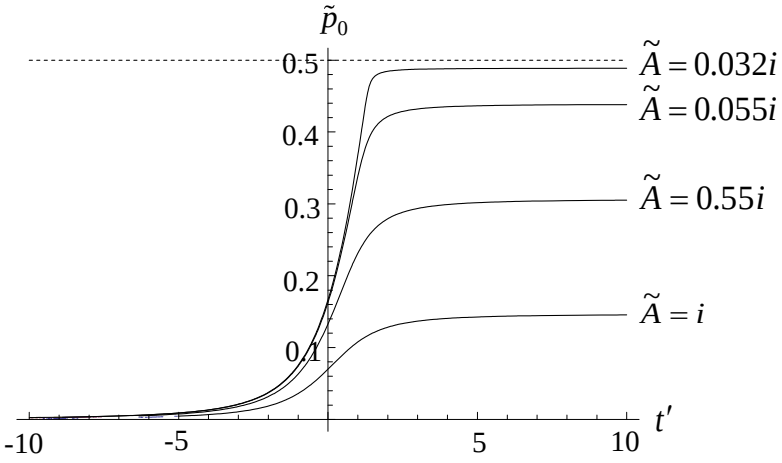


Fig. 2.7. The approximate expression for the molecular state probability $\tilde{p}_0 = 1/2[(q_0')^2 + (p_0')^2]$ in the improved adiabatic approximation (2.47) versus time t' $(t' = \sqrt{\delta_0}\, t)$, for different values of an imaginary parameter $\tilde{A}$ $(\sqrt{\lambda/2} > |\tilde{A}| > 0)$ and fixed $\lambda = 4$.

obeying the following set of equations:

$$0 = \frac{1}{\sqrt{2}} U(t)[1 - 3(p_0')^2 - (q_0')^2] + \delta_t(t)\, p_0', \qquad \tilde{A} = \sqrt{2}\, U(t) \cdot p_0' q_0' - \delta_t(t) q_0'. \tag{2.47}$$

Studying the solution of these equations, we arrive at an interesting result: the approximate expression for the molecular state probability $\tilde{p}_0 = 1/2[(q_0')^2 + (p_0')^2]$ is a bounded step-like function starting from zero at $t = -\infty$, if and only if $\tilde{A}$ is a pure imaginary constant, i.e., $\mathrm{Re}(\tilde{A}) = 0$ (see Fig. 2.7). This result is quite unexpected since the quantity dp'/dt, which we have tried to approximate by the constant $\tilde{A}$, never takes imaginary values. This statement has been verified for several level crossing models, such as the Landau-Zener and Demkov-Kunike models.

One can look at the emergence of the constant $\tilde{A}$ from a different angle. Let's consider an effective system described by the following complex Hamiltonian:

$$H(t, q', p') = \frac{U(t)}{\sqrt{2}}\, p'[1 - (p')^2 - (q')^2] + \frac{\delta_t(t)}{2}[(p')^2 + (q')^2] + \tilde{A} q'. \tag{2.48}$$

If we now write Hamilton's equations of motion for it and neglect the higher order derivatives, we will again arrive at the set of equations (2.47). Hence, the valid zero-order approximation (2.47) has

been constructed by introducing a complex term into the Hamiltonian (2.16).

Note that the precise value of the parameter $\tilde{A}$ has not been specified yet: it plays a role of a variational parameter.

2.7. Review of the results by Ishkhanyan *et al.* [62]

In what follows we juxtapose the presented developments with the results obtained in Refs. [61-62], where a completely different approach has been implemented. We show how the results of these works and the presented developments are related and complement each other.

First of all we compare the notations used in the present chapter with those of Refs. [61-62]. In these references the unitary transformation (1.3) to the basic set of equations (1.2) has been applied, thus the canonic form (1.4) of the governing set of equations has been used.

The approach presented in those works is based on the exact equation for the molecular state probability (1.12). When considering the Landau-Zener model (2.20) in Refs. [61-62] time has been rescaled as $t' = \sqrt{\delta_0}\, t$ and the dimensionless Landau-Zener parameter $\lambda = U_0^2 / \delta_0$ has been introduced. Thus, for the Landau-Zener model, the equation for the molecular state probability (1.12) takes the following form:

$$p_{ttt} - \frac{p_{tt}}{t} + \left[4t^2 + 4\lambda(1-3p)\right]p_t + \frac{\lambda}{t}(1-8p+12p^2) = 0, \tag{2.49}$$

where the prime of t' has been omitted.

In Ref. [62], a highly accurate approximate solution of Eq. (2.49) has been constructed; this approximation is written as a sum of two terms:

$$p = p_0(A,t) + C_1 \frac{p_{LZ}(\lambda_1,t)}{p_{LZ}(\lambda_1,\infty)}. \tag{2.50}$$

The first term, $p_0(A,t)$, is defined as a solution of an augmented limit equation :

$$\left[4t^2 + 4\lambda(1-3p_0)\right]p_{0_t} + \frac{\lambda}{t}(1-8p_0+12p_0^2) - \frac{A}{t} = 0, \tag{2.51}$$

such that $p_0(A, t=-\infty) = 0$ while the second term, $p_{LZ}(\lambda_1,t)$, is the solution of the *linear* Landau-Zener problem [72] for an effective Landau-Zener parameter λ_1:

$$\left(\frac{d}{dt}-\frac{1}{t}\right)\left(\frac{d^2 p_{LZ}}{dt^2}+4\lambda_1 p_{LZ}-2\lambda_1\right)+4t^2\frac{dp_{LZ}}{dt}=0. \tag{2.52}$$

The solution p_{LZ} should satisfy the following initial conditions:

$$p_{LZ}(t)\big|_{t=-\infty}=0,\quad \left.\frac{dp_{LZ}}{dt}\right|_{t=-\infty}=0. \tag{2.53}$$

In the case of the Landau-Zener problem, the initial conditions imposed on the molecular state probability and its first derivative [see Eq. (2.53)] unambiguously define the solution of equation (2.52). The function $p_{LZ}(\lambda_1,t)$ can be written explicitly in terms of the confluent hypergeometric functions:

$$p_{LZ}(t)=\left|C_{01}\cdot F_1+C_{02}\cdot F_2\right|^2 \tag{2.54}$$

with

$$C_{01}=\sqrt{\lambda_1 e^{-\pi\lambda_1/4}\cosh(\pi\lambda_1/4)}\,\frac{i}{2}\,\frac{\Gamma(1/2-i\lambda_1/4)}{\Gamma(1-i\lambda_1/4)},\quad C_{02}=\sqrt{\lambda_1 e^{-\pi\lambda_1/4}\cosh(\pi\lambda_1/4)}\sqrt{i}, \tag{2.55}$$

and

$$F_1={}_1F_1(i\lambda_1/4;1/2;it^2),\quad F_2=t\,{}_1F_1(1/2+i\lambda_1/4;3/2;it^2), \tag{2.56}$$

where Γ is the Euler gamma-function [85] and ${}_1F_1$ is the Kummer confluent hypergeometric function [85]. The limits of p_{LZ} for $t\to 0$ and $t\to+\infty$ are written as

$$p_{LZ}(0)=\frac{1-e^{-\pi\lambda_1/2}}{2},\quad p_{LZ}(+\infty)=1-e^{-\pi\lambda_1}. \tag{2.57}$$

Regarding the limit solution $p_0(A,t)$, integration of Eq. (2.51) via transformation of the independent variable followed by interchange of dependent and independent variables results in a *quartic* polynomial equation for p_0:

$$\frac{\lambda}{4t^2}=\frac{C_0+p_0(p_0-\beta_1)(p_0-\beta_2)}{9(p_0-\alpha_1)^2(p_0-\alpha_2)^2}, \tag{2.58}$$

where C_0 is an integration constant and the involved parameters $\alpha_{1,2}$, $\beta_{1,2}$ are defined as

$$\alpha_{1,2}=\frac{1}{3}\mp\frac{1}{6}\sqrt{1+\frac{6A}{\lambda}},\quad \beta_{1,2}=\frac{1}{2}\mp\sqrt{\frac{A}{2\lambda}}. \tag{2.59}$$

For the initial condition $p_0(-\infty)=0$ one obtains $C_0=0$. For a positive A, such that $\lambda/2>A>0$, the solution of the equation (2.58) defines a bounded, monotonically increasing function which tends to a finite value less than $1/2$ when $t\to+\infty$ (Fig. 2.7). In Ref. [61] it has been shown that

$$p_0(+\infty)=\beta_1. \tag{2.60}$$

By combining Eqs. (2.50), (2.59), and (2.60), it is readily seen that the approximate expression for the final transition probability can be written as follows:

$$p(t=+\infty)=\frac{1}{2}-\sqrt{\frac{A}{2\lambda}}+C_1. \tag{2.61}$$

In Ref. [62] the following analytic expressions for the variational parameters $A(\lambda)$, $C_1(\lambda)$, and $\lambda_1(\lambda)$ have been obtained:

$$A=\frac{\lambda}{2}\,{}_2F_1\left(1,2;1.385;-\frac{\lambda^2}{2}\right), \tag{2.62}$$

$$C_1=\frac{P_{LZ}(\lambda,+\infty)}{4}\sqrt{{}_2F_1\left(1,2;1.2767;-\frac{\lambda^2}{2.75}\right)}, \tag{2.63}$$

and

$$\lambda_1=\lambda\,(1-3\beta_1-3C_1)=\lambda\,(1-3p(+\infty)), \tag{2.64}$$

where ${}_2F_1$ is the Gauss hypergeometric function [85]. We would like to note that because of a misprint, the third parameter of the hypergeometric function ${}_2F_1$ in the expression for C_1 (2.63) differs from that presented in the original paper [62]. For all the variation range of the input Landau-Zener parameter λ, the deviation of the formulae (2.62)-(2.64) from the numerical results is of the order of or less than 10^{-4}. Moreover, it has been shown that the absolute error of the analytical formula for the final transition probability with the fitting parameters A, C_1, and λ_1 defined by Eqs. (2.62)-(2.64) is also of the order of or less than 10^{-4}.

2.8. Interrelation between the two approaches

Note that if we now take $A=0$, Eq. (2.58) will degenerate to a quadratic one because in this

case three of four parameters $\alpha_{1,2}$, $\beta_{1,2}$ become equal, $\alpha_2 = \beta_1 = \beta_2 = 1/2$. An interesting observation is that the solutions of this quadratic equation identically coincide with the function (2.26) derived within the adiabatic approximation. Thus, application of the adiabatic approximation is equivalent to removing the two higher order derivative terms from the exact equation for the molecular state probability (2.49). In this connection it would be interesting to find out whether there exists an analogous interrelation between the function $p_0(A,t)$ [see Eq. (2.58)] and the improved zero-order approximation for the molecular state probability $\tilde{p} = 1/2[(q_0')^2 + (p_0')^2]$, where the functions $\{q_0', p_0'\}$ are defined as a solution of the set (2.47) with the initial condition $\tilde{p}(-\infty) = 0$.

To clarify this issue, we rewrite the complex Hamiltonian (2.48) in terms of the coordinates $\{q, p\}$ [see Eqs. (2.14)-(2.15)] and derive the corresponding equations of motion. This results in the following set of equations for the variables q and p:

$$\begin{aligned} \frac{dq}{dt} &= p^{-1/2}\left(\frac{1}{2} - 3p\right)\cdot U(t)\cos q + \delta_t(t) + \frac{\tilde{A}}{\sqrt{2p}}\sin q, \\ \frac{dp}{dt} &= p^{1/2}(1-2p)\cdot U(t)\sin q - \tilde{A}\sqrt{2p}\sin q\,. \end{aligned} \tag{2.65}$$

To construct an improved adiabatic approximation, equivalent to that given by the set of equations (2.47), we neglect the derivatives of q and p in the system (2.65). To compare the obtained set of equations with the solution of the augmented limit equation (2.58), we eliminate the coordinate q from this set. This immediately yields an equation for the determination of the molecular state probability. In the case of the Landau-Zener model the improved adiabatic approximation is written as follows:

$$\frac{U^2(t)}{\delta_t^2(t)} = \frac{p_0(p_0 - \tilde{\beta}_1)(p_0 - \tilde{\beta}_2)}{9(p_0 - \tilde{\alpha}_1)^2(p_0 - \tilde{\alpha}_2)^2}, \tag{2.66}$$

where

$$\tilde{\alpha}_{1,2} = \frac{1}{3} \mp \frac{1}{6}\sqrt{1 - \frac{6\tilde{A}^2}{\lambda}}, \quad \tilde{\beta}_{1,2} = \frac{1}{2} \mp \frac{i\tilde{A}}{\sqrt{2\lambda}}. \tag{2.67}$$

If we now choose $\tilde{A}$ as $\tilde{A} = \pm i\sqrt{A}$, the molecular state probability calculated in the improved adiabatic approximation will identically coincide with the solution of the augmented limit equation $p_0(A,t)$. If the negative sign is chosen then $\tilde{\beta}_{1,2} = \beta_{1,2}$; otherwise $\tilde{\beta}_{1,2} = \beta_{2,1}$.

Further, taking into account the fact that the change in the action is coupled with the initial (at $t = -\infty$) and final (at $t = -\infty$) probabilities of the molecular state [see Eqs. (2.41)-(2.42)], we use formulae (2.61)-(2.64) to obtain the following asymptotic expression for the action variable at $t \to +\infty$.

$$I(t = +\infty) = \frac{1}{2}\sqrt{{}_2F_1\left(1, 2; 1.385; -\frac{\lambda^2}{2}\right)} - \frac{P_{LZ}(\lambda, +\infty)}{4}\sqrt{{}_2F_1\left(1, 2; 1.2767; -\frac{\lambda^2}{2.75}\right)}. \tag{2.68}$$

The absolute error of this formula does not exceed 10^{-4}, and it is applicable without any limitations on the value of the Landau-Zener parameter λ. Note that this formula is explicitly expressed in terms of the input parameters of the problem. To write Eq. (2.68) in terms of elementary functions, we apply the asymptotic expansion for $\lambda >> 1$ to each of the hypergeometric functions in (2.68), thus reducing it to the following form:

$$I(t = +\infty) \approx \frac{0.22067}{\lambda} + \frac{1}{\lambda^3}(0.10589 \ln\lambda - 0.24181). \tag{2.69}$$

The asymptotically exact expression for the action variable at $t \to +\infty$, $I(t = +\infty)$, for very slow resonance sweep rates has been derived in Ref. [69]:

$$I(t = +\infty) = \frac{\ln 2}{\pi}\frac{1}{\lambda} \approx \frac{0.220636}{\lambda} \tag{2.70}$$

(recall that λ is inversely proportional to the resonance sweep rate). As it has been mentioned in Ref. [69], for $\lambda = 20$ numerical calculations reproduce the coefficient $\ln 2/\pi \approx 0.220636$ with 5-digit accuracy; for larger values of λ, the absolute error of formula (2.70) will be even smaller. Thus, as compared to formulas (2.68) and (2.69), formula (2.70) is more precise in the case of very slow sweep rates, but both formulas (2.68) and even (2.69) have wider applicability range. For example, the analysis of Eq. (73) indicates that, within the applicability range of the presented

formula, the total change in the action, $I(t=+\infty)-I(t=-\infty)$, in the case of large values of the Landau-Zener parameter ($\lambda >> 1$) can be written as a power-law function of the sweep rate through the resonance. However, Eqs. (2.68) and (2.69) clearly show that in the case of arbitrary values of the Landau-Zener parameter the total change in the action is not given by a power-law function of the sweep rate. Moreover, the total change of the action is not given by a power law function of the sweep rate also in the case of the strong nonlinearity limit which corresponds to $\lambda > 1$ (for a detailed discussion of the strong and weak nonlinearity limits see Ref. [62]).

Finally, we conclude this section with some qualitative observations. The exact equation for the molecular state probability (1.12) indicates that the passage of the system through the resonance can increase the number of the singularities of the equation: if $\delta_{tt} \neq 0$ at the resonance crossing then the logarithmic derivative of the detuning δ_{tt} / δ_t necessarily becomes infinite at this point. Hence, the resonance crossing strongly affects the dynamics of molecule formation. However, the phase space of the time-independent version of the system does not provide a straightforward evidence for the relevance of the resonance crossing. Instead, when studying the phase space of the system, we arrived at a conclusion that the crossing point of the system's exact phase trajectory with the separatrix of the "frozen" system is the essential concept. Indeed, at the separatrix crossing the action substantially changes its value, and due to this crossing the system changes the type of motion. The separatrix crossing point is the singular point of the exact equation for p' (2.18). A natural conclusion is that the separatrix crossing plays an important role in emergence of the small-amplitude oscillations in the molecular state probability which come up after the separatrix crossing (see Fig. 2.4).

While studying the linear set of equations (2.31) we have shown that the corresponding classical phase space does not contain separatrices. However, as it is in the nonlinear case, in the linear case also, certain time after the system has crossed the resonance, small-amplitude oscillations in the molecular state probability appear. In the parameter variation domain, where the adiabatic approximation is applicable (approximately $\lambda > 3.5$), the amplitude of these oscillations is negligibly small, and the function $p_L(t)$ can be regarded as an almost monotonic one. But if we

consider the values of the Landau-Zener parameter such that the adiabatic approximation is not applicable (approximately $\lambda < 3.5$), the small amplitude oscillations cannot be neglected (see Fig. 2.5). By comparing this situation with the one we have in the nonlinear case we see that in the nonlinear case the small-amplitude oscillations cannot be neglected for any values of the Landau-Zener parameter λ. Hence, we arrive at a conclusion that in the nonlinear case these small-amplitude oscillations are more persistent due to the crossing of the separatrix.

2.9. Conclusion

We have studied the nonlinear mean-field dynamics of molecule formation at coherent photo- and magneto-association of an atomic Bose-Einstein condensate focusing on the case when the external field configuration is defined by the constant-coupling linear resonance-crossing Landau-Zener model. We have studied a condensate initially being in all-atomic state since under contemporary experimental conditions one faces this case most frequently.

Assuming that the sweeping rate through the resonance is small, we have applied the theory of adiabatic invariants. First, we have discussed the classical phase space of the time-independent version of the problem in terms of the canonically conjugate variables $\{q', p'\}$ [see Eq. (2.13)]. Taking into account that the considered initial condition corresponds to the case of zero initial action we have constructed an expression for the molecular state probability within the adiabatic approximation [see Eq. (2.26)]. The constructed solution quite accurately describes the temporal dynamics of the coupled atom-molecular system up to the point of time where the approximation, deviating from the numerical solution, starts to go to infinity. Thus, the adiabatic approximation fails to provide a prediction for the final number of the formed molecules.

The reason for the divergence of the adiabatic approximation is that the exact phase trajectory of the system inevitably crosses the separatrix of the system's time-independent version. Hence, the necessary conditions of the adiabatic theorem are not satisfied in this case. However, we have managed to construct a valid zero-order approximation by introducing an imaginary term in the Hamiltonian, writing equations of motion for this augmented Hamiltonian and neglecting the higher order derivative terms. This procedure results in a step-like bounded function that starts from

zero. Thus, the introduced complex term has enabled us to eliminate the divergence of the adiabatic approximation.

Further, we have compared the developments of the present paper with those presented in Ref. [62]. We have shown that the application of the adiabatic approximation is equivalent to removing the two higher order derivative terms from the exact equation for the molecular state probability (2.49) while the constructed zero-order approximation is identical with the solution of the augmented limit equation (2.51). Taking into account that the molecular conversion efficiency is coupled with the total change of the action $[I(t=+\infty)-I(t=-\infty)]$, we have calculated this change [see Eq. (2.68)] using a highly accurate approximate formula for the final transition probability presented in Ref. [62]. The absolute error of the presented formula for the action change is on the order of or less than 10^{-4}. Interestingly, the total change of the action is not given as a power-law function of the sweep rate through the resonance.

Finally, we recall that the Hamiltonian we have studied is not restricted to the description of the coupled dynamics of the atomic and molecular condensates only. As it has been mentioned above, it can be mapped to the Hamiltonian describing the formation of ultracold molecules at magneto-association in degenerate Fermi gases [50]. Moreover, it is shown to be equivalent to the time-dependent Dicke model [104]. (Detailed discussion on the correspondence of various quantum models is presented in Ref. [67]). Thus, the results of this paper are equally applicable to all these cases.

Chapter 3

Strong nonlinearity limits: two distinct scenarios

In the present chapter we show that two distinct strongly nonlinear scenarios of molecule formation in an atomic Bose-Einstein condensate are available: the association process in the first case is almost non-oscillatory in time, while in the second case the evolution of the system displays strongly pronounced Rabi-type oscillations. By analyzing the exact differential equation for the molecular state probability, we construct highly accurate approximate solutions for both interaction regimes. Investigation of the constructed analytical solutions leads to several qualitative conclusions of practical significance. In particular, we show that, in the almost non-oscillatory regime of the strong nonlinearity limit, the non-crossing models are able to provide conversion of no more than one third of the initial atomic population.

3.1. Introduction

As it has been mentioned above, the two major routes leading to creation of ultracold molecules are the Raman photoassociation and Feshbach association of degenerate atomic gases. In this context, it is commonly believed that large coupling is favorable for molecule formation. In particular, it is expected that in the case of photoassociation, application of higher laser field intensities will result in larger molecular population. This supposition originates from the analysis of the Landau-Zener model (1.36) [72] which is typically employed when treating the level crossing processes. However, the knowledge accumulated from the analysis of quantum nonadiabatic transitions in linear systems (see, e.g., Refs. [86-87,89-90]) suggests that the Landau-Zener-based predictions are substantially altered when more realistic models are discussed. Therefore, one may expect that in the nonlinear case, when the formation of mesoscopic or macroscopic numbers of molecules are discussed, the changes in the interaction picture caused by the deviation of the coupling and detuning shapes from those defined by the Landau-Zener model may even be more essential.

To address this topic systematically, we examine the level crossing as well as non-crossing processes in general, i.e., we assume arbitrary coupling-shape and energy-detuning configurations. Discussing possible scenarios of molecule formation in the case of the strong coupling limit, we show that two qualitatively distinct interaction regimes may occur. In the first interaction regime, which, e.g., for the Rosen-Zener model (1.41) corresponds to the large detuning and large values of the peak coupling, the transition of atoms into the molecular state takes place almost non-oscillatory in time (only weakly pronounced oscillations between the two population modes are observed). On the contrary, in the second interaction regime, which, e.g. for the Rosen-Zener model, corresponds to the small detuning and large values of the peak coupling, the hybrid atomic-molecular system displays large-amplitude Rabi-type oscillations between the populations. We illustrate the peculiarities of these two regimes using several models with distinct properties, such as the first Nikitin exponential-crossing model (1.42) that differs from the Landau-Zener case mainly in the finite final detuning at $t \to +\infty$, the first Demkov-Kunike quasi-linear level-crossing model (1.40) with a finite pulse and finite detuning, and the Rosen-Zener finite-pulse constant-detuning, hence, non-crossing model (1.41). Multiple level-crossing models are not considered.

First we present a thorough analysis of the system's dynamics for the case when the external field configuration is defined by the Rosen-Zener model. For completeness of the analysis, we treat both strong and weak coupling limits for this model. Further, we generalize the developed mathematical approach to the case of arbitrary time-dependent coupling and detuning. We construct an approximate solution to describe temporal dynamics of molecule formation in this general case. Our analysis leads to some important results. For example, we show that in the case of the almost non-oscillatory regime of the strong nonlinearity limit, a non-crossing model is not capable of converting into molecules more than $1/3$ of atoms. Thus, in this interaction regime, tuning through the resonance is crucial for molecule production efficiency. However, it should be noted that the constructed approximate solution suffers from essential shortcomings. For example, in the case of the Landau-Zener and Demkov-Kunike models, it does not provide a sufficiently accurate prediction for the final (at $t \to \infty$) transition probability to the molecular state and does not contain an adjustable parameter. To conclude this chapter, we present a general prescription for

modification of the mentioned approximate solution and illustrate its virtues on the example of the Demkov-Kunike and Landau-Zener models. Importantly, the resultant approximation is a smooth bounded step-wise function which contains an adjustable fitting parameter.

3.2. General overview of the Rosen-Zener model

For the non-crossing models next, after the basic constant-amplitude Rabi one (1.35), comes the Rosen-Zener model (1.41) for which the detuning is supposed constant while the coupling varies in time according to the hyperbolic secant law. Though the governing set of equations (1.4) analyzed in this work is relevant to the cold molecule formation processes via both photo- and magneto-association, this field configuration is directly applicable to the photoassociation only. This is due to the fact that, in the case of Feshbach association of molecules, the coupling is constant: it cannot be adjusted by variation of the external field. On the contrary, in the case of photoassociation the pulse duration cannot be infinite (this would mean infinite energy). Hence, finite pulse duration should necessarily be discussed if experimental realization is considered. Finally, the knowledge accumulated from the linear theory suggests that one should be careful with the optical pulse start-up and shutdown scenarios – the particular form of the time variation of the field amplitude plays a substantial role. A well discussed shape of such a time-variable pulse in the linear theory is the Rosen-Zener hyperbolic-secant model. This is a motivation to explore the Rosen-Zener field-configuration for the photoassociation technique.

One should note, however, that this model is applied, though indirectly, to the Feshbach resonance as well. This is achieved by applying a transformation of the independent variable (1.14) that changes the governing equations to a constant-amplitude form. Changing to the constant-amplitude form turns the model into a variable-detuning field configuration. Yet, strictly speaking, the model remains non-crossing. However, this constant-amplitude form reveals a prominent property of the model, namely, a hidden singularity due to the field rise rate at $t = -\infty$. It is this singularity that makes the major difference of this model from the Rabi one, which does not reveal the different evolution scenarios inherent in the Rosen-Zener model as discussed below. The mentioned singularity effectively acts as a resonance-touching. Finally, it should be noted that the

constant-amplitude form of the model makes it relevant to the experiment [30]. Thus, the model is equally useful for the magneto-association via Feshbach resonances.

In the present chapter we explore both the weak and strong coupling regimes for the Rosen-Zener field configuration and compare the results with those for the linear Rosen-Zener model [87] and the nonlinear Rabi problem [70]. Our starting point is the nonlinear coupled set of equations (1.4):

$$i\frac{da_1}{dt} = U(t)e^{-i\delta(t)}a_2\bar{a}_1, \quad i\frac{da_2}{dt} = \frac{U(t)}{2}e^{i\delta(t)}a_1a_1. \tag{3.1}$$

The probability amplitudes a_1 and a_2 are normalized as: $|a_1|^2 + 2|a_2|^2 = 1$. Since we consider a condensate initially being in all-atoms state, the initial conditions imposed are $a_1(-\infty) = 1, a_2(-\infty) = 0$. The external field configuration of the Rosen-Zener model is given as

$$U(t) = U_0\,\mathrm{sech}(t), \quad \delta(t) = 2\delta_0 t \tag{3.2}$$

[compare with Eq. (1.41); recall that $\delta(t)$ is the integral of the detuning $\delta_t(t)$]. We also rewrite here the linear system (1.19) associated with the nonlinear one (3.1)

$$i\frac{da_{1L}}{dt} = U(t)e^{-i\delta(t)}a_{2L}, \quad i\frac{da_{2L}}{dt} = U(t)e^{i\delta(t)}a_{1L} \tag{3.3}$$

with the same functions $U(t), \delta(t)$. Following the prescription of Section 1.4 we choose the motion integral of the linear system as $|a_{1L}|^2 + |a_{2L}|^2 = 1/4$ and impose the following initial conditions: $|a_{1L}(-\infty)| = 1/2$, $a_{2L}(-\infty) = 0$. This choice ensures the coincidence of the solutions of nonlinear and linear systems (3.1) and (3.3), respectively, in the vicinity of $t = -\infty$. The solution of system (3.3) for $I_L = 1$ is written as [87]

$$\begin{aligned} a_{1RZ} &= {}_2F_1(U_0, -U_0; 1/2 + i\delta_0; x), \\ a_{2RZ} &= -iU_0((1-x)/x)^{-i\delta_0}\sqrt{x(1-x)}\cdot{}_2F_1(1+U_0, 1-U_0; 3/2 + i\delta_0; x)/(1/2 + i\delta_0), \end{aligned} \tag{3.4}$$

where $x = (1 + \tanh(t))/2$, and ${}_2F_1(\alpha, \beta; \gamma; x)$ is the Gauss hypergeometric function [85]. Hence, up to a phase factor, the solution of system (3.3) satisfying the normalization $I_L = 1/4$ is

$a_{1L} = a_{1RZ}/2$, $a_{2L} = a_{2RZ}/2$ (for a detailed discussion on the correspondence between the linear and nonlinear systems (3.1) and (3.3), respectively, see Section 1.4).

The final (at $t \to +\infty$) probability of transition to the second level is given by the Rosen-Zener's formula:

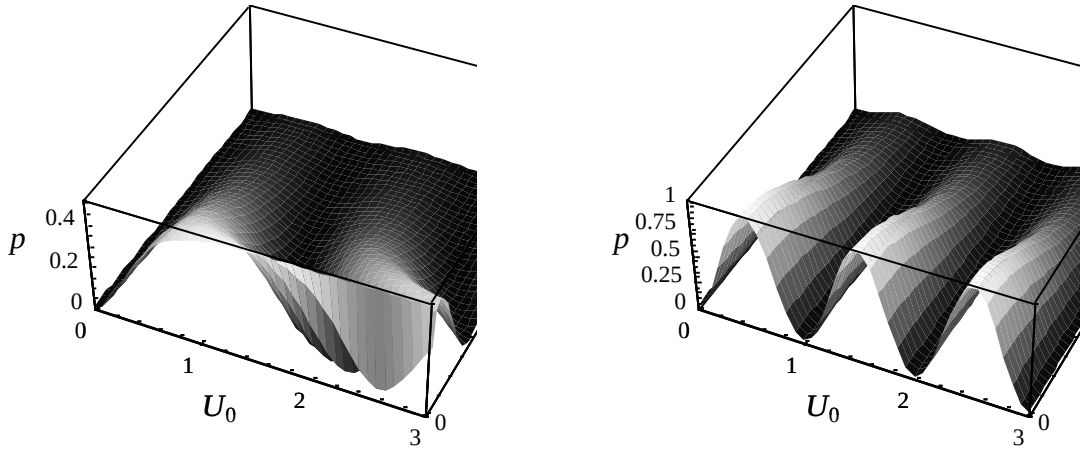
$$P_{RZ} = [\sin(\pi U_0)]^2 \cdot [\mathrm{sech}(\pi \delta_0)]^2 . \tag{3.5}$$

This formula states the well-known π-theorem [87] according to which the system returns to the initial state $(a_{1RZ}, a_{2RZ}) = (1,0)$ if $U_0 = n$ with $n = 0, 1, 2...$, and reaches the highest transition probability possible for the given fixed detuning at $U_0 = 1/2 + n$ ($P_{RZ}^{\max} = [\mathrm{sech}(\pi \delta_0)]^2$). Note that the system may completely be inverted at exact resonance only.

In Fig.3.1 we show the numerical plots of the final transition probability to the molecular state in the nonlinear case and final transition probability to the second state in the linear case as functions of the peak value of the coupling U_0 and the detuning parameter δ_0. As it can be seen, the nonlinear behavior displays considerable deviations from the linear one. First, at exact resonance the dependence of the final transition probability on the Rabi frequency in the nonlinear case is monotonic. Second, though at non-zero detuning atom/molecule oscillations are always observed in the p versus U_0 graph, the π-theorem is no longer valid. However, at fixed detuning the final transition probability depends periodically on the field amplitude and approximately periodic ***returns*** to the initial state are observed. (Therefore, it is likely that a modified form of the π-theorem holds in this nonlinear case as well.) This is demonstrated in Fig.3.2. Furthermore, examining the graphs in this figure, we see that the oscillation shape, amplitude and frequency are changed depending on the detuning. Clearly, the oscillation nature is close to that of the nonlinear Rabi-solution (see, e.g., [70]). Finally, we note that in the nonlinear case the transition probability decreases considerably faster as the detuning is increasing, and becomes negligible already at $\delta_0 \approx 1$.

Our study is based on two different ***exact*** nonlinear equations written for the molecular state probability $p = |a_2|^2$: a Volterra integral equation and a third-order differential equation. Being

equivalent in general, these two equations are efficient if applied to opposite limits: the first equation is useful at weak nonlinearity while the second one will be applied in the strong nonlinearity limit.



a) b)

Fig. 3.1. Final transition probability as a function of the peak value of the coupling U_0 and the detuning parameter δ_0 : a) nonlinear problem; b) linear problem.

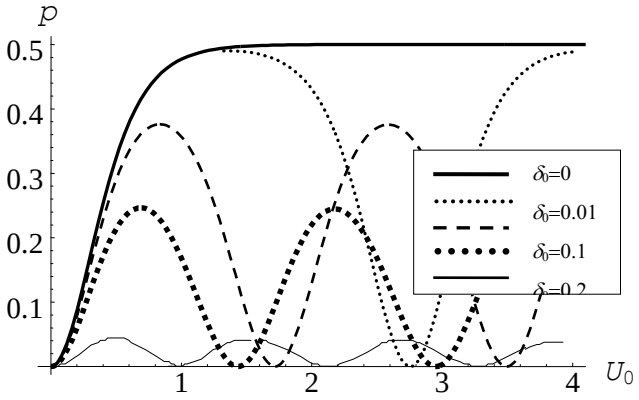


Fig. 3.2. Nonlinear Rosen-Zener model. At fixed non-zero detuning the transition probability depends periodically on the field amplitude. The oscillation shape, amplitude and frequency undergo changes analogous to those observed for the nonlinear Rabi-problem.

We start from the weak nonlinearity limit, corresponding to the small values of the peak coupling U_0 $(U_0 \leq 1)$, that is a commonly encountered situation under current experimental conditions. Using the nonlinear Volterra integral equation, we show that, applying Picard's successive approximations for this limit, an accurate approximate solution in terms of the solution to the linear quantum-optics problem can be constructed. We determine the final molecule conversion probability and show that, because of the inherent properties of the Rosen-Zener model under consideration, the strict limit of weak nonlinearity (when no essential deviations from the linear evolution are observed) corresponds to smaller field intensities as compared with the Landau-Zener case. We discuss the specific reasons for such a behavior and construct an approximation that is valid also for the intermediate regime of moderate coupling strength.

Further, we pass to the strong nonlinearity limit corresponding to large values of the peak coupling U_0 $(U_0 > 1)$ and show that the system reveals two different time-evolution pictures depending on the detuning $2\delta_0$ of the associating field. At large detuning $(\delta_0 \geq 1)$ the molecule formation process occurs almost non-oscillatory in time. In contrast to the large detuning regime of the strong nonlinearity limit, at small detuning $(\delta_0 < 1)$ the evolution of the system displays strongly pronounced large-amplitude Rabi-type oscillations. The third-order differential equation in each case is reduced to a limit equation of a lower order. In the case of large detuning this equation is of the first order, while in the small detuning case it is an effective Rabi-equation of the second order. Using these limit equations, we derive two accurate approximate formulas for the molecular state probability applicable to the two mentioned regimes. The results show that in the large detuning regime the system always returns to the initial all-atomic state independently of the field intensity, hence, the final molecule formation efficiency in this case is nearly zero. In the small detuning regime, because of large-amplitude oscillations, the peak Rabi frequency (or, equivalently, the Rosen-Zener pulse area) should be adjusted in order to achieve efficient conversion, if the photoassociation terminology is used.

3.3. Weak coupling limit for the Rosen-Zener model

Consider the transformation of the independent variable $dz/dt = \mathrm{sech}(t)$ [see Eq. (1.14)] that changes system (3.1) to the following ***constant-amplitude*** form

$$i\frac{da_1(z)}{dz} = U_0 e^{-i\delta(z)}\overline{a}_1(z)\cdot a_2(z), \quad i\frac{da_2(z)}{dz} = \frac{U_0}{2}e^{+i\delta(z)}a_1(z)\cdot a_1(z), \tag{3.6}$$

where $z = \pi/2 + 2\arctan\left(\tanh(t/2)\right)$ ($z \in [0,\pi]$) and

$$\delta(z) = 4\delta_0 \operatorname{arctanh}\left(\tan\left(\frac{z}{2}-\frac{\pi}{4}\right)\right) \Rightarrow \delta_z(z) = \frac{2\delta_0}{\sin(z)}. \tag{3.7}$$

To treat the weak coupling limit of such problems with arbitrary detuning and constant coupling U_0, we have earlier developed an adapted mathematical approach based on the reduction of system (3.6) to the following nonlinear Volterra integral equation [105] for the molecular state probability $p(z) = |a_2(z)|^2$ [59]:

$$p(z) = \frac{\lambda}{4}f(z) - 4\lambda\int_0^z K(z,\eta)\left(p(\eta) - \frac{3}{2}p^2(\eta)\right)d\eta, \tag{3.8}$$

where $\lambda = U_0^2$ and the kernel, $K(z,\eta)$, and the forcing function, $f(z)$, are given as

$$K(z,\eta) = \left(C_\delta(z) - C_\delta(\eta)\right)\cos(\delta(\eta)) + \left(S_\delta(z) - S_\delta(\eta)\right)\sin(\delta(\eta)), \tag{3.9}$$

$$f(z) = C_\delta^2(z) + S_\delta^2(z), \quad C_\delta(z) = \int_0^z \cos(\delta(\xi))d\xi, \quad S_\delta(z) = \int_0^z \sin(\delta(\xi))d\xi. \tag{3.10}$$

Note that if the term proportional to p^2 is discarded, Eq. (3.8) turns into an exact equation equivalent to the linear system (3.3). In the case of ***weak coupling*** ($U_0^2 < 1$), a series solution of the problem is constructed by means of Picard's successive approximations [105] to equation (3.8). Furthermore, noting that the first three terms of this expansion and that of the corresponding linear integral equation coincide, it is possible to construct a faster converging series using the substitution $p = p_L + u$ where $p_L = |a_{2L}|^2$. For the function $u(z)$ we get a new integral equation of the Hammerstein type [105]:

$$u(z)=6\lambda\int_0^z K(z,\eta)\,p_L^2\,d\eta-4\lambda\int_0^z K(z,\eta)\left[(1-3p_L)u-\frac{3}{2}u^2\right]d\eta\,. \tag{3.11}$$

It is not difficult to see that it is sufficient to take only the first term on the right-hand side of Eq. (3.11). Thereby, the approximate solution of the nonlinear system (3.6) is expressed via the solution of the linear system (3.3):

$$p(z)=p_L(z)+6\lambda\int_0^z K(z,\eta)\,p_L^2\,d\eta\,. \tag{3.12}$$

This formula is checked to be pretty accurate for an appropriate variation range of $\lambda=U_0^2$. Now, let us calculate the integral of Eq. (3.12). Note that, to achieve a preset accuracy in powers of λ, the approximation of p_L by a finite number of terms of its Picard's series can be used. Restricting to the accuracy up to $O(\lambda^4)$ (the first order of the expansion), one may put $p_L(z)\approx\lambda f(z)/4$ [see Eq. (3.8)]. To improve this approximation, a correction factor can be introduced, thereby applying an approximation of the form $p_L(z)\cong A\,f(z)$. Furthermore, the functions C_δ and S_δ are explicitly determined by considering an auxiliary integral:

$$F(z)\equiv C_\delta+iS_\delta=\int e^{i\delta(\xi)}d\xi=B_y(1/2+i\delta_0,1/2-i\delta_0)\,,\quad y=\sin^2(z/2)\,, \tag{3.13}$$

where B_y is an incomplete Beta function [85]. Hence,

$$C_\delta=\mathrm{Re}[B_y(1/2+i\delta_0,1/2-i\delta_0)],\quad S_\delta=\mathrm{Im}[B_y(1/2+i\delta_0,1/2-i\delta_0)]. \tag{3.14}$$

These functions are shown in Fig.3.3.

Then, the correction term u at $z=\pi$ $(t=+\infty)$ is readily calculated. The result reads $u(\pi)\approx 6\lambda A^2C_\infty^3$, where $C_\infty=\pi\,\mathrm{sech}(\pi\delta_0)$. Hence, for A chosen as $A=\lambda/4$, the solution of nonlinear problem (3.1), accurate to $O(\lambda^4)$, is given by the following formula:

$$p_{+\infty}\equiv p(z=\pi)\approx\frac{P_{RZ}}{4}+\frac{3\lambda^3}{8}C_\infty^3\,. \tag{3.15}$$

This formula works quite well up to $U_0\approx 0.3$ $(\lambda\approx 0.1)$. As for $U_0>0.3$, significant deviations of the prediction (3.15) from the numerical result is observed. To understand the reason for this deviation to occur, we investigate the structure of formula (3.15). Since $P_{RZ}\le 1$ and C_∞

does not depend on U_0, $p_{+\infty}$ defined by formula (3.15) grows infinitely as U_0 increases, exceeding, already at $U_0 \approx 0.53$ (for $\delta_0 \approx 0$), the maximum value 1/2 allowed by the normalization.

However, the derived formula can be modified to essentially improve the result. This can be done by noting that p_L at small non-zero λ is much better approximated by a formula of the form $p_L \approx (P_{RZ}/4)(f[z(t)]/f[z(t\to\infty)] = P_{RZ} f/(4C_\infty^2)$. This corresponds to the choice $A = P_{LZ}/(4C_\infty^2)$ that leads to a formula of significantly better structure:

$$p_{+\infty} \approx \frac{P_{RZ}}{4} + \frac{6\lambda}{C_\infty}\left(\frac{P_{RZ}}{4}\right)^2. \tag{3.16}$$

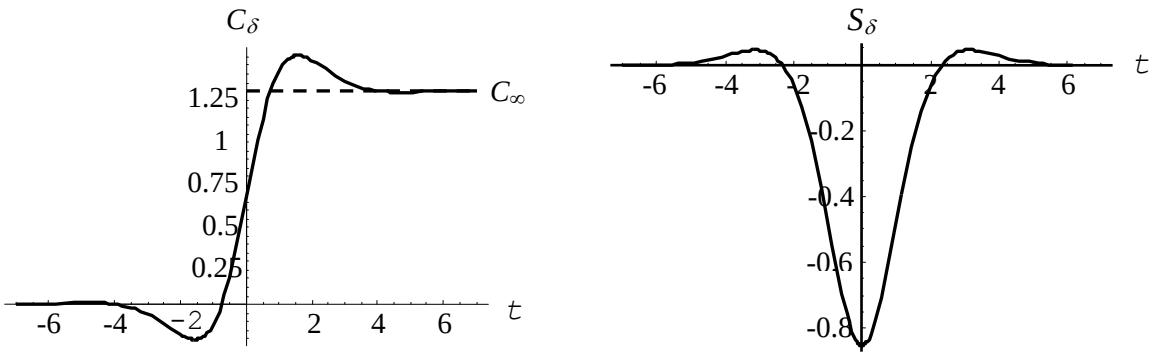


Fig. 3.3. The functions $C_\delta(t)$ and $S_\delta(t)$, $\delta_0 = 0.5$.

Indeed, unlike formula (3.15), the transition probability $p_{+\infty}$ defined by the given formula remains less than 1/2 under $\lambda \le 1$, i.e., in the whole range where it makes sense to confine ourselves only to the first term of Picard's series expansion for u. However, the obtained formula gives a numerically satisfactory approximation only up to $\lambda \le 0.15$. Reasons for the latter additional restriction deserve special discussion and we will return to this a little later. But before, we will show that there is a non-trivial way to improve this result even more. Note first that, with up to a constant factor, $F(z) = \lim_{\lambda\to 0}(e^{i\pi/2} a_{2RZ}/\sqrt{\lambda})$. This observation suggests replacing the functions C_δ

and S_δ in (3.11) by $-\mathrm{Im}(a_{2RZ})/\sqrt{\lambda}$ and $\mathrm{Re}(a_{2RZ})/\sqrt{\lambda}$, respectively, $\cos(\delta(z))$ and $\sin(\delta(z))$ by the corresponding derivatives. As is easily seen, this is nearly equivalent to the substitution $C_\infty = \sqrt{P_{RZ}/\lambda}$ in formula (3.16). As a result, we have

$$p_{+\infty} \approx \frac{P_{RZ}}{4} + 3\left(\lambda \frac{P_{RZ}}{4}\right)^{3/2}. \tag{3.17}$$

More accurate calculations taking into account the properties of a_{2RZ} show that

$$p_{+\infty} \approx \frac{P_{RZ}}{4} + 3(1+2\lambda)\left(\lambda \frac{P_{RZ}}{4}\right)^{3/2}. \tag{3.18}$$

The derived formula gives a very good approximation up to $\lambda \le 0.25$ ($U_0 < 0.5$), the relative error being of the order of fractions of a percent, see Fig. 3.4.

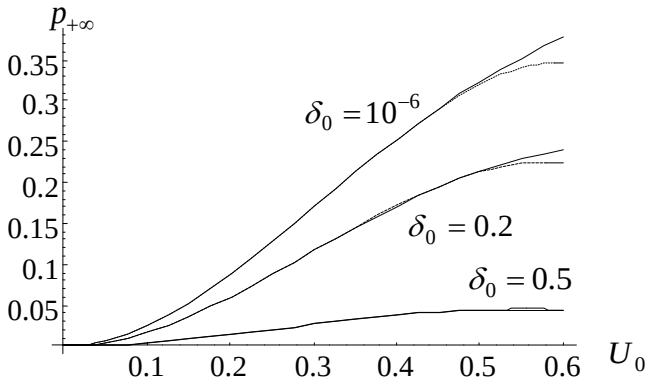


Fig. 3.4. Final probability of the transition to the molecular state as a function of U_0: solid line - numerical result, dashed line - Eq. (3.18).

Let us now discuss the applicability range for the obtained formulas and the origin of the restriction imposed on λ. The calculations presented above rest upon the presumption of smallness of Picard's successive approximations for u as compared to the first term of Picard's series. As follows from Eq. (3.11), the second Picard term has the form

$$u_1 = -4\lambda \int_0^z K(z,\eta)\left[(1-3p_L)u_0 - \frac{3}{2}u_0^2\right]d\eta . \qquad (3.19)$$

As it can be easily seen, whenever at $\lambda << 1$, the condition $u_0 \sim \lambda$ [$p_L = O(\lambda)$] is fulfilled, and the assumption $u_1 << u_0$ will be the case. Of course, this takes place under $\lambda \le 0.1$ and, as was mentioned above, it is this fact that defines the applicability range of formulas (3.15) and (3.16). The situation, however, is drastically changed already at $\lambda \approx 0.2 - 0.3$. First, one should no longer consider λ as being much less than unity, and, second, what is more important, the linear transition probability p_L is not any longer much less than unity. The latter is already seen from Rosen-Zener formula (3.5): the final probability of the linear transition $p_L(t = +\infty) = P_{RZ} / 4$ at $\delta_0 \approx 0$ is about 0.25. Thus, the nonlinear Rosen-Zener problem can be treated as a weakly nonlinear one, when the dimensionless amplitude obeys the condition $U_0 \le 0.3$ ($\lambda \le 0.1$). Recall that in the weakly nonlinear cases, a zero-order approximation can be chosen as a solution of the corresponding linear problem. Note that this conclusion is not ***a priori*** evident. For instance, in the case of the Landau-Zener model, the weak nonlinearity limit corresponds to the values of $\lambda < 1$ [59-60,62]. Thus, fields with $U_0 > 0.3$ ($\lambda > 0.1$) belong to the intermediate type, between the strong nonlinear and weak nonlinear ones. It is for this reason that modifications (3.17) and (3.18) applicable up to $U_0 < 0.5$ ($\lambda \le 0.25$) are of substantial importance. One might hope that the latter formula will be applicable for a little larger λ if $\delta_0 \ge \lambda$, since then, due to the presence of the factor $[\mathrm{sech}(\pi\delta_0)]^2$ in formula (3.5), $p_L(t = +\infty) << 1$. To some extent, this assumption is valid. However in this parameter variation domain the relative error is significantly greater; already at $U_0 \approx 0.7$ it is of the order of several percents. The reason for this lies in the fact that in the vicinity of the point $t = 0$ the linear solution $p_{2RZ}(t)$ [see (3.4)] reaches values of the order of unity, irrespective of value of δ_0 (at moderate and large values of δ_0, there is a pronounced maximum). The mentioned property can be demonstrated by studying, e.g., the behavior of the linear solution at $U_0 = 1$. In this case, the hypergeometric series in solution (3.4) are terminated, which results in an elementary solution,

$p_{2RZ} = (\mathrm{sech}(t))^2/(1+4\delta_0^2)$. As it can be seen, at moderate $\delta_0 \approx 0.5$ we have $p_{2RZ}(0) \approx 0.5$. Thus, the general conclusion is that under $U_0 > 0.5-0.6$, one may not confine himself only to the first term of Picard's series for u since the successive terms play an important role. Therefore, the given regime should be viewed as a strongly nonlinear one.

3.4. Strong coupling limit for the Rosen-Zener model

In the strong coupling limit of high field intensities, $U_0^2 >> 1$, the nonlinearity is well pronounced. In this case, however, the Volterra equation (3.8) is of little help, because the successive Picard's approximation terms become larger and larger. Instead, we use the exact nonlinear differential equation of third order (1.12). For the Rosen-Zener model under consideration the frequency detuning is constant, and the equation is considerably simplified:

$$p_{ttt} + 2\tanh(t)\,p_{tt} + [(4\delta_0^2+1) + 4U_0^2\,\mathrm{sech}^2(t)(1-3p)]p_t + \frac{U_0^2}{2}\mathrm{sech}^2(t)\tanh(t)(1-8p+12p^2) = 0. \quad (3.20)$$

To construct an approximate solution of this equation, we compare the magnitudes of involved terms keeping in mind that we suppose $U_0^2 >> 1$. It can be then immediately seen that there are two basic possibilities depending on the magnitude of the detuning, $\delta_0 << 1$ and $\delta_0 >> 1$. This conclusion is also guessed from Fig.3.1. Indeed, as has already been noted above, at small detuning, the final conversion probability (i.e., the molecular state probability at $t \to +\infty$) reveals large amplitude oscillatory dependence on the peak coupling U_0. In the meanwhile, the probability rapidly decreases as the detuning is increased; the molecular state probability becomes practically negligible at $\delta_0 \approx 1$. These observations are further confirmed by examining the temporal evolution of the transition probability (Fig.3.5). We see that at $\delta_0 \le 0.5$ strong temporal oscillations of the atom-molecule populations occur (see the detailed picture in Fig.3.6), while at larger detuning the oscillations are highly suppressed (Fig.3.7); they can be neglected already at $\delta_0 \approx 2$.

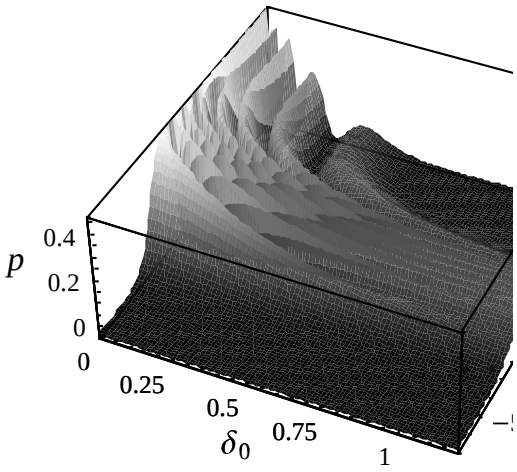


Fig. 3.5. Molecule formation probability versus time and detuning ($U_0 = 10$).

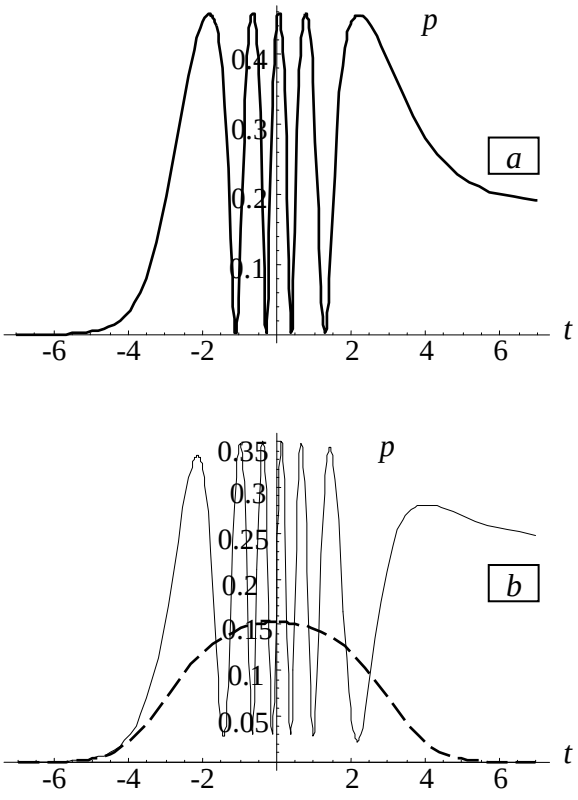


Fig. 3.6. Temporal evolution of the molecular state probability at small detuning: a) $\delta_0 = 0.05$, b) $\delta_0 = 0.2$ ($U_0 = 10$).

Solid line - numerical solution, dashed line - limit solution (3.27).

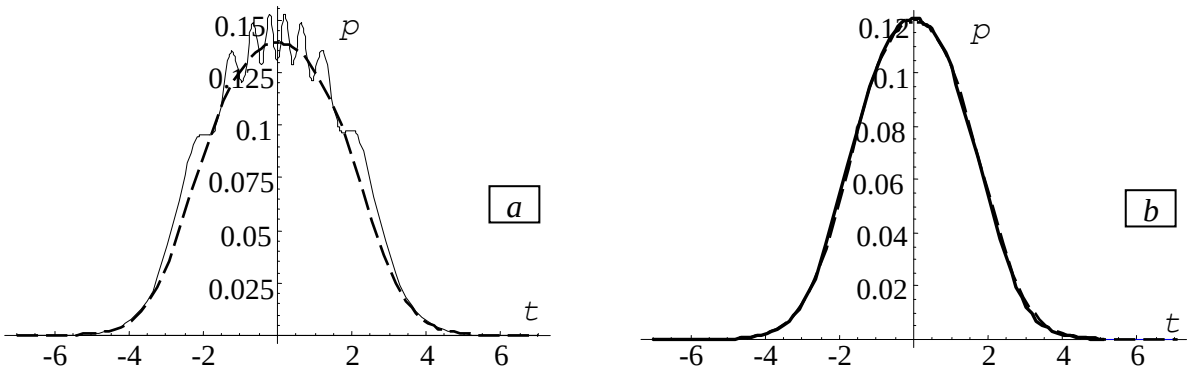


Fig. 3.7. Molecular state probability vs. time at large detuning: a) $\delta_0 = 1$, b) $\delta_0 = 2$ $(U_0 = 10)$.

Solid line - numerical solution, dashed line - limit solution (3.27).

Large detuning case: $\delta_0 >> 1$.

Since both U_0 and δ_0 are large parameters, the leading terms in Eq. (3.20) are the last two. By retaining only these terms and denoting the constructed solution by p_0, we obtain the following ***limit*** equation:

$$[(4\delta_0^2 + 1)\cosh^2(t) + 4U_0^2(1 - 3p_0)]p_{0t} + \frac{U_0^2}{2}\tanh(t)(1 - 8p_0 + 12p_0^2) = 0. \qquad (3.21)$$

This equation is solved by a change of the independent variable followed by interchange of the roles of the independent and dependent variables. Indeed, the transformation

$$\frac{d}{dt} = \alpha \tanh(t) \cdot s\frac{d}{ds} \quad \Leftrightarrow \quad \sqrt{4\delta_0^2 + 1}\cosh(t) = C_0 s^{1/\alpha} \qquad (3.22)$$

changes Eq. (3.21) to the form

$$s\alpha\frac{dp_0}{ds}[C_0^2 s^{2/\alpha} + 4U_0^2(1 - 3p_0)] + \frac{U_0^2}{2}(1 - 8p_0 + 12p_0^2) = 0. \qquad (3.23)$$

Choosing now $\alpha = -2$ and $C_0 = U_0$ we arrive at an equation

$$[1 + 4s(1 - 3p_0)]\frac{dp_0}{ds} - \frac{1}{4}(1 - 8p_0 + 12p_0^2) = 0, \qquad (3.24)$$

that can further be solved by considering s as a dependent variable since in this case the differential

equation (3.24) becomes linear with respect to s. The result reads

$$\frac{U_0^2}{(4\delta_0^2+1)\cosh^2(t)} = \frac{C_1 + p_0(p_0-1/2)^2}{9(p_0-1/2)^2(p_0-1/6)^2}. \tag{3.25}$$

For the initial condition $p_0(-\infty)=0$ considered here, we obtain $C_1=0$, hence the polynomial equation (3.25) is considerably simplified reducing to a quadratic equation for p_0:

$$\frac{U_0^2}{(4\delta_0^2+1)\cosh^2(t)} = \frac{p_0}{9(p_0-1/6)^2}, \tag{3.26}$$

whereby we arrive at the following principal result:

$$p_0(t) = \frac{1}{6} + \frac{4\delta_0^2+1}{18U_0^2}\cosh(t)\left(\cosh(t) - \sqrt{\cosh^2(t) + \frac{6U_0^2}{4\delta_0^2+1}}\right). \tag{3.27}$$

This is a highly accurate approximation. For $U_0 > 5$ and $\delta_0 > 2$ the probability calculated by this formula and the numerical result are practically indistinguishable (Fig.3.7b). Besides, it allows one to linearize the exact equation for the molecular state probability (3.20) (by substitution $p = p_0 + u$) thereby covering the whole range $\{U_0 \geq 1, \delta_0 \geq 1\}$. Two immediate conclusions follow from this formula. First, since $p_0(t \to +\infty) \to 0$, the final molecular state probability at strong coupling is nearly zero if the detuning is large, i.e., the system subjected to a large-detuning Rosen-Zener pulse returns to its initial all-atomic state. Second, $p_0(t)$ is a bell-shaped non-oscillatory function of time and its maximum is achieved at $t=0$:

$$p_0^{\max} = \frac{1}{6} + \frac{4\delta_0^2+1}{18U_0^2}\left(1 - \sqrt{1 + \frac{6U_0^2}{4\delta_0^2+1}}\right). \tag{3.28}$$

For $6U_0^2/(4\delta_0^2+1) >> 1$ this is close to $1/6$. However, $p_0^{\max}$ is always less than $1/6$. Hence, at large detuning a Rosen-Zener pulse is not able to associate more than one third of atoms ($p_{\text{molecule}} = 1/6$ corresponds to $1/3$ of atoms). This limitation for the conversion efficiency has been noted to be the case in the adiabatic limit (which is equivalent to the discussed case of high field intensities and large detuning) for other non-crossing models too (see, e.g., [106]).

Finally, it is of interest to compare the above nonlinear behavior under strong coupling and

large detuning conditions with the linear Rosen-Zener counterpart. In the linear case, instead of Eq. (3.21), we have the following linear limit equation (here, the normalization $I_L = 1/4$ is adopted)

$$[(4\delta_0^2 + 1)\cosh^2(t) + 4U_0^2]p_{0Lt} + \frac{U_0^2}{2}\tanh(t)(1 - 8p_{0L}) = 0. \qquad (3.29)$$

The solution to this equation reads

$$p_{0L}(t) = \frac{1}{8}\left(1 - 1/\sqrt{1 + \frac{4U_0^2}{4\delta_0^2 + 1}\mathrm{sech}^2(t)}\right). \qquad (3.30)$$

This formula displays the same qualitative features as the nonlinear solution, Eq. (3.27); i.e., in the linear case again a return to the initial state is observed if the applied Rosen-Zener pulse is of a large detuning, and there is a maximum possible transition probability achieved at $t = 0$. This time, this probability is $1/8$ (i.e., $1/2$ for the normalization $I_L = 1$).

Small detuning case: $\delta_0 << 1$.

To treat this regime we first rewrite Eq. (3.20) in the following factorized form

$$\left(\frac{d}{dt} + \tanh(t)\right)\left[p_{tt} + \tanh(t)p_t - \frac{U_0^2\mathrm{sech}^2(t)}{2}(1 - 8p + 12p^2)\right] + 4\delta_0^2 p_t = 0. \qquad (3.31)$$

The arguments now are as follows. Though the detuning is supposed to be small, one cannot completely neglect the term $4\delta_0^2 p_t$. Indeed, putting $\delta_0 = 0$ results in a monotonically increasing solution:

$$p = \frac{1}{2}\tanh^2\left(\frac{U_0 z}{\sqrt{2}}\right), \qquad (3.32)$$

where

$$z = \pi/2 + 2\arctan\left(\tanh(t/2)\right), \quad z \in [0, \pi]. \qquad (3.33)$$

However, the numerical simulations reveal that for any non-zero small δ_0 the solution is oscillatory (this is well seen from Figs. 3.5 and 3.6). Hence, in a sense, the exact resonance case $\delta_0 = 0$ is degenerate. This degeneracy can be resolved by introducing a small perturbation when constructing the initial approximation. Intuitively, in order to get an approximation that would be close to the

real solution as much as possible, one should try to introduce a perturbation as small as possible. On the other hand, one should choose a form of this perturbation that allows construction of an analytic solution. From this point of view, the form of Eq. (3.31) suggests introducing the perturbation inside the square brackets since then the truncated equation, that remains after disregarding the term $4\delta_0^2 p_t$, can be immediately integrated once. One may further try to choose a specific form of the perturbation that allows the complete integration of the reduced equation. The listed requirements are satisfied by introducing a trial term of the form $A\cdot\mathrm{sech}^2(t)$ with some constant A (depending, in general, on δ_0 and U_0) in the square brackets of Eq. (3.31). We suppose that A is small (say, of the order of δ_0^2 as δ_0 goes to zero). The value of this constant is then defined by requiring the resulting approximation to be as close to the exact solution as possible with the chosen form of the introduced perturbation.

To proceed with the outlined approach, we rewrite Eq. (3.31) in the following equivalent form:

$$\left(\frac{d}{dt}+\tanh(t)\right)\left[p_{tt}+\tanh(t)\,p_t-\frac{U_0^2\mathrm{sech}^2(t)}{2}\left(1-8p+12p^2-\frac{2A}{U_0^2}\right)-A\cdot\mathrm{sech}^2(t)\right]+4\delta_0^2 p_t=0\,. \quad (3.34)$$

Now, supposing $A<<1$, we make an attempt to construct a valid approximation via dropping the last term of this equation and the last term in the brackets, and integrating the remaining equation once. Taking into account the initial conditions applied here, we arrive at the following second order equation

$$p_{tt}+\tanh(t)\,p_t-\frac{U_0^2\mathrm{sech}^2(t)}{2}\left(1-8p+12p^2-\frac{2A}{U_0^2}\right)=0\,, \quad (3.35)$$

which is easily turned into another one with constant parameters by the change of the independent variable given by Eq. (3.33):

$$p_{zz}-\frac{U_0^2}{2}\left(1-8p+12p^2-\frac{2A}{U_0^2}\right)=0\,. \quad (3.36)$$

Multiplying this equation by p_z and integrating once, we obtain an equation that is immediately identified as an equation for an effective Rabi problem with for some field parameters – an effective

field amplitude and an effective detuning (see, e.g., [70]). Correspondingly, the zero-order approximation is written in terms of the Jacobi elliptic sine function [85]:

$$p_0 = p_1 \,\mathrm{sn}^2[\sqrt{p_2}U_0 z; m], \tag{3.37}$$

where the parameters p_1, p_2 and m are defined as

$$p_{1,2} = \frac{1}{2} \mp \sqrt{\frac{A}{2U_0^2}}, \quad m = \frac{p_1}{p_2}. \tag{3.38}$$

The period of the oscillations is given as

$$T(m) = \frac{\pi}{\sqrt{p_2}U_0} \,{}_2F_1(1/2, 1/2; 1; m). \tag{3.39}$$

Comparing this solution with the exact resonant solution we first note that the solution given by Eq. (3.32) is also written in terms of the Jacobi sn -function if one takes $m = 1$ ($\tanh(z) = \mathrm{sn}[z;1]$). Furthermore we note that Eq. (3.37) is reduced to Eq. (3.32) for $A = 0$. These observations clearly suggest that the performed procedure, the introduction of an A-term, should be equivalent to changing the parameters of the resonant solution (3.32) written in the Jacobi sn -function form. Hence, the approach we applied can be viewed as a modification of the well-known method of strained parameters [107].

The obtained solution (3.37) presents an oscillatory function whose behavior displays all the qualitative features of the exact solution. Moreover, a few numerical simulations shortly reveal that for any small enough δ_0 one may always find such a value of the parameter A for which this solution is practically indistinguishable from the numerical solution. To derive an analytic expression for this value of A, we examine the neglected terms with p defined by this solution:

$$R = \left(\frac{d}{dt} + \tanh(t)\right)\left[-A \cdot \mathrm{sech}^2(t)\right] + 4\delta_0^2 p_{0t} = \mathrm{sech}^2(t)\left[A \cdot \tanh(t) + \frac{4\delta_0^2 p_{0t}}{\mathrm{sech}^2(t)}\right]. \tag{3.40}$$

Here, the idea is to choose the parameter A so that this remainder becomes as small as possible. Strictly speaking, one should look for such a value of A for which the ***influence*** of the neglected terms is minimal. To address the latter question mathematically, one should examine the behavior

of the next approximation term constructed by using p_0 of Eq. (3.37) as zero-order approximation. However, it is difficult to proceed in this way because the analytic expression for the next approximation term is not known. For this reason, we look for indirect criteria. A possibility opens up when examining the behavior of the function $4\delta_0^2 p_{0t}/\mathrm{sech}^2(t)$. This is a step-like function that exponentially slowly decreases from a relatively large value $\sim \delta_0^2 U_0^2$ at $t=-\infty$, then sharply goes to zero at some negative time and remains negligible in a large vicinity of the point $t=0$ where the field intensity is the highest. Noting now that a rather similar qualitative behavior is displayed by the term $A\cdot\tanh(t)$, we see that the remainder R will be essentially suppressed for a large time interval, covering the effective interaction region, i.e., the vicinity of the point $t=0$, if we require the term in the square brackets in Eq. (3.40) be vanishing at the beginning of the interaction, i.e. at $t\to-\infty$. Then, since

$$4\delta_0^2 p_{0t}\Big|_{t\to-\infty} \sim 8\delta_0^2 p_1 p_2 U_0^2 \mathrm{sech}^2(t)\,, \tag{3.41}$$

we immediately get

$$A=\frac{2\delta_0^2 U_0^2}{1+4\delta_0^2}\,. \tag{3.42}$$

This is already a good approximation showing the order of the parameter A: $A\sim\delta_0^2 U_0^2$. Indeed, the comparison with the numerical solution shows that the approximate solution (3.37) with this value of A describes well the process for many oscillations (see Fig. 3.8a).

Nevertheless, it can be seen that the deviation from the exact solution slowly increases during time and eventually becomes rather noticable at the end of the interaction process. Fortunately, the result can be essentially improved by trying a perturbation with two fitting parameters, namely a perturbation of the form $(A+Bp)\mathrm{sech}^2(t)$. Since the parameters p_1 and p_2 of Eq. (3.37) are then changed independently [compare with Eq. (3.38)], it is understood that this is more elaborate realization of the strained parameters method. Interestingly, it turns out that for high field intensities the result is effectively equivalent to the single-parameter A-perturbation approach with a slightly modified value of A as compared with that of Eq. (3.42):

$$A = \frac{\sqrt{2}\,\delta_0^2 U_0^2}{1 + 4\delta_0^2}. \tag{3.43}$$

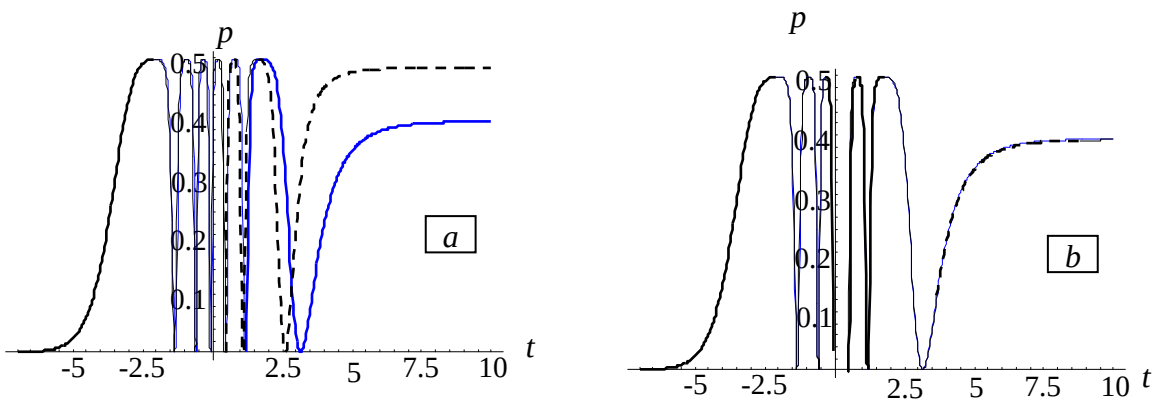


Fig. 3.8. Comparison of the approximation (3.37) (dashed line) with the numerical result (solid line) for $\delta_0 = 0.001$, $U_0 = 23.5$: a) A is given by Eq. (3.42) and b) A is given by Eq. (3.43).

The parameters p_1 and p_2 are finally given by simple formulas:

$$p_{1,2} \approx \frac{1}{2} \mp \frac{\delta_0}{\sqrt{\sqrt{2}}}. \tag{3.44}$$

This is a really good approximation. The Jacobi sine solution (3.37) with these parameters produces graphs practically indistinguishable from the numerical solution as far as δ_0 is small enough and $U_0 >> 1$ (Fig. 3.8b). If needed, one may further improve the results by linearization of the problem using this solution as an initial approximation.

Thus, we have seen that at small detuning the Rosen-Zener pulse causes large amplitude oscillations during the time evolution of the coupled atom-molecule ensemble which are described by the Jacobi sn -function. According to the properties of this function, the shape of the oscillations is defined by the parameter $m = p_1 / p_2$. Hence, we conclude from Eq. (3.44) that at small detuning the time shape of the atom-molecule oscillations is in first approximation defined by the detuning only. On the other hand, the number of the oscillations is mainly defined by the value of

$\int_{-\infty}^{+\infty} U_0 \,\mathrm{sech}(t)\,dt$ i.e., by the pulse area.

It is interesting to analyze the construction of the approximation for the small detuning regime of the Rosen-Zener model (3.37) from a different point of view. We have seen that the constant A, which determines both the qualitative and quantitative properties of the solution, has eventually been calculated by examining the behavior of the system at the beginning of the interaction. This observation leads to a notable speculation. Indeed, it seems rather unexpected that the vicinity of the point $t=-\infty$, where the amplitude of the field is exponentially small, plays such an important role, a much more important role than that of the vicinity of point $t=0$, where the field amplitude is maximal. This clearly indicates that the time point $t=-\infty$ actually presents a hidden singularity. The origin and the nature of this singularity are understood by rewriting Eq. (3.31) for the variable z [see Eq. (1.17)]:

$$\left(\frac{d}{dz}-\frac{\delta_{zz}^*}{\delta_z^*}\right)\left(p_{zz}-\frac{U_0^2}{2}\left(1-8p+12p^2\right)\right)+\delta_z^{*2}\,p_z=0, \tag{3.45}$$

where $z=\int_{-\infty}^{t}\mathrm{sech}(t)\,dt$ and the effective detuning δ_z^* is given as

$$\delta_z^*(z)=2\delta_0/\sin(z) \tag{3.46}$$

so that

$$\frac{\delta_{zz}^*}{\delta_z^*}=-\frac{\cos(z)}{\sin(z)}. \tag{3.47}$$

It is then immediately seen from the last relation that the point $z=0$ corresponding to $t=-\infty$ is indeed singular because the operator δ_{zz}^*/δ_z^* diverges at this point. Notably, this divergence does not depend on the parameter δ_0 which is the only characteristic of the detuning $\delta_t(t)$. The divergence is of course caused by the transformation from t to z, hence, exclusively by the form of the time evolution of the field amplitude, $U(t)$, more precisely, by the field rise rate. Naturally, this singularity can be viewed as an effective resonance touching (but not crossing) because the divergence of the operator δ_{zz}^*/δ_z^* at the crossing point is the main characteristic of the (constant-

amplitude) crossing models (e.g., for the Landau-Zener case we have $\delta_{tt}/\delta_t = 1/t \to \infty$ at $t = 0$). Strictly speaking, there is another singular point, $z = \pi$, however, this corresponds to $t = +\infty$, where the interaction process ends. Since the interaction exponentially vanishes when we approach this point and there is no further time for this point to display its influence, the role of this point is in practice negligible. Note finally that the left-hand side of Eq. (3.25) which describes the other evolution regime corresponding to the large detuning case can be written as $\approx 4U_0^2/\delta_z^{*2}$. Since this term vanishes at $z = 0$, thus leading to a zero integration constant C_1, we conclude that in this regime too the behavior of the system is essentially determined by the mentioned hidden singularity.

3.5. Two strongly nonlinear distinct scenarios of cold molecule formation

In the present section we analyze the strong nonlinearity limit of the coherent molecule formation, assuming an arbitrary external field configuration. Two distinct strongly nonlinear scenarios of the system's evolution are shown to be available – almost non-oscillatory and strongly oscillatory regimes [73]. By generalizing the mathematical approach used for the treatment of the nonlinear Rosen-Zener problem (see Sections 3.3-3.4), we construct simple analytical approximations for both interaction regimes.

First, to get a better intuitive understanding of the problem at hand, we examine the exact equation for the molecular state probability (1.12). The nonlinearity is determined by the current value of the transition probability p. Hence, one may expect that if p remains small enough (note that, anyway, $p \le 1/2$) the role of the nonlinearity will be rather restricted. In this case, neglecting the nonlinear terms in equation (1.15), we get the linear equation, satisfied by the function $p_L = |a_{2L}|^2$ [see Eq. (1.18)]. Studying now the solution of the linear two-state problem $p_L(t)$ we see that, if the dimensionless peak Rabi frequency U_0 is small enough ($U_0 << 1$), or if it is much smaller compared to the sweep rate through the resonance ($U_0 << \delta_0$), then the function p_L does not attain large values. From this, one can infer that in these cases the transition probability defined

by the nonlinear two-state problem is close to that defined by the linear two-state problem.

Now, let us define the coupling and detuning parameter variation range that corresponds to the strong nonlinearity limit. To this end, we again address the exact equation for the molecular state probability (1.15). It can easily be seen that the nonlinear terms in Eq. (1.15) are proportional to the peak coupling squared: U_0^2. Hence, the strong nonlinearity regime corresponds to high field intensities, if the photoassociation terminology is used, and we thus suppose that U_0^2 is a large parameter. Note now that the function δ_z^{*2} may also adopt large values (e.g., in the Landau-Zener model $\delta_z^{*2} \sim z^2 = t^2$ diverges at $t \to \pm\infty$). Furthermore, note that the nonlinearity is merely determined by the current value of $p(t)$. Hence, at strong coupling the probability $p(t)$ should reach large values during the evolution of the system (of course, relatively large, since the normalization constraint p cannot exceed $1/2$). Having these observations in mind, we suppose that the leading terms in the exact equation for the molecular state probability (1.15) are the last two so that we neglect, for the moment, the first two terms thus arriving at the following ***limit*** nonlinear equation of the first order:

$$\left[\delta_z^{*2} + 4U_0^2(1-3p_0)\right]p_{0z} + \frac{U_0^2}{2}\frac{\delta_{zz}^*}{\delta_z^*}\left(1-8p_0+12{p_0}^2\right) = 0\,. \qquad (3.48)$$

This is a productive equation. In spite of the singular way it was derived (the higher-order derivatives have been disregarded) the equation works well due to its rich structure that incorporates all the principal features of the exact equation (1.15), i.e., the form of the nonlinearity, the interplay between the nonlinearity and the detuning modulation, etc.

This equation has two trivial constant solutions $p_0 = 1/2$ and $p_0 = 1/6$ that are also stationary solutions to the exact equation (1.15). These solutions play, as we will see below, a pronounced role in the determination of the asymptotes of the approximate solution. Furthermore, in spite of the complexity of the limit equation (3.48), its ***general*** solution can be found for ***arbitrary*** effective detuning δ_z^*. To this end, we apply such a transformation of the independent variable $z \to s$ that reduces the nonlinear limit equation (3.48) to a linear one, if s is considered as a ***dependent*** variable, p_0 serving then as an independent variable. This is achieved by applying the

transformation $s = U_0{}^2 / \delta_z^{*2}$. The resulting equation for s is written as

$$\left(p_0 - \frac{1}{6}\right)\left(p_0 - \frac{1}{2}\right)\frac{ds}{dp_0} + 4\left(p_0 - \frac{1}{3}\right)s - \frac{1}{3} = 0. \tag{3.49}$$

After simple integration we arrive at the following main result:

$$\frac{U_0{}^2}{\delta_z^{*2}} = \frac{C_0 + p_0(p_0 - 1/2)^2}{9(p_0 - 1/6)^2(p_0 - 1/2)^2}, \quad C_0 = \text{const}. \tag{3.50}$$

This algebraic equation defines a limit solution $p_0(t)$ in terms of the effective detuning $\delta_z^*(z(t))$. Already at this stage, Eq. (3.50) leads to several immediate conclusions. Indeed, note that if the effective detuning $\delta_z^*(z(t))$ goes to zero at some point of time, the limit solution $p_0(t)$ should inevitably adopt $1/6$ (or $1/2$ if $C_0 \neq 0$) at this point. Hence, the molecular state probability is strictly equal [indeed, within the applicability limitations of the limit equation (3.48)] to $1/6$ at the frequency resonance crossing point. It then follows that for non-crossing models the molecular state probability cannot exceed $1/6$, hence, the sweep through the resonance is a necessary condition for creation of a considerable molecular population (recall that we start from the all-atoms state).

A short examination shows that to define the constant C_0 in Eq. (3.50), the behavior of the function δ_z^{*2} at $t \to -\infty$ should be considered. It is not difficult to verify that for all the four particular models listed in Section 1.6, the Landau-Zener, the first Nikitin, the first Demkov-Kunike and Rosen-Zener models, holds $\lim_{t\to-\infty}\left|\delta_z^*\right| = \infty$. Imposing now the initial condition $p_0(t = -\infty) = 0$, we obtain that for these models $C_0 = 0$. Hence, in these cases the quartic equation (3.50) is reduced to a quadratic one. As a result, we finally arrive at the following explicit expression for the limit solution p_0:

$$p_0 = \frac{1}{6} + \frac{\delta_z^*}{18U_0}\left(\frac{\delta_z^*}{U_0} - S\sqrt{\left(\frac{\delta_z^*}{U_0}\right)^2 + 6}\right), \quad S = \text{sgn}\left(\lim_{t\to-\infty}\delta_t(t)\right). \tag{3.51}$$

In the case of the Rosen-Zener model this expression exactly coincides with the previously derived approximation (3.27). The derived solution (3.51) is a rather accurate approximation.

This is demonstrated in Figs 3.7 and 3.9, where we compare the limit solution (3.51) with the numerical solution of the problem for different external field configurations. Note that the function (3.51) is not necessarily bounded: for example in the case of the Landau-Zener and Demkov-Kunike models it goes to infinity when $t \to +\infty$. To eliminate this divergence and construct an approximation valid for all times, we combine the limit function (3.51) with the trivial solution $p_0 = 1/2$. Thus, generally speaking, if at some point $t = t_c$, the limit solution (3.51) attains the maximal value $1/2$ allowed by the normalization, it must be combined with the trivial solution $p_0 = 1/2$ for $t > t_c$.

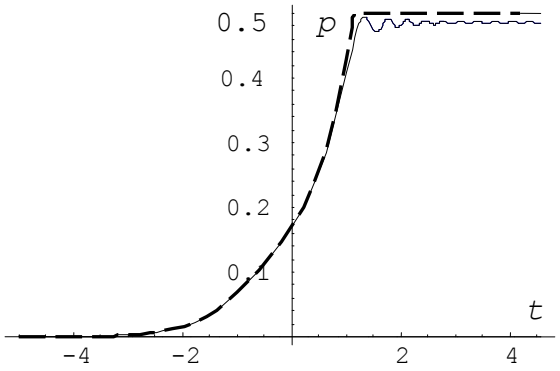


Fig. 3.9. Molecule formation probability vs. time for the Demkov-Kunike model ($U_0 = 20$, $\delta_0 = 10$).

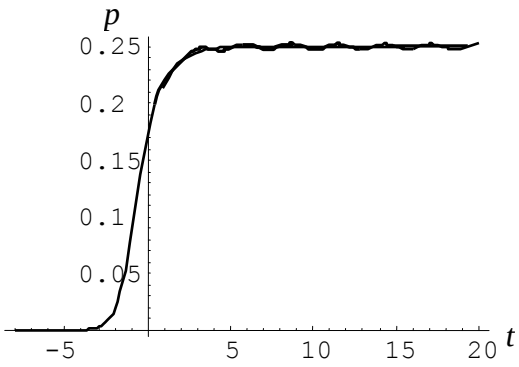


Fig. 3.10. Nikitin exponential model, $U_0^2/\Delta^2 = 4$. Monotonic curve represents the solution (3.51).

Furthermore, the limit solution (3.51) allows to draw several qualitative conclusions of

practical significance. First, suppose that the limit solution p_0 always remains less than $1/2$ or, equivalently, $\delta_t / U \le \sqrt{2}$, if $S = -1$, and $\delta_t / U \ge -\sqrt{2}$, if $S = 1$. In this case if $\lim_{t \to -\infty} \delta_z^*(z(t)) = \lim_{t \to +\infty} \delta_z^*(z(t))$, then after the interaction the system will ***return*** to its initial, all-atoms state. This happens, for instance, when the external field configuration is defined by the Rosen-Zener model (Fig. 3.7). Note that the maximum molecular population achieved at this non-crossing process is less than $1/6$. Second, let p_0 always remain less than $1/2$ and, in addition δ_z^* remain restricted in the neighborhood of $t = +\infty$ for any finite values of the detuning and coupling parameters. Then the final transition probability tends to $1/6$, when U_0 tends to infinity. This behavior is observed in the case of the Nikitin exponential model (Fig. 3.10). This curious result proves that the application of high field intensities (if the photoassociation terminology is used) is not always efficient to achieve large final molecular population.

The common feature of the limit solutions for the four considered models is their non-oscillatory behavior. To find out the conditions under which the system displays almost non-oscillatory behavior, we analyze the numerical solutions of the problem for the Rosen-Zener and first Demkov-Kunike models. Our analysis shows that for $U_0 > 1$, the process of molecule formation is almost non-oscillatory if, in the case of the Rosen-Zener model, the detuning is large enough: $\delta_0 > 1$, and in the case of the Demkov-Kunike model, the sweep through the resonance is sufficiently fast: again, $\delta_0 > 1$ (see Figs. 3.6, 3.7, and 3.11). Finally, we conclude that the limit solution (3.51) is a good approximation when $U_0 >> 1$ and $\delta_0 > 1$.

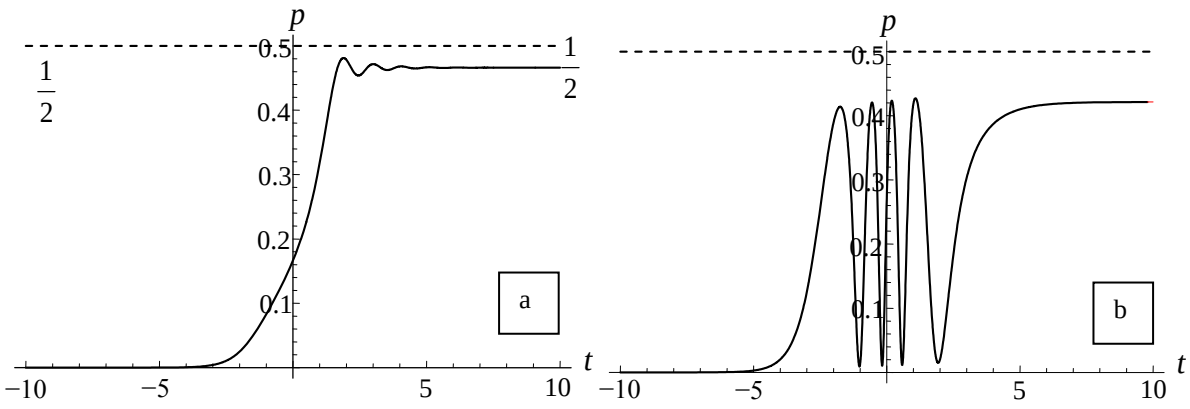


Fig. 3.11. The probability of the molecular state versus time for the DK model. a) The fast resonance sweep regime of the strong nonlinearity limit ($U_0 = 8$, $\delta_0 = 8$). b) The slow resonance sweep regime of the strong nonlinearity limit ($U_0 = 8$, $\delta_0 = 0.1$).

Thus, to construct an approximate solution for the parameter variation range $U_0 >> 1$ and $\delta_0 < 1$ a different approach should be developed. The numerical examination shows that in this case the behavior of the system is much more "unstable": the time evolution of the molecular state probability reveals oscillations with large amplitude and varying frequency. These peculiarities of the solution suggest that for construction of an analytical approximation (in this interaction regime), the two higher order derivative terms in the exact equation for the molecular state probability (1.12) should necessarily be preserved. In Section 3.4, we have already managed to construct a highly accurate approximate solution of the problem, valid in the oscillatory regime of the strong nonlinearity limit. In the present section we generalize the presented mathematical approach.

Again, our starting point should be the exact equation for the molecular state probability written in the factorized form (1.17):

$$\left(\frac{d}{dz} - \frac{\delta^*_{zz}}{\delta^*_z}\right)\left(p_{zz} - \frac{U_0^2}{2}\left(1 - 8p + 12p^2\right)\right) + \delta^{*2}_z p_z = 0\,. \qquad (3.52)$$

Following the arguments presented in Section 3.4, we see that, by neglecting the last term of this

equation, it is impossible to construct a valid approximation, regardless of the smallness of $\delta_z^{*2} p_z$. As it has been proved, putting $\delta_z^{*2} p_z \equiv 0$ results in a monotonically increasing solution that contradicts the numerically observed behavior. Thus, to construct a valid approximation, we not just simply remove the term $\delta_z^{*2} p_z$, but simultaneously add a small perturbation, such that the solution of the constructed equation is an oscillatory function. The chosen perturbation should also be of such a form that the resulting equation is analytically solvable. Finally, we try to construct a valid approximation as a solution of the following differential equation:

$$\left(\frac{d}{dz} - \frac{\delta_{zz}^*}{\delta_z^*}\right)\left(p_{0zz} - \frac{U_0^2}{2}\left(1 - 8p_0 + 12p_0^2\right) + A\right) = 0, \tag{3.53}$$

where A is an adjustable parameter. This equation is readily integrated, and the approximation p_0 is readily given in terms of the Jacobi elliptic sine function [20]:

$$p_0 = p_1 \,\mathrm{sn}^2[\sqrt{p_2} U_0 z; m], \tag{3.54}$$

where parameters p_1, p_2, and m are defined as

$$p_{1,2} = \frac{1}{2} \mp \sqrt{\frac{A}{2U_0^2}}, \quad m = \frac{p_1}{p_2}. \tag{3.55}$$

When analyzing the Rosen-Zener model, an analytical expression for the fitting parameter A has been defined [see Eq. (3.43)].

The solution (3.54) is analogous to the nonlinear Rabi-solution. As it can immediately be seen, it is of a universal form for arbitrary pulse shape and detuning modulation functions; the change of the laser field configuration only affects the argument and the expression for the fitting parameter A leaving the function itself unchanged. Hence, the qualitative behavior of the system in this regime is less sensitive to the concrete form of the laser excitation. Another interesting feature is the subtle dependence of the oscillation frequency of the atom-molecule mixture on the parameters of the laser field modulation.

3.5. Improvement of the approximation (3.51) for the weakly oscillatory regime of the strong nonlinearity limit

In the previous section we have shown that in the case of large values of the peak coupling U_0, two strongly nonlinear distinct scenarios of the system's evolution are available – the highly oscillatory and the almost non-oscillatory interaction regimes. By neglecting two higher order derivative terms in the exact equation for the molecular state probability (1.15), we constructed an approximation (3.51) to describe the temporal dynamics of molecule formation in the almost non-oscillatory regime of the strong nonlinearity limit. The presented approximation is valid for an arbitrary external field configuration. Though the approximation constructed in this way describes the association process quite well before the resonance crossing and not long after the crossing, it suffers from substantial shortcomings: it does not predict the correct value for the final transition probability and it has a derivative discontinuity at the point $t = t_0$. However, as it will be shown below, it is possible to modify the limit equation (3.48) in such a way that it will have a bounded step-like solution.

We first note that if one takes a non-zero value for the integration constant C_0 then, in general, the quartic equation (3.50) is not reduced to a quadratic one, and the function $p_0(t)$ does not diverge at $t \to +\infty$. But for non-zero C_0 the constructed approximate solution does not satisfy the initial condition $p_0(-\infty) = 0$. This observation gives a hint that when constructing an approximation one should try to avoid the degeneracy of the quartic polynomial equation to a quadratic one. It is possible to resolve this issue via an appropriate modification of the limit equation (3.48) by introducing therein a term of the form $A\delta^*_{zz}/\delta^*_z$, where A is an adjustable parameter. In this way, we arrive at the following *augmented limit equation*:

$$\left[\delta_z^{*2} + 4\lambda(1-3p_0)\right]p_{0z} + \frac{\lambda}{2}\frac{\delta^*_{zz}}{\delta^*_z}\left(1-8p_0+12p_0^2\right) - A\frac{\delta^*_{zz}}{\delta^*_z} = 0, \tag{3.56}$$

which can be integrated using the same method as for solving Eq. (3.48). The integration leads to a remarkable result:

$$\frac{\lambda}{\delta_z^{*2}(z(t))} = \frac{p_0(p_0-\beta_1)(p_0-\beta_2)+C_0}{9(p_0-\alpha_1)^2(p_0-\alpha_2)^2}, \tag{3.57}$$

where

$$\alpha_{1,2} = \frac{1}{3} \mp \frac{1}{6}\sqrt{1+\frac{6A}{\lambda}}, \quad \beta_{1,2} = \frac{1}{2} \mp \sqrt{\frac{A}{2\lambda}}. \tag{3.58}$$

This relation defines a *quartic algebraic equation* for the determination of the function $p_0(t)$. The determination of the fitting parameter A will be discussed later.

Now we analyze in detail the solution of the quartic equation (3.57) for the case of the DK model. First of all, we note that for the initial condition $p_0(-\infty)=0$, we obtain $C_0=0$. Then we note that at $t\to+\infty$ the left-hand side of Eq. (3.57) tends to zero. Hence, $p_0(+\infty)$ equals either β_1 or β_2. Since $\beta_2 > 1/2$, we conclude that $p_0(+\infty)=\beta_1$. Furthermore, considering the behavior of p_0 at $t=0$ we see that at $t\to 0$ the left-hand side of Eq. (3.57) diverges, hence, $p_0(0)=\alpha_1$ because $\alpha_2 > 1/2$. Summarizing the results, we have:

$$p_0(0) = \frac{1}{3} - \frac{1}{6}\sqrt{1+\frac{6A}{\lambda}}, \quad p_0(+\infty) = \frac{1}{2} - \sqrt{\frac{A}{2\lambda}}. \tag{3.59}$$

Note that $p_0(0) < 1/6$ and $p_0(+\infty) < 1/2$. The limit solution $p_0(z(t),A)$ is a monotonically increasing function that starts from zero at $t=-\infty$, reaches some value less than $1/6$ at $t=0$, and tends to a finite positive value less than $1/2$ for $t\to+\infty$ when $0<A<\lambda/2$ (see Fig. 3.12).

To develop general principles from which the fitting parameter A could be determined, we insert the approximate solution $p_0(z,A)$ into the exact equation for the molecular state probability (1.15) and consider the behavior of the remainder

$$R = \left(\frac{d}{dz} - \frac{\delta_{zz}^*}{\delta_z^*}\right)(p_{0zz} - A). \tag{3.60}$$

It is intuitively understood that the better approximation p_0 is the smaller the remainder R will become [it would identically be zero if p_0 were the exact solution of Eq. (1.15)]. Thus, we try to minimize the remainder via an appropriate choice of the fitting parameter A. The remainder R is

not bounded at the resonance point $z=0$. To eliminate the divergence of the remainder at this point of singularity, we choose the parameter A as a solution of the equation

$$p_{0zz}(0)-A=0. \tag{3.61}$$

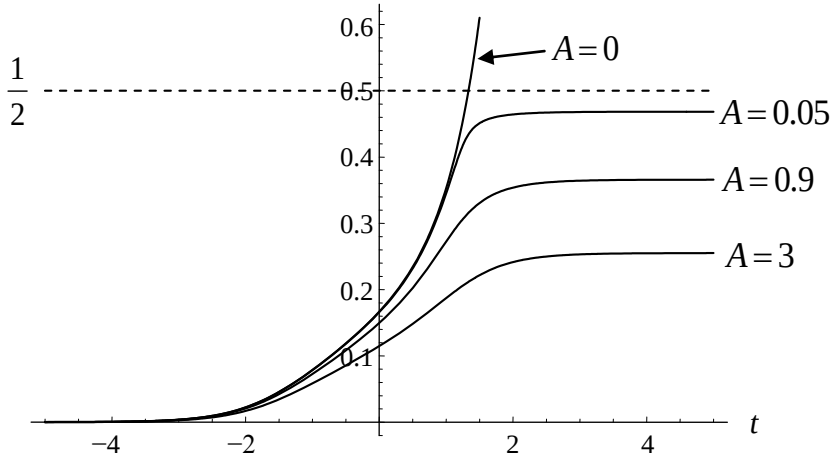


Fig. 3.12. The limit solution $p_0(t)$ [see Eq. (3.57)] versus time at $\lambda=25$ for $A=0$, $A=0.05$, $A=0.9$, and $A=3$.

Taking into account the definition of p_0, i.e., Eqs. (3.57)-(3.58), one can try to obtain an analytical expression for the parameter A. For example, in the case of the strong nonlinearity limit of the Landau-Zener model ($\lambda>>1$), Eq. (3.61) provides the following value for the adjustable parameter A:

$$A\approx\frac{4}{9\lambda}. \tag{3.62}$$

Thus, in the strong nonlinearity limit of the Landau-Zener model, the fitting parameter A is inversely proportional to the Landau-Zener parameter. Further, by analyzing the strong coupling ($\lambda>>1$, where $\lambda=U_0^2$) and moderate values of the sweep rate δ_0 ($1<\delta_0<\sqrt{\lambda}$) of the Demkov-Kunike model we obtain the following approximate expression for the parameter A:

$$A\approx\frac{\lambda}{27\delta_0^{\sqrt{3}}}. \tag{3.63}$$

It should be noted that a more accurate approximation for A valid for a larger region of variation of δ_0 and λ is of the form $A \approx \lambda / g(\delta_0)$ with a complicated function $g(\delta_0)$ vanishing at $\delta_0 \to \infty$. From the qualitative point of view, however, the approximation (3.63) reveals an important peculiarity that we would like to note here, namely, the linear dependence of A on λ in the strong coupling limit.

To conclude this section, we note that the limit solution p_0 still misses several essential features of the association process. Indeed, for instance, the coherent oscillations between atomic and molecular populations which arise after the system has passed through the resonance are not contained in this solution [see Figs. 3.11(a) and 3.12]. Furthermore, the final transition probability at $t \to +\infty$ predicted by p_0, with the parameter A defined by Eq. (3.63), is always lower than what is shown by the numerical solution of the exact equation.

A natural conclusion is that the shortcomings of the suggested limit solution are due to the singular procedure we have employed to derive it. Indeed, we have constructed p_0 by neglecting the two higher order derivative terms in Eq. (1.15). Of course, these terms played a role in determination of the appropriate value of A, hence, to some extent, they have been taken into account. However, for a considerable improvement of the obtained result, we need the next correction term that accounts for the second and third order derivatives of p. One can use the presented solution p_0 as a zero-order approximation to construct the next approximation term to the problem. The presented developments are not restricted to the case of the Demkov-Kunike or Landau-Zener models only: they are equally applicable to other level-crossing models.

3.6. Summary

Thus, we have examined the temporal dynamics of molecule formation in a Bose-Einstein condensate of atoms, assuming arbitrary coupling-shape and energy-detuning configurations. First, we have presented a thorough analysis of the system's dynamics in the case when the external field is defined by the non-crossing Rosen-Zener model. For completeness of the analysis, we have treated both strong and weak nonlinearity limits for this model.

Using an exact nonlinear Volterra integral equation, we have shown that in the weak nonlinearity limit the solution of the nonlinear Rosen-Zener problem is written in terms of the solution to an auxiliary linear Rosen-Zener problem. We have derived a simple expression for the final transition probability. We have found that for the Rosen-Zener model the strict limit of weak nonlinearity corresponds to smaller field intensities than for other known models such as the Landau-Zener and Nikitin-exponential ones. We have shown that this is due to the inherent properties of the particular hyperbolic secant pulse shape under consideration.

Further, we have treated the strong coupling limit of the nonlinear Rosen-Zener problem when the nonlinearity is most pronounced in the molecule formation process. We have shown that here there are two different regimes of the time evolution of the coupled atom-molecule system corresponding to large and small detuning of the associating field. In the first case the behavior of the system is almost non-oscillatory while in the second case large amplitude coherent oscillations in the population dynamics are observed.

Discussing the large detuning regime, we have shown that the conversion process is effectively described by a limit first-order nonlinear equation for the molecular state probability. Using the exact solution of this equation, we have shown that in this regime the molecular fraction qualitatively follows the field amplitude time variation, i.e., the probability of the molecular state first monotonically increases, reaches its maximum at the time when the field intensity is maximal, and then decreases as the field amplitude decreases. Eventually, the system returns to the initial all-atoms state. The maximal possible molecular fraction is found to be $1/6$, i.e., in this regime a Rosen-Zener pulse is capable of capturing no more than the third of the initial atomic population (this is an argument why for high molecule production efficiency a resonance-crossing is needed). In accordance with this prediction, the JILA experiment [30] have shown a maximum molecular conversion of about 16%.

Furthermore, discussing the small detuning limit, we have shown that in this case the system is well described by a second order nonlinear equation that is shown to be the equation of an effective Rabi problem with changed parameters. We have derived accurate approximations for the parameters of the corresponding Rabi-solution written in terms of the Jacobi elliptic sine function.

We have seen that the number of oscillations, as in the linear case, is mainly defined by the pulse area. In the meantime, we have shown that the oscillation shape is mostly defined by the field detuning; the influence of the field intensity here presents a small correction of higher order.

Importantly, we have indicated an inherent singularity of the Rosen-Zener model, a hidden singularity that stands for many of the qualitative and quantitative properties of the model. This singularity, which is shown to be due to the time-variation law of the field amplitude in the beginning of the interaction, can be viewed as an effective resonance-touching.

Further, we have analyzed the strong nonlinearity limit of the coherent molecule formation, assuming an arbitrary external field configuration. We have shown that, as in the Rosen-Zener case, there are two distinct strongly nonlinear scenarios of the system evolution – almost non-oscillatory and strongly oscillatory interaction regimes. By generalizing the mathematical approach used for the treatment of the nonlinear Rosen-Zener problem (see Sections 3.3-3.4), we have constructed simple analytical approximations for both interaction regimes

The approximation for the problem in the almost non-oscillatory regime of the strong interaction limit has been defined as a solution of the first-order nonlinear equation (3.48). The exact solution (3.51) of this equation satisfying the considered initial conditions is given as a solution of the polynomial equation of ***second*** order. Though the approximation constructed in this way describes the association process quite well before the resonance crossing and not long after the crossing, it suffers from substantial shortcomings: it does not predict the correct value for the final transition probability and it has a derivative discontinuity. We have constructed a zero-order approximation for the problem which has been defined as a solution of the augmented limit equation (3.56). We have shown that the exact solution of this equation is given as a solution of the polynomial equation of ***fourth*** order [see Eq. (3.57)]. The constructed approximation contains a fitting parameter which has been determined through a variational procedure. Being a step-like bounded smooth function (see Fig. 3.12), p_0 can be used as a zero-order approximation to construct the next approximation term.

The approximate solution of the problem in the strongly oscillatory interaction regime is expressed in terms of the Jacobi sn-function (3.54), thus having a universal form for arbitrary pulse

shape and detuning modulation functions; the change of the external field configuration only affects the argument and the expression for the fitting parameter A leaving the function itself unchanged. The origin of the oscillations observed in this interaction regime is qualitatively understood by examining the effective interaction time. Consider the example of the Demkov-Kunike model, assuming that the peak coupling is larger than unity ($U_0 > 1$). If the resonance sweep rate and final detuning are large ($\delta_0 > 1$) then in the regions relatively far from the crossing point, the interaction is rather weak since the coupling is small there, and the system does not change its state considerably. However, in the case of small detuning the effective interaction time is large, hence, during this time period the system will considerably change its state despite the smallness of the Rabi frequency: large-amplitude Rabi oscillations start.

Chapter 4

Landau-Zener model with inter-particle elastic scattering included

In the present chapter we study the strong coupling limit of a quadratic-nonlinear Landau-Zener problem for coherent photo- and magneto-association of cold atoms taking into account the atom-atom, atom-molecule, and molecule-molecule elastic scattering. Using an exact third-order nonlinear differential equation for the molecular state probability, we develop a variational approach which enables us to construct a highly accurate and simple analytic approximation describing the time dynamics of the coupled atom-molecule system. We show that the approximation describing time evolution of the molecular state probability can be written as a sum of two distinct terms; the first one, being a solution to a limit first-order nonlinear equation, effectively describes the process of the molecule formation while the second one, being a scaled solution to the linear Landau-Zener problem (but now with a negative effective Landau-Zener parameter as long as the strong coupling regime is considered), corresponds to the remaining oscillations which arise when the process of molecule formation is over

4.1. Introduction

In the present chapter we investigate the influence of atom-atom, atom-molecule, and molecule-molecule elastic scattering on the dynamics of coherent molecule formation subject to an external field configuration of the resonance-crossing Landau-Zener model. The basic version of the nonlinear Landau-Zener problem [defined by Eqs. (1.4) and (1.36)] has extensively been analyzed, e.g., in Refs. [60-69]. In these references, the quartic nonlinear terms are not included in the Hamiltonian that, for the case of the cold molecule formation, describe inter-particle elastic scattering. One of the main conclusions one gains from the obtained results is that in the strong coupling limit the non-transition probability turns to be proportional to the inverse sweep rate, in contrast to the linear two-state case when the dependence is exponential [72]. Further, by juxtaposing the results of Refs. [60-69], we see that, in contrast to the other listed works, Refs.

[61,62] not only provide a prediction for the final transition probability but also suggest highly accurate analytical formulas to describe the whole temporal dynamics of the system. In particular, the absolute error of the analytical formula for the number of the associated molecules, presented in Ref. [62], does not exceed 10^{-4} at the end of the interaction $(t \to +\infty)$ while for particular time points it may increase up to 10^{-3}. The mentioned formula provides the same accuracy at arbitrary values of the problem's input parameters.

The role of inter-particle interactions in the cold atom coherent association dynamics has already been discussed, e.g., in Refs. [108-111,55,99]. It has been shown that these interactions strongly affect the process of molecule formation. In particular, it has been shown that, in the case when the external field configuration is defined by the Landau-Zener model, inter-particle elastic scattering is described by a sole combined parameter [111]. Moreover, it has been revealed that depending on the sign of this parameter the molecule conversion efficiency can both diminish or increase. In the present chapter, by analyzing both molecule conversion efficiency and temporal dynamics of the atom association, we first define favorable conditions for formation of molecules. Further, we develop a version of the variational method [112] which not only enables one to predict the final transition probability to the molecular state but also provides a highly accurate and simple analytical formula describing the temporal dynamics of the coupled atom-molecular system for the case when the inter-particle elastic scattering is included in the basic version of the nonlinear Landau-Zener problem. The constructed analytical approximation is valid in the strong coupling limit and moderate values of the mentioned combined parameter which describes inter-particle elastic scattering. We also show that inter-particle elastic scattering results in a nonlinear shift of the effective resonance point and find an analytical expression for the effective resonance crossing time point (applicable in the strong coupling limit) written in terms of the input parameters of the problem. It should be emphasized that our approach gives an accurate analytical description of the whole temporal dynamics of the molecule formation process.

4.2. General observations

We consider the following nonlinear system of mean-field coupled Gross-Pitaevskii-type

equations describing atomic and molecular condensates as classical fields [41-45]:

$$
\begin{aligned}
i\frac{da_1}{dt} &= U(t)e^{-i\delta(t)}a_1^* a_2 + (\Lambda_{11}|a_1|^2 + \Lambda_{12}|a_2|^2)a_1, \\
i\frac{da_2}{dt} &= \frac{U(t)}{2}e^{i\delta(t)}a_1 a_1 + (\Lambda_{21}|a_1|^2 + \Lambda_{22}|a_2|^2)a_2,
\end{aligned}
\tag{4.1}
$$

where, again, a_1 and a_2 are the atomic and molecular state probability amplitudes, respectively. In the set of equations (4.1), the cubic nonlinearities describe the inter-particle elastic scattering processes. The coefficients Λ_{jk} $(j,k=1,2)$ in the diagonal case $j=k$ are given by $\Lambda_{jj} = 4\pi n\hbar\tilde{a}_j / m_j$, where $\tilde{a}$ is the background off-resonant *s*-wave scattering length and m_j is the mass of a single particle for the *j*th species, respectively, while the nondiagonal terms are given by $\Lambda_{jk} = \Lambda_{kj} = 2\pi n\hbar\tilde{a}_{jk} / \mu_{jk}$, where $\tilde{a}_{jk}$ is the interspecies background off-resonant *s*-wave scattering length and $\mu_{jk} = m_j m_k /(m_j + m_k)$ are the reduced masses. The parameter n denotes the mean density of particles: $n = N/V$, where N is the number of "atomic particles" and V is the volume of trapped particles (each molecule is being considered as two "atomic particles"), and $\hbar$ is Planck's constant divided by 2π. In the case of Feshbach association of utracold bosonic atoms the atom-molecule coupling is given as $U = \sqrt{n}g/\hbar$, where $g = \hbar\sqrt{8\pi\tilde{a}_1\Delta B\Delta\mu / m_1}$ [79-80] (see Section 1.1). In this expression ΔB is the width of the resonance, $\Delta\mu$ is the difference in magnetic momentum between the atomic and the bound molecular states. The detuning δ_t is given as $\delta_t = \Delta\mu[B(t) - B_0]/\hbar$, where $B(t)$ is the external magnetic field, B_0 denotes the position of the Feshbach resonance. System (4.1) describes a lossless process, i.e., it preserves the total number of particles that we normalize to unity: $|a_1|^2 + 2|a_2|^2 = \text{const} = 1$. We consider the basic situation when the system starts from the all-atomic state: $|a_1(-\infty)| = 1$, $a_2(-\infty) = 0$. In the present paper we discuss the case of the LZ model hence hereafter we put $U(t) = U_0 = \text{const}$ and $\delta_t = 2\delta_0 t$.

It can be shown that the dynamics of the molecular state probability $p = |a_2|^2$ is described by the following nonlinear ordinary differential equation of third order:

$$p_{ttt} - \frac{G_t}{G} p_{tt} + \left[G^2 + 4\lambda(1-3p)\right] p_t + \frac{\lambda}{2} \frac{G_t}{G} (1 - 8p + 12p^2) = 0 \ , \tag{4.2}$$

where

$$G = 2t - \Lambda_a + 2\Lambda_s p \, , \tag{4.3}$$

$$\Lambda_a = 2\Lambda_{11} - \Lambda_{21}, \quad \Lambda_s = \Lambda_a + \frac{1}{2}(\Lambda_{22} - 2\Lambda_{12}) \, , \tag{4.4}$$

$(\Lambda_{12} = \Lambda_{21})$ and λ is the standard Landau-Zener parameter: $\lambda = U_0^2 / \delta_0$. In Eqs. (4.2)-(4.4)the independent variable and the parameters involved have been scaled as follows: $t' = \sqrt{\delta_0} t$ and $\Lambda'_{jk} = \Lambda_{jk} / \sqrt{\delta_0}$ $(j,k = 1,2)$ and, for simplicity of notations, the primes have been omitted. Note that the variation range of the function p is $p \in [0,1/2]$. However, since the quantity $N\,p(t)$ defines the number of molecules existing in the system at the time t, we conventionally refer to a_2 as to molecular sate probability amplitude, and to $p = |a_2|^2$ as the molecular sate probability.

If the cubic nonlinearities are not taken into account, i.e., if we put $\Lambda_{jk} = 0$ $(j,k = 1,2)$, then the function G coincides with the Landau-Zener detuning $2t$. Hence, in a sense, the function G plays the role of the effective (nonlinear) detuning and the point $t = t_{res}$ defined from the condition $G(t_{res}) = 0$ is the point of the effective resonance. Thus, we conclude that the introduction of the cubic nonlinearities results in a *nonlinear shift of the resonance*. Moreover, the structure of the effective detuning G suggests that at sufficiently large absolute values of the variable t, when the condition $|2t| >> |\Lambda_a - 2\Lambda_s p|$ holds, the role of the terms proportional to the parameter Λ_s becomes negligible.

Further we notice that the parameter Λ_a merely leads to a constant shift in the detuning which can be eliminated by the following change of the time variable: $t'' = t - \Lambda_a / 2$. This change does not affect the initial conditions since they are imposed at infinity $(t = -\infty)$. Again, for simplicity of notation, we omit the double prime in what follows. [This is formally equivalent to removing the summand Λ_a in Eq. (4.3)]. Hence the inter-particle elastic scattering is now described by a sole combined parameter Λ_s. As it can be seen from Eq. (4.2), there exist some nonzero

parameters Λ_{jk} for which the inter-particle elastic interactions merely result in the shift of the detuning by a constant which can be eliminated by the above mentioned change of the time variable. This occurs when the parameter Λ_s is equal to zero.

We start our discussion by outlining some observations gained from numerical simulations. The dependence of the final transition probability to the molecular state $p(+\infty)$ on the parameters λ and Λ_s is shown in Fig. 4.1. As it is immediately seen, for a fixed Λ_s, the final transition probability is a monotonic function of λ (see also Fig. 4.2a). Furthermore, $p(+\infty)$ is also a monotonic function of Λ_s for fixed λ (see Fig. 4.2b). This is an important conclusion gained from the 3-dimensional plot. Compared with the case when no inter-particle interactions are included ($\Lambda_s = 0$), the transition probability is always higher for negative Λ_s and it is lower when Λ_s is positive (Figs. 4.2a, 4.2b). Physically, this implies that atom-atom and molecule-molecule repulsive interactions diminish the molecule conversion efficiency while atom-molecule repulsion results in its increase. Thus, we conclude that the atom-atom, molecule-molecule attractive and atom-molecule repulsive interactions are favorable for molecule conversion efficiency. Time-dynamics of molecule formation also exhibits remarkable differences depending on whether the value of the parameter Λ_s is negative or positive (see Fig. 4.3). Compared to the case when $\Lambda_s = 0$, at $\Lambda_s < 0$, the passage through the effective resonance occurs later, the transition to the molecular state takes place more slowly, and the amplitude and the frequency of the emerging oscillations are smaller. At $\Lambda_s > 0$ one observes the opposite behavior of these features. Hence, the general conclusion is that for the Landau-Zener model higher laser field intensities and large negative effective interactions Λ_s are the favorable conditions for the formation of molecules.

Figure 4.3 also indicates that besides the time of the effective resonance crossing $t = t_{res}$, there exists another important time characterizing the association process – the point $t = t_{osc}$ at which the nonoscillatory evolution of the molecular state probability changes to an oscillatory behavior. Analyzing the system (4.1) from the point of view of classical Hamiltonian mechanics, one can see that the observed oscillations appear after the exact phase trajectory of the system

crosses the separatrix in the phase space of the time-independent version of the system (see Chapter 2).

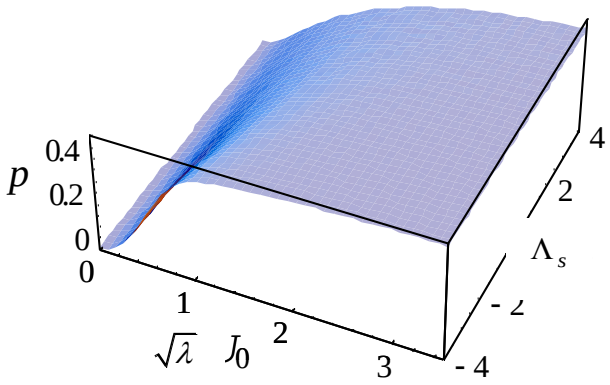


Fig. 4.1. Final transition probability to the molecular state versus $\sqrt{\lambda}$ and Λ_s. It is seen that the probability is a monotonic function of λ for a fixed Λ_s and it is also a monotonic function of Λ_s for fixed λ.

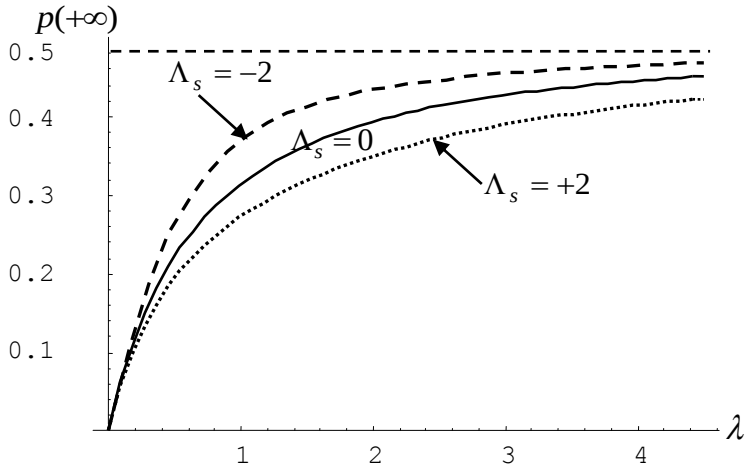


Fig. 4.2a. Final transition probability to the molecular state versus λ for different values of Λ_s.

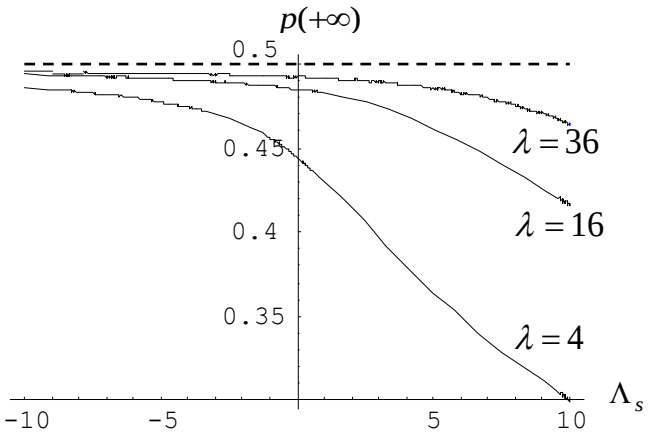


Fig. 4.2b. Final transition probability to the molecular state versus Λ_s for different values of λ.

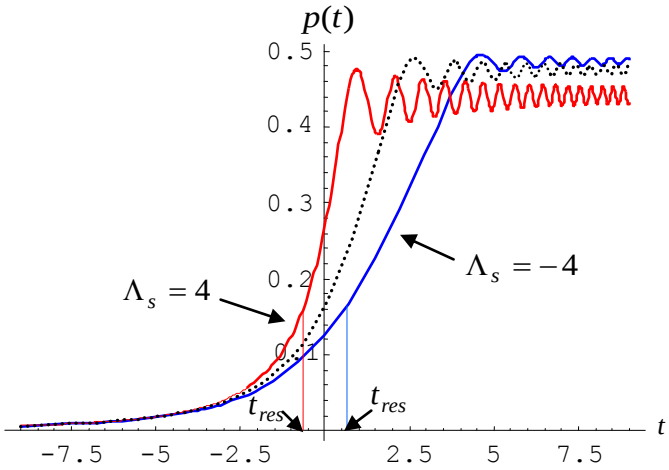


Fig. 4.3. The molecular state probability as a function of time at $\lambda = 9$. Dotted line corresponds to the case $\Lambda_s = 0$ while the solid lines correspond to the cases $\Lambda_s = +4$ and $\Lambda_s = -4$.

4.3. Mathematical treatment

To describe the presented features of the association process quantitatively, we proceed to the analysis of the equation for the molecular state probability (4.2). We consider *the strong nonlinearity regime* corresponding to high field intensities and we thus suppose that λ is a large parameter. Since the function G also adopts large values, we suppose that the leading terms in

equation (4.2) are the last two. Hence, we make an attempt to construct an approximation by neglecting the two higher order derivative terms in the exact equation (4.2) and adding to the obtained truncated equation a term of the form AG_t / G:

$$\left[G^2 + 4\lambda(1-3p_0)\right]p_{0t} + \frac{\lambda}{2}\frac{G_t}{G}(1-8p_0+12p_0^2) - A\frac{G_t}{G} = 0, \tag{4.5}$$

where A is a fitting parameter that will be specified afterwards. Applying the method presented in [73], we find the general solution to the limit equation (4.5):

$$\frac{1}{G^2(p_0)} = \frac{1}{9\lambda}\frac{p_0(p_0-\beta_1)(p_0-\beta_2)+C_0}{(p_0-\alpha_1)^2(p_0-\alpha_2)^2}, \tag{4.6}$$

where

$$\alpha_{1,2} = \frac{1}{3} \mp \frac{1}{6}\sqrt{1+\frac{6A}{\lambda}}, \quad \beta_{1,2} = \frac{1}{2} \mp \sqrt{\frac{A}{2\lambda}} \tag{4.7}$$

and C_0 is the integration constant. This relation defines a *quintic algebraic equation* for the determination of the function $p_0(t)$. First of all, we note that the initial condition $p_0(-\infty) = 0$ implies that $C_0 = 0$. Further, we see that at $t \to +\infty$ the left-hand side of Eq. (4.6). tends to zero and hence $p_0(+\infty)$ must be either β_1 or β_2. But since $\beta_2 > 1/2$ and the probability function p_0 cannot exceed $1/2$, we conclude that

$$p_0(+\infty) = \beta_1. \tag{4.8}$$

Thus, the approximate value of the final probability for the molecular state equals to β_1. Furthermore, one can determine a time $t = t_{res}$ such that $G(t_{res}) = 0$, i.e., a time at which the effective detuning G passes through the effective resonance:

$$2t_{res} + 2\Lambda_s p_0(t_{res}) = 0. \tag{4.9}$$

From Eq. (4.6) it is clear that either $p_0(t_{res}) = \alpha_1$ or $p_0(t_{res}) = \alpha_2$. However, since $\alpha_2 > 1/2$, it must be

$$p_0(t_{res}) = \alpha_1. \tag{4.10}$$

Thus, the parameter α_1 defines the approximate value of the molecular state probability at the effective resonance-crossing point. From Eqs. (4.9)-(4.10) it follows that

$$t_{res} = -\Lambda_s \alpha_1 . \tag{4.11}$$

In order to develop general principles from which the fitting parameter A can be determined, we insert the approximate solution $p_0(t, A)$ into the exact equation for the molecular state probability (4.2) and consider the behavior of the remainder

$$R = p_0''' - \frac{G_t}{G} p_0'' + A \frac{G_t}{G} . \tag{4.12}$$

It is intuitively clear that a better approximation p_0 should yield a smaller remainder [the latter would be identically zero if p_0 is the exact solution to Eq. (4.2)]. Thus, we try to minimize the remainder via appropriate choice of the fitting parameter A. We choose the fitting parameter A by the condition that the remainder should not diverge at the effective resonance crossing t_{res}. This condition leads to the equation

$$p_0''(t_{res}) - A = 0 . \tag{4.13}$$

The analysis of Eq. (4.13) then yields

$$A = \frac{4}{9\lambda} \mathrm{Exp}\left[\left(1 - \frac{1}{2\lambda} \right) \frac{\Lambda_s}{\sqrt{\lambda}} + \frac{|\Lambda_s|}{2\pi} \sin\left(\frac{\pi \Lambda_s}{\lambda} \right) \right] . \tag{4.14}$$

If the condition $\Lambda_s << \sqrt{\lambda}$ holds then the following approximation can be used:

$$A = \frac{4}{9\lambda} \left(1 + \sqrt{\frac{2}{3}} \frac{\Lambda_s}{\sqrt{\lambda}} \right) . \tag{4.15}$$

Comparison of the limit solution p_0 with the numerical solution shows that p_0 still misses several essential features of the association process (see Fig. 4.4). Indeed, for instance, the coherent oscillations between atomic and molecular populations which come up after the system passes through the resonance point are not contained in this approximation. The shortcomings of the limit solution p_0 are caused by the singular procedure used to obtain it. Indeed, we have constructed p_0 by neglecting the two highest order derivative terms in Eq. (4.2). Of course, when determining the optimal value of A we have afterwards taken into account these terms, to some extent.

To improve the result, we need a next correction term that takes into account the second and third order derivatives of p. However, it turns out that this is not a simple task because the equation

obeyed by the exact correction term $u \equiv p - p_0$ is still an essentially non-linear one.

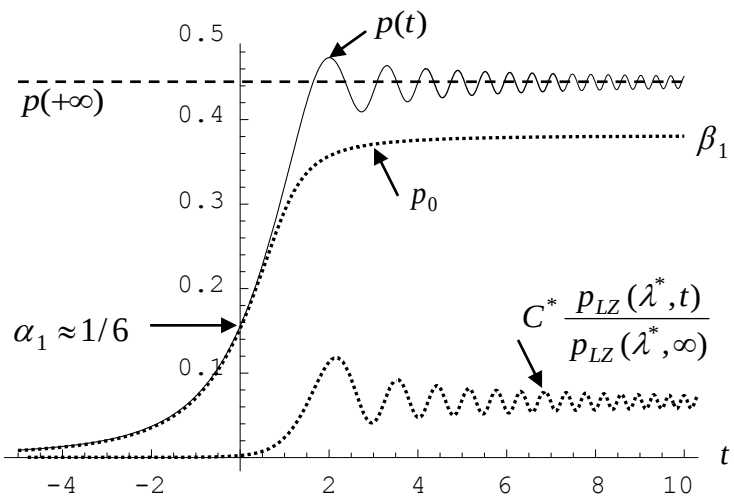


Fig. 4.4. Molecular state probability $p(t)$, the limit solution p_0 determined from Eq. (4.6), and the scaled solution to the linear Landau-Zener problem with modified parameters [Eq. (4.18)].

To develop an appropriate approach, we first consider the Landau-Zener crossing in the relatively simple case when the cubic nonlinearities are neglected, i.e., we take $\Lambda_s = 0$. Now, by introducing in Eq. (4.2) the change of dependent variable

$$p = p_0 + u\,, \tag{4.16}$$

we obtain an exact nonlinear differential equation for the correction u which we write in the following factorized form:

$$\left(\frac{d}{dt} - \frac{1}{t}\right)\left(u'' + 4\left[t^2 + \lambda(1-3p_0)\right]u + p_0'' - A - 6\lambda u^2\right) - 4tu = 0\,. \tag{4.17}$$

Since the function p_0 is already a good first approximation, the correction u is supposed to be small. Further we notice that if in (4.17) we neglect the nonlinear term $-6\lambda u^2$ and consider p_0 as a constant then the solution of the equation can be written as a scaled solution of the linear Landau-Zener problem with a modified Landau-Zener parameter. This observation gives an argument to make the conjecture that the exact solution of Eq. (4.17) can be approximated as

$$u = C^* \frac{P_{LZ}(\lambda^*, t)}{P_{LZ}(\lambda^*, \infty)}, \tag{4.18}$$

where $P_{LZ}(\lambda^*, t)$ is the solution of the linear Landau-Zener model [see Eqs. (2.54)-(2.56)], which can be expressed in terms of confluent hypergeometric functions, and C^* and λ^* are fitting parameters which will be determined afterwards. This conjecture is well confirmed by numerical analysis; the numerical simulations show that one can always find C^* and λ^* such that the function (4.18) accurately fits the numerical solution of the exact equation (4.17).

To obtain analytical expressions for the fitting parameters C^* and λ^*, we substitute the trial function (4.18) into the exact equation (4.17) and aim at minimization of the remainder

$$R = \left(\frac{d}{dt} - \frac{1}{t}\right)\left\{4\left[\lambda(1-3p_0) - \lambda^*\right]\frac{P_{LZ}(\lambda^*, t)}{P_{LZ}(\lambda^*, \infty)} + \frac{2\lambda^*}{P_{LZ}(\lambda^*, \infty)} + \frac{1}{C^*}\left(p_0'' - A\right) - 6\lambda C^* \frac{P_{LZ}^2(\lambda^*, t)}{P_{LZ}^2(\lambda^*, \infty)}\right\} \tag{4.19}$$

via appropriate choice of C^* and λ^*.

The analysis of the behavior of the first term in the curly brackets suggests that the remainder is strongly suppressed if one chooses

$$\lambda^* = \lambda(1 - 3p_0(+\infty)). \tag{4.20}$$

Taking into account the value of $p_0(+\infty)$ [defined by Eq. (4.8)], we rewrite Eq. (4.20) as follows:

$$\lambda^* = -\frac{\lambda}{2} + 3\sqrt{\frac{A\lambda}{2}}. \tag{4.21}$$

Hence, for $\lambda >> 1$, λ^* is a large *negative* parameter. This choice of λ^* leads to an important observation. It is known that [see Eq. (2.57)]

$$\lim_{t \to +\infty} P_{LZ}(\lambda, t) = 1 - e^{-\pi\lambda}, \tag{4.22}$$

hence, in the case of negative λ^* the function $P_{LZ}(\lambda^*, \infty)$ grows exponentially with $|\lambda^*|$. Consequently, for this choice of λ^* the second term in the curly brackets in Eq. (4.19) is also essentially suppressed. Regarding the two last terms in Eq. (4.19), one should minimize them with respect to the parameter C^*. This implies the condition

$$\frac{\partial(R/C^*)}{\partial C^*} = \left(\frac{d}{dt} - \frac{1}{t}\right)\left(-\frac{1}{C^{*2}}\left(p_0'' - A\right) - 6\lambda\frac{P_{LZ}^2(\lambda^*,t)}{P_{LZ}^2(\lambda^*,\infty)}\right) = 0\,. \tag{4.23}$$

Since the last term is proportional to (large) λ and $P_{LZ}(\lambda^*,t)$ is an increasing function of time the "worst" point is $t = +\infty$. Hence, we look for minimization at $t = +\infty$. This immediately leads to the following value for C^*:

$$C^* = \sqrt{\frac{A}{6\lambda}}\,. \tag{4.24}$$

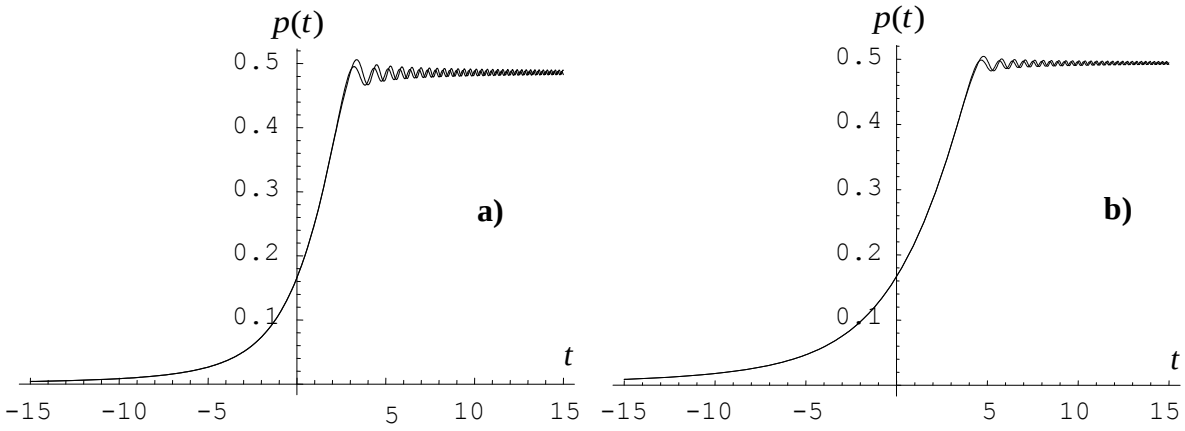


Fig. 4.5. Molecular state probability $p(t)$ and the approximate solution given by Eqs. (16) and (18) as functions of time for a) $\lambda = 15$ and b) $\lambda = 36$. The fitting parameters are taken as $A = 4/(9\lambda)$, $C^* = \sqrt{A/(6\lambda)}$, and $\lambda^* = -\lambda/2$. The analytical formula slightly overestimates the final transition probability.

The comparison of the constructed approximation with the numerical solution shows that formulas (4.21) and (4.24) define a quite good approximation which describes the dynamics of the system qualitatively well (see Fig. 4.5). Taking into account Eqs. (4.8), (4.16), and (4.18), it can easily be seen that the final $(t \to +\infty)$ transition probability to the molecular state is given by the

following relation:

$$p(+\infty) = \frac{1}{2} - \sqrt{\frac{A}{2\lambda}} + C^* . \tag{4.25}$$

This relation shows that the final transition probability does not depend on the parameter λ^*. Obviously, it is changed with variation of A and C^* (note that variation of A inevitably leads to variation of C^*) . By analyzing the structure of the constructed approximate equation [see Eqs. (4.16) and (4.18)], we see that the first term of the constructed two-term solution is a step-like function while the second one describes the oscillations which come up after the system has passed through the resonance (see Fig. 4.4). The frequency of these oscillations is defined by the value of the parameter λ^* only. Variation of the parameter C^* is not able to change the frequency of the oscillations since C^* is just the scaling parameter in Eq. (4.18). Summing up these observations we arrive at a conclusion that the introduced parameters λ^* and C^* characterize qualitatively different physical processes; the parameter C^* describes the final transition probability to the molecular state, whereas the parameter λ^* determines the frequency of the oscillations, emerging some time after the system has passed through the resonance. Though to construct an approximate solution we use a solution of a linear equation $P_{LZ}(\lambda^*, t)$, the parameters involved in the constructed approximation (4.18), λ^* and C^*, are essentially determined by the nonlinear terms involved. Note that the values of the parameters λ^* and C^* depend on the value of the fitting parameter A.

The analytical expressions (4.21) and (4.24) have been obtained when attempting to suppress the remainder (4.19) as much as possible. However, from the mathematical point of view, to obtain an accurate approximation, one should minimize the next approximation term $w = p - p_0 - u$ and not the remainder itself. It can be seen that the remainder (4.19) serves as the inhomogeneous term of the exact equation obeyed by w. Thus, we try to minimize the next approximation term w via appropriate variation of the remainder. By applying the described approach we arrive at a conclusion that the result given by Eqs. (4.21) and (4.24) can be

considerably improved if we redefine the fitting parameters as follows:

$$C^* = \sqrt{\frac{A}{6\lambda}} - \frac{1}{54\lambda} \quad \text{and} \quad \lambda^* = \lambda(1-3[p_0(+\infty)+C^*]). \tag{4.26}$$

The comparison of the refined approximation with the numerical solution shows that it is a very good approximation at $\lambda > 2$.

Now, we return to the general case with $\Lambda_s \neq 0$. Based on the experience gained for $\Lambda_s = 0$, we make the conjecture that the approximate solution in this general case has an analogous structure:

$$p = p_0 + C^* \frac{P_{LZ}(\lambda^*, t - t_{ph})}{P_{LZ}(\lambda^*, \infty)}, \tag{4.27}$$

where the parameters λ^* and C^* are still defined by formula (4.26) and t_{ph} is the newly introduced fitting parameter. Eq. (4.27) along with expressions (4.14) and (4.26) for the involved fitting parameters is the main result of the present paper. The first summand of Eq. (4.27), p_0, is a step-like function while the second one monotonically increases until the small-amplitude oscillations appear (see Fig. 4.4). When presenting general observations, we have already mentioned that inter-particle elastic scattering results in the shift of both the effective resonance point, $t = t_{res}$, and the point where the small-amplitude oscillations start, $t = t_{osc}$, as compared to the case when the inter-particle elastic scattering is neglected. Hence, the fitting parameter t_{ph} introduced in the approximation (4.27) is supposed to describe the shift of the point where the small-amplitude oscillations start. Supposing that the fitting parameter t_{ph} is related to the effective resonance crossing point $t_{ph} = t_{ph}(t_{res})$ we further try to derive an analytical expression for this dependence. To this end, assuming that t_{ph} is proportional to t_{res}, we determine the coefficient of proportionality numerically: $t_{ph} \approx 2.8 t_{res}$. The physical processes emerging due to inter-particle scattering are described via the dependence of the parameters A and t_{res} on Λ_s. Comparison of the approximation (4.27) with the numerical solution shows that it is a very good approximation for

$\lambda > 2$ and $-0.5 \le \Lambda_s / \sqrt{\lambda} \le 0.25$; it accurately describes the association process for almost all the time range.

To analyze the behavior of the final transition probability, we substitute the values of the fitting parameters A, λ^* and C^* determined by Eqs. (4.14) and (4.26) into expression for the final probability of transition to the molecular state (4.25). This results in the following relation:

$$p(+\infty) = \frac{1}{2} - \frac{1}{\lambda}\left(\left[\frac{\sqrt{2}}{3} - \frac{\sqrt{6}}{9}\right]e^{\gamma/2} + \frac{1}{54}\right) \approx \frac{1}{2} - \frac{1}{\lambda}\left(0.1992 e^{\gamma/2} + 0.0185\right), \tag{4.28}$$

where

$$\gamma = \left(1 - \frac{1}{2\lambda}\right)\frac{\Lambda_s}{\sqrt{\lambda}} + \frac{|\Lambda_s|}{2\pi}\sin\left(\frac{\pi\Lambda_s}{\lambda}\right). \tag{4.29}$$

Formula (4.28) is one of the most relevant results of the present chapter. This formula agrees well with the results of numerical simulations (Fig. 4.6); it also confirms the statement that negative effective scattering $\Lambda_s < 0$ is favorable for molecule formation (within the applicability range of the formula). Indeed, if $\Lambda_s < 0$ then $\gamma < 0$, hence, the final transition probability increases. Obviously, when $\Lambda_s > 0$ the final transition probability decreases. The maximum discrepancy between numerical and analytical solutions shown in Fig. 4.6 corresponds to $\lambda = 5$, $\Lambda_s = 0.7$ and equals 0.001540. In the case $\Lambda_s = 0$ expression (4.28) takes the following form:

$$p(+\infty) = \frac{1}{2} - \frac{1}{\lambda}\left(\frac{\sqrt{2}}{3} + \frac{1}{54} - \frac{\sqrt{6}}{9}\right) \approx \frac{1}{2} - \frac{0.2178}{\lambda}. \tag{4.30}$$

This formula confirms the result of Refs. [61-62] stating that in the strong coupling limit, the final probability for non-transition to the molecular state is inversely proportional to the Landau–Zener parameter [in contrast to the linear two-state case when the dependence is exponential (2.57)].

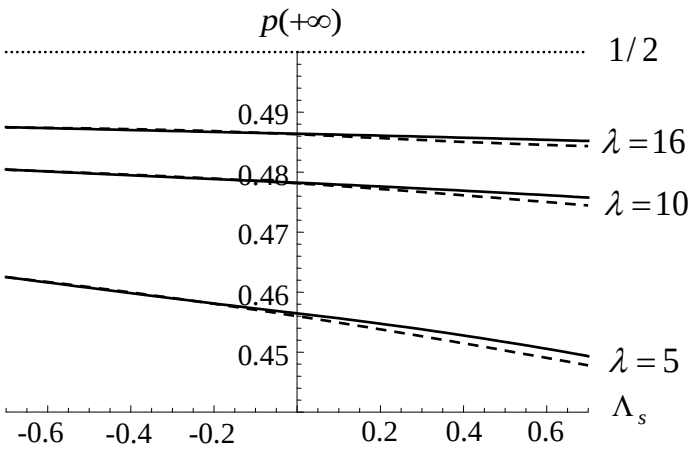


Fig. 4.6. Final transition probability versus Λ_s for $\lambda = 5$, $\lambda = 10$, and $\lambda = 16$.

Solid line - analytical solution (4.28), dashed line – numerical solution.

The method we apply in the present paper to tackle the problem is analogous to that presented in Refs [61-62], where the basic nonlinear version of the nonlinear Landau-Zener problem has been considered. In these papers the inter-particle elastic scattering has not been taken into account. It has been shown that the approximate solution of the problem can be written as a sum of two distinct terms, a solution of a limit first-order nonlinear equation and a scaled solution of the linear Landau-Zener problem with modified parameters. In this case the solution of the limit equation has been shown to be determined as a solution of a polynomial equation of *fourth* order. However, as we have seen above, the inclusion of the cubic-nonlinear terms describing inter-particle elastic scattering results in the modification of the limit equation [see Eq. (4.5)]: now, the solution of this equation is given as a solution of a polynomial equation of *fifth* order (4.6). Note that if we put $\Lambda_s = 0$ the polynomial equation of fifth order will reduce to a polynomial equation of fourth order used in Refs. [61-62].

Finally, we would like to mention that the physical situation we have been discussing is realized under current experiments (for a comprehensive review see Ref. [34]). A typical example is the 85Rb experiment performed by Hodby and co-workers in JILA [91], where coherent formation of Rb_2 molecules via sweep of the magnetic field through the Feshbach resonance located at $155\,G$

is implemented. The magnetic field is changed at a given linear sweep rate $\dot{B}$, and the molecule conversion efficiency is measured as a function of the inverse sweep rate. Thus, the external field configuration applied in this experiment corresponds to the Landau-Zener model. The initial density of the atomic cloud n is of the order of 10^{11}cm^{-3}, the background scattering length of atoms is $\tilde{a}_1 = -443a_0$, where a_0 is the Bohr radius, the resonance width is $\Delta B = 10.71G$, the difference in magnetic moment between the atomic and the bound molecular channels is $\Delta\mu = -2.33\mu_B$, where μ_B is the Bohr magneton. The Landau-Zener parameter is written as $\lambda = 16\pi n\hbar\tilde{a}_1\Delta B/(\dot{B}m_1)$. At the small enough sweep rates and high enough atomic densities applied at this experiment the molecule formation is described by the strong interaction regime $\lambda >> 1$ discussed here; indeed, for the sweep rate $1/\dot{B} = 1000\mu s/G$ and $n = 5\cdot 10^{11}\text{cm}^{-3}$ one has $\lambda \approx 5$. Furthermore, estimating the value of the dimensionless parameter Λ_s, we see that in this particular experiment $\Lambda_s \approx 10^{-2} << \lambda$. Hence, the presented theory is helpful for interpretation of the mentioned experiment.

4.4. Summary

We have presented a nonlinear version of the Landau-Zener problem that arises in the theory of coherent photoassociation or Feshbach resonances in atomic Bose-Einstein condensates, focusing on the role of the atom-atom, atom-molecule, and molecule-molecule scattering which are described by the cubic nonlinear terms in the system (4.1). We have shown that the interparticle interactions strongly affect the dynamics of the molecule formation in the vicinity of the resonance, resulting in the nonlinear shift of the resonance point [see Eqs. (4.3)-(4.4)]. We have proven that in the case of the Landau-Zener model the inter-particle elastic scattering is described by a sole combined parameter Λ_s (this fact has already been noticed in Ref. [111]). By studying both the final $(t \to +\infty)$ transition probability to the molecular state and the temporal dynamics of molecule formation, we have arrived at a general conclusion that for large values of the Landau-Zener parameter λ and large negative effective interactions Λ_s are the most favorable conditions for the

formation of molecules.

Further, we have undertaken a variational treatment to the nonlinear Landau-Zener problem in the strong coupling limit. Using the third-order nonlinear differential equation for the molecular state probability (4.2), we have constructed an approximate solution of the problem in three steps.

1. Neglecting two higher order derivative terms in the exact equation for the molecular state probability (4.2), we define the nonlinear limit equation (4.5) in which we introduce an adjustable parameter A. We explicitly solve the limit equation (4.5) and further determine A from the condition of minimization of the remainder (4.19). Note that the obtained value of A depends on Λ_s.

2. Then, we consider the case $\Lambda_s = 0$. We insert $p = p_0 + u$, into the exact equation (4.2) and make a conjecture that the correction u can be represented as a scaled solution of the linear Landau-Zener problem, containing some effective Landau-Zener parameter λ^* [see Eq. (4.18)]. Again, the fitting parameters λ^* and C^* are determined via minimization of the remainder (4.19). This defines λ^* and C^* in terms of the parameter A [see Eq. (4.26)].

3. To construct an appropriate approximation in the general case when $\Lambda_s \neq 0$, we make a conjecture that in this case the approximate solution has the same structure as for the case $\Lambda_s = 0$ and the parameters C^* and λ^* are still determined from Eq. (4.26) but now the function (4.27) takes into account the interparticle elastic scattering due to the dependence of the parameter A on Λ_s and the introduced shift in the argument of the function.

The described approach can be viewed as a variational method. It enables one to construct a highly accurate and simple analytic approximation describing the time dynamics of the coupled atom-molecular system at $\lambda > 2$ and $-0.5 \leq \Lambda_s / \sqrt{\lambda} \leq 0.25$ (Fig. 4.6). Moreover, the decomposition (4.27) shows that the solution can be separated into two distinct parts: p_0, describing the process of molecule formation, and u, describing the remaining oscillations which come up after the system has passed through the effective resonance. This decomposition clearly indicates that the process of molecule formation is mainly governed by the nonlinear limit equation

(4.5). It should be stressed that the derived approximate solution for the first time describes the whole temporal dynamics of the nonlinear Landau-Zener problem with inter-particle elastic interactions included.

Finally, we note that the presented approach is not restricted to the particular Landau-Zener problem treated here. It can be easily generalized to other time-dependent models. Hence, the developed method is a general strategy for attacking analogous nonlinear two-state problems.

Conclusion

We have studied the nonlinear mean-field dynamics of diatomic molecule formation at coherent photo- and magneto-association of ultracold atoms focusing on the case when the system is initially in all-atomic state.

First, we have considered the case when the external field configuration is defined by the constant-coupling linear resonance-crossing Landau-Zener model. Assuming that the sweeping rate through the resonance is small, we have applied the theory of adiabatic invariants. First, we have discussed the classical phase space of the time-independent version of the problem. Taking into account that the considered initial condition corresponds to the case of zero initial action we have constructed an expression for the molecular state probability within the adiabatic approximation. The constructed solution quite accurately describes the temporal dynamics of the coupled atom-molecular system up to the point of time where the approximation, deviating from the numerical solution, starts to go to infinity. Thus, the adiabatic approximation fails to provide a prediction for the final number of the formed molecules.

The reason for the divergence of the adiabatic approximation is that the exact phase trajectory of the system inevitably crosses the separatrix of the system's time-independent version. Hence, the necessary conditions of the adiabatic theorem are not satisfied in this case. However, we have managed to construct a valid zero-order approximation by introducing an imaginary term in the Hamiltonian, writing equations of motion for this augmented Hamiltonian and neglecting the higher order derivative terms. This procedure results in a step-like bounded function that starts from zero. Thus, the introduced complex term has enabled us to eliminate the divergence of the adiabatic approximation.

Further, we have compared the developments of the present paper with those presented in Ref. [62]. We have shown that the application of the adiabatic approximation is equivalent to removing the two higher order derivative terms from the exact equation for the molecular state probability (2.49) while the constructed zero-order approximation is identical with the solution of the augmented limit equation (2.51). Taking into account that the molecular conversion efficiency is

coupled with the total change of the action, we have calculated this change [see Eq. (2.68)] using a highly accurate approximate formula for the final transition probability presented in Ref. [62]. The absolute error of the presented formula for the action change is on the order of or less than 10^{-4}. Interestingly, the total change of the action is not given as a power-law function of the sweep rate through the resonance.

Further, we have examined temporal dynamics of ultracold molecule formation, assuming arbitrary coupling-shape and energy-detuning configurations. As a first step, we have presented a thorough analysis of the system's dynamics in the case when the external field is defined by the non-crossing Rosen-Zener model. For completeness of the analysis, we have treated both strong and weak interaction limits for this model.

Using an exact nonlinear Volterra integral equation, we have shown that in weak interaction limit the solution to the nonlinear Rosen-Zener problem is written in terms of the solution of an auxiliary linear Rosen-Zener problem. We have derived a simple expression for the final transition probability. We have found that for the Rosen-Zener model the strict limit of weak nonlinearity corresponds to smaller values of the peak coupling than for other known models such as the Landau-Zener and Nikitin-exponential ones. We have shown that this is due to the inherent properties of the particular hyperbolic secant pulse shape under consideration.

Further, we have treated the strong nonlinearity limit of the nonlinear Rosen-Zener problem when the nonlinearity is most pronounced in the molecule formation process. We have shown that, in the strong nonlinearty limit, there are two different regimes of the time evolution of the coupled atom-molecule system corresponding to large and small detuning of the associating field. In the first case the behavior of the system is almost non-oscillatory while in the second case large amplitude coherent oscillations in the population dynamics are observed.

Discussing the large detuning regime, we have shown that the conversion process is effectively described by a limit first-order nonlinear equation for the molecular state probability. Using the exact solution of this equation, we have shown that in this regime the molecular fraction qualitatively follows the field amplitude time-variation, i.e., the probability of the molecular state first increases monotonically, reaches a maximum at the time when the field intensity is maximal,

and then decreases as the field amplitude decreases. Eventually, the system returns to the initial all-atomic state. The maximal possible molecular fraction is found to be $1/6$, i.e., in this regime a Rosen-Zener pulse is capable to capture no more than the third of the initial atomic population (this is an argument why a resonance-crossing is needed for molecule production efficiency). In accordance with this prediction, the JILA experiments [30] have shown a maximum molecular conversion of about 16%.

Furthermore, discussing the small detuning limit, we have shown that in this case the system is well described by a second order nonlinear equation that is shown to be the equation for an effective Rabi problem with changed parameters. We have derived accurate approximations for the parameters of the corresponding Rabi-solution written in terms of the Jacobi elliptic sine function. We have seen that the number of the oscillations, as in the linear case, is mainly defined by the pulse area. In the meantime, we have shown that the oscillation shape is mostly defined by the field detuning; the influence of the field intensity here presents a small correction of higher order.

We have indicated an inherent singularity of the Rosen-Zener model, a hidden singularity that stands for many of the qualitative and quantitative properties of the model. This singularity, which is shown to be due to the time-variation law of the field amplitude at the beginning of the interaction, can be viewed as an effective resonance-touching.

Next, we have analyzed the strong nonolinearity limit of the coherent molecule formation, assuming arbitrary external field configuration. We have shown that, like in the Rosen-Zener case, there are two distinct strongly nonlinear scenarios of the evolution of the system – almost non-oscillatory and strongly oscillatory interaction regimes. By generalizing the mathematical approach used for the treatment of the nonlinear Rosen-Zener problem we have constructed simple analytical approximations for both interaction regimes.

The approximation to the problem in the almost non-oscillatory regime of the strong interaction limit has been defined as a solution of the first-order nonlinear limit equation (3.48), and as it has been mentioned above, coincides with the adiabatic approximation. The exact solution (3.51) of this equation satisfying the considered initial conditions is given as a solution of a polynomial equation of ***second*** order. Though the approximation constructed in this way describes

quite well the association process before the resonance crossing and not long after the crossing, it suffers from substantial shortcomings: it does not predict the correct value for the final transition probability and it has a derivative discontinuity. However, by modifying the mentioned first-order nonlinear limit equation (3.48), we have constructed a zero-order approximation to the problem which has been defined as a solution of the augmented limit equation (3.56). We have shown that the exact solution of this equation is given as a solution of the polynomial equation of ***fourth*** order [see Eq. (3.57)]. The constructed approximation contains a fitting parameter which has been determined through a variational procedure. Being a step-like bounded smooth function, p_0 can be used as a zero-order approximation to construct the next approximation term to the problem.

The approximate solution of the problem in the strongly oscillatory interaction regime is expressed in terms of the Jacobi sn-function (3.54), thus having a universal form for arbitrary pulse shape and detuning modulation functions; the change of the external field configuration only affects the argument and the expression for the fitting parameter A leaving the function itself unchanged. The origin of the oscillations observed in this interaction regime can be qualitatively understood by examining the effective interaction time. Consider the example of the Demkov-Kunike model, assuming that the peak coupling is larger than unity ($U_0 > 1$). If the resonance sweep rate and final detuning are large ($\delta_0 > 1$) then in the regions relatively far from the crossing point, where the coupling is small, the interaction is rather weak, and the system does not change its state considerably. However, in the case of small detuning the effective interaction time is large, hence, during this time interval the system will considerably change its state despite the smallness of the coupling: large-amplitude Rabi oscillations start.

Finally, we investigate the influence of atom-atom, atom-molecule, and molecule-molecule elastic scattering on the dynamics of coherent molecule formation subject to an external field configuration defined by the resonance-crossing Landau-Zener model. We have shown that the interparticle interactions strongly affect the dynamics of the molecule formation in the vicinity of the resonance, resulting in the nonlinear shift of the resonance point. We have proven that in the case of the Landau-Zener model the inter-particle elastic scattering is described by a sole combined

parameter Λ_s (this fact has already been noticed in Ref. [111]). By studying both the final $(t \to +\infty)$ transition probability to the molecular state and the temporal dynamics of molecule formation, we have arrived at a general conclusion that the large values of the Landau-Zener parameter λ and large negative effective interactions Λ_s are the most favorable conditions for the formation of molecules.

Further, we have undertaken a variational treatment to the nonlinear Landau-Zener problem in the strong coupling limit. Using the third-order nonlinear differential equation for the molecular state probability, we have constructed a highly accurate and simple analytic approximation describing the ***temporal*** dynamics of the coupled atomic-molecular system in the case of strong coupling and weak interparticle elastic scattering ($\lambda > 2$ and $-0.5 \le \Lambda_s / \sqrt{\lambda} \le 0.25$). The constructed approximation can be written as a sum of two distinct terms; the first one, being a solution to a limit first-order *nonlinear* equation, effectively describes the process of the molecule formation while the second one, being the scaled solution to the *linear* Landau-Zener problem (but now with *negative* effective Landau-Zener parameter when the strong coupling regime is considered), corresponds to the oscillations which come up after the system has passed through the effective resonance. This decomposition of the approximate solutionclearly indicates that the process of molecule formation is mainly governed by the nonlinear limit equation. The derived approximate solution for the first time describes the whole temporal dynamics of the nonlinear Landau-Zener problem with inter-particle elastic interactions included.

References

1.**W.D. Phillips**, Rev. Mod. Phys. **70**, 721-741 (1998).

2.**C.N. Cohen-Tannoudji**, Rev. Mod. Phys. **70**, 707-719 (1998).

3.**S. Chu**, Rev. Mod. Phys. **70**, 685-706 (1998).

4.**K.B. Davis, M.-O. Mewes, M.R. Andrews, N.J. van Druten, D.S. Durfee, D.M. Kurn, and W. Ketterle**, "Bose-Einstein Condensation in a Gas of Sodium Atoms", Phys. Rev. Lett. **75**, 3969-3973 (1995).

5.**M.H. Anderson, J.R. Ensher, M.R. Matthews, C.E. Wieman, and E.A. Cornell**, "Observation of Bose-Einstein Condensation in a Dilute Atomic Vapor", Science **269**, 198-201 (1995).

6.**W. Ketterle**, "Nobel lecture: When atoms behave as waves: Bose-Einstein condensation and the atom laser", Rev. Mod. Phys. **74**, 1131-1151 (2002).

7.**E. Cornell and C. Wieman**, "Nobel Lecture: Bose-Einstein condensation in a dilute gas, the first 70 years and some recent experiments", Rev. Mod. Phys. **74**, 875-893 (2002).

8.**C.J. Pethick and H. Smith**, *Bose-Einstein condensation in dilute gases* (Cambridge University Press, Cambridge, 2002).

9.**S. Bose**, Z. Phys. **26**, 178-181 (1924).

10.**A. Einstein**, Sitzungsber. Kgl. Preuss. Akad. Wiss. 3-14 **(**1925).

11.**M. Greiner, C.A. Regal, and D.S. Jin**, "Emergence of a molecular Bose-Einstein condensate from a Fermi gas", Nature **426**, 537-540 (2003).

12. **M.W. Zwierlein, C.A. Stan, C.H. Schunck, S.M.F. Raupach, S. Gupta, Z. Hadzibabic, and W. Ketterle**, "Observation of Bose-Einstein Condensation of Molecules", Phys. Rev. Lett. **91**, 250401, 1-4 (2003).

13.**S. Jochim, M. Bartenstein, A. Altmeyer, G. Hendl, S. Riedl, C. Chin, J. Hecker Denschlag, and R. Grimm**, "Bose-Einstein Condensation of Molecules", Science **302**, 2101-2103 (2003).

14.**N.R. Claussen, S.J.J.M.F. Kokkelmans, S.T. Thompson, E.A. Donley, E. Hodby, and C.E. Wieman**, "Very-high-precision bound-state spectroscopy near a ^{85}**Rb** Feshbach resonance", Phys. Rev. A **67**, 060701(R), 1-4 (2003).

15. **S. Kotochigova, T. Zelevinsky, and J. Ye**, "Prospects for application of ultracold $\mathbf{Sr}_2$ molecules in precision measurements", Phys. Rev. A **79**, 012504, 1-7 (2009).

16.**D.J. Heinzen, R. Wynar, P.D. Drummond, and K.V. Kheruntsyan**, "Superchemistry: Dynamics of Coupled Atomic and Molecular Bose-Einstein Condensates", Phys. Rev. Lett. **84**, 5029-5033 (2000).

17.**E.R. Meyer and J.L. Bohn**, "Prospects for an electron electric-dipole moment search in metastable **ThO** and $\mathbf{ThF}^+$", Phys. Rev. A **78**, 010502(R), 1-4 (2008).

18. **B.C. Regan, E.D. Commins, C.J. Schmidt, and D. DeMille**, "New Limit on the Electron Electric Dipole Moment", Phys. Rev. Lett. **88**, 071805, 1-4 (2002).

19.**D. DeMille**, "Quantum Computation with Trapped Polar Molecules", Phys. Rev. Lett. **88**, 067901, 1-4 (2002).

20.**K.-A. Brickman Soderberg, N. Gemelke, and Ch. Chin**, "Ultracold molecules: vehicles to scalable quantum information processing", New J. Phys. **11**, 055022, 1-14 (2009).

21.**T. Zelevinsky, S. Blatt, M.M. Boyd, G.K. Campbell, A.D. Ludlow, and J. Ye**, "Highly Coherent Spectroscopy of Ultracold Atoms and Molecules in Optical Lattices", ChemPhysChem **9**, 375-382 (2008).

22.**W.C. Stwalley**, "Stability of Spin-Aligned Hydrogen at Low Temperatures and High Magnetic Fields: New Field-Dependent Scattering Resonances and Predissociations", Phys. Rev. Lett. **37**, 1628-1631 (1976); **E. Tiesinga, B.J. Verhaar, and H.T.C. Stoof**, "Threshold and resonance phenomena in ultracold ground-state collisions", Phys. Rev. A **47**, 4114 (1993).

23. **E. Tiesinga, A.J. Moerdijk, B.J. Verhaar, and H.T.C. Stoof**, "Conditions for Bose-Einstein condensation in magnetically trapped atomic cesium", Phys. Rev. A **46**, R1167-R1170 (1992).

24.**A.J. Moerdijk, B.J. Verhaar, and A. Axelsson**, "Resonances in ultracold collisions of ^{6}Li, ^{7}Li, and ^{23}Na," Phys. Rev. A **51**, 4852-4861 (1995).

25.**S. Inouye, M.R. Andrews, J. Stenger, H.-J. Miesner, D.M. Stamper-Kurn, and W. Ketterle**,

"Feshbach resonances", Nature (London) **392**, 151-154 (1998).

26. **P. Courteille, R.S. Freeland, D.J. Heinzen, F.A. van Abeelen, and B.J. Verhaar**, "Observation of a Feshbach Resonance in Cold Atom Scattering", Phys. Rev. Lett. **81**, 69-72 (1998).

27.**A. Fioretti, D. Comparat, A. Crubellier, O. Dulieu, F. Masnou-Seeuws, and P. Pillet**, "Formation of Cold $\mathbf{Cs}_2$ Molecules through Photoassociation", Phys. Rev. Lett. **80**, 4402-4405 (1998).

28. **A.N. Nikolov, E.E. Eyler, X.T. Wang, J. Li, H. Wang, W.C. Stwalley, and P.L. Gould**, "Observation of Ultracold Ground-State Potassium Molecules", Phys. Rev. Lett. **82**, 703-706 (1999).

29.**J. Weiner, V.S. Bagnato, S. Zilio, and P.S. Julienne**, "Experiments and theory in cold and ultracold collisions", Rev. Mod. Phys. **71**, 1-85 (1999); **F. Masnou-Seeuws and P. Pillet**, "Formation of ultracold molecules $T \leq 200\mu K$ via photoassociation in a gas of lasercooled atoms," Adv. At., Mol., Opt. Phys. **47**, 53-127 (2001).

30.**E.A. Donley, N.R. Claussen, S.T. Thompson, C.E. Wieman**, "Atom–molecule coherence in a Bose–Einstein condensate", Nature **417**, 529-533 (2002).

31.**K.E. Strecker, G.B. Partridge, and R.G. Hulet**, "Conversion of an Atomic Fermi Gas to a Long-Lived Molecular Bose Gas", Phys. Rev. Lett. **91**, 080406, 1-4 (2003).

32.**S. Jochim, M. Bartenstein, A. Altmeyer, G. Hendl, C. Chin, J. Hecker Denschlag, and R. Grimm**, "Pure Gas of Optically Trapped Molecules Created from Fermionic Atoms", Phys. Rev. Lett. **91**, 240402, 1-4 (2003).

33.**T. Koehler, K. Goral, and P. Julienne**, "Production of cold molecules via magnetically tunable Feshbach resonances", Rev. Mod. Phys. **78**, 1311-1361 (2006).

34.**C. Chin, R. Grimm, P. Julienne, and E. Tiesinga**, "Feshbach Resonances in Ultracold Gases", Rev. Mod. Phys. **82**, 1225-1286 (2010).

35.**R. Wynar, R.S. Freeland, D.J. Han, C. Ryu, and D.J. Heinzen**, "Molecules in a Bose-Einstein condensate", Science **287**, 1016-1019 (2000).

36.**C. McKenzie, J. Hecker Denschlag, H. Häffner, A. Browaeys, Luís E.E. de Araujo, F.K.**

Fatemi, K.M. Jones, J.E. Simsarian, D. Cho, A. Simoni, E. Tiesinga, P.S. Julienne, K. Helmerson, P.D. Lett, S.L. Rolston, and W.D. Phillips, "Photoassociation of sodium in a Bose-Einstein condensate", Phys. Rev. Lett. **88**, 120403, 1-4 (2002).

37.**K.M. Jones, E. Tiesinga, P.D. Lett, and P.S. Julienne**, "Ultracold photoassociation spectroscopy: Long-range molecules and atomic scattering", Rev. Mod. Phys. **78**, 483-535 (2006).

38.**E. Taylor-Juarros, R. Côté, and K. Kirby**, "Formation of ultracold polar molecules via Raman excitation", Eur. Phys. J. D **31**, 213-219 (2004).

39. **E. Juarros, K. Kirby, and R. Côté**, "Laser-assisted ultracold lithium-hydride molecule formation: stimulated versus spontaneous emission", J. Phys. B **39**, S965-S980 (2006).

40.**P. Pellegrini, M. Gacesa, and R. Côté**, "Giant Formation Rates of Ultracold Molecules via Feshbach-Optimized Photoassociation", Phys. Rev. Lett. **101**, 053201, 1-4 (2008).

41.**J. Javanainen and M. Mackie**, "Coherent photoassociation of a Bose-Einstein condensate", Phys. Rev. A **59**, R3186-R3189 (1999).

42.**M. Koštrun, M. Mackie, R. Côté, and J. Javanainen**, "Theory of coherent photoassociation of a Bose-Einstein condensate", Phys. Rev. A **62**, 063616, 1-23 (2000).

43.**M. Mackie and J. Javanainen**, "Quasicontinuum modeling of photoassociation", Phys. Rev. A **60**, 3174-3187 (1999).

44. **A. Carmichael and J. Javanainen**, "Mean-field stationary state of a Bose gas at a Feshbach resonance", Phys. Rev. A **77**, 043616, 1-15 (2008).

45.**P.D. Drummond, K.V. Kheruntsyan, and H. He**, "Coherent Molecular Solitons in Bose-Einstein Condensates", Phys. Rev. Lett. **81**, 3055-3058 (1998).

46.**E.P. Gross**, Nuovo Cimento **20**, 454-477 (1961).

47.**E.P. Gross**, J. Math. Phys. **4**, 195-207 (1963).

48.**L.P Pitaevskii**, Zh. Eksp. Teor. Fiz. **40**, 646-651 (1961).

49.**L.P Pitaevskii**, Sov. Phys. JETP **13**, 451-454 (1961).

50.**I. Tikhonenkov, E. Pazy, and A. Vardi**, "Boson-like quantum dynamics of association in ultracold Fermi gases", Opt. Commun. **264** (1), 321-325 (2006).

51.**S.A. Akhmanov and R. V. Khokhlov**, *Problems of Nonlinear Optics* (Gordon and Breach, New York, 1972).

52. **T. Ditmire, A.M. Rubenchik, D. Eimerl, and M. D. Perry**, J. Opt. Soc. Am. B **13**, 649-655 (1996); **O. Bang, T. W. Graversen, and J.F. Corney**, Opt. Lett. **26**, 1007-1009 (2001).

53.**Y.R. Shen**, *The Principles of Nonlinear Optics* (Wiley, New York, 2002); **R.W. Boyd**, *Nonlinear Optics* (Academic Press, Boston, 1992).

54. **P.N. Butcher and D. Cotter**, *The Elements of Nonlinear Optics* (Cambridge University Press, Cambridge, England, 1991).

55.**J.J. Hope, M.K. Olsen, and L.I. Plimak**, "Multimode model of the formation of molecular Bose-Einstein condensates by Bose-stimulated Raman adiabatic passage", Phys. Rev. A **63**, 043603, 1-6 (2001).

56.**B.J. Cusack, T.J. Alexander, E.A. Ostrovskaya, and Yu.S. Kivshar**, "Existence and stability of coupled atomic-molecular Bose-Einstein condensates", Phys. Rev. A **65**, 013609, 1-4 (2002).

57. **T.J. Alexander, E.A. Ostrovskaya, Yu.S Kivshar, and P.S. Julienne**, "Vortices in atomic-molecular Bose-Einstein condensates", J. Opt. B: Q. Semiclass. Opt. **4**, S33-S38 (2002).

58.**G. Baym and C. Pethick**, "Ground-State Properties of Magnetically Trapped Bose-Condensed Rubidium Gas", Phys. Rev. Lett. **76**, 6-9 (1996).

59.**A. Ishkhanyan, J. Javanainen, and H. Nakamura**, "A basic two-state model for bosonic field theories with a cubic nonlinearity", J. Phys. A **38**, 3505-3516 (2005).

60.**A. Ishkhanyan, J. Javanainen, and H. Nakamura**, "Landau–Zener transition in photoassociation of cold atoms: strong interaction limit", J. Phys. A **39**, 14887-14894 (2006).

61.**R. Sokhoyan, H. Azizbekyan, C. Leroy, and A. Ishkhanyan**, "Strong interaction regime of the nonlinear Landau-Zener problem for photo- and magneto-association of cold atoms", e-print arXiv:0909.0625, 1-13.

62.**A. Ishkhanyan, B. Joulakian, and K.-A. Suominen**, "Variational ansatz for the nonlinear Landau–Zener problem for cold atom association", J. Phys. B **42**, 221002, 1-5 (2009).

63.**R.A. Barankov and L.S. Levitov**, "Dynamical projection of atoms to Feshbach molecules at strong coupling", e-print arXiv:0506323, 1-5 (2005).

64.**E. Altman and A. Vishwanath**, "Dynamic Projection on Feshbach Molecules: A Probe of Pairing and Phase Fluctuations", Phys. Rev. Lett. **95**, 110404, 1-4 (2005).

65.**I. Tikhonenkov, E. Pazy, Y.B. Band, M. Fleischhauer, and A. Vardi**, "Many-body effects on adiabatic passage through Feshbach resonances", Phys. Rev. A **73**, 043605, 1-9 (2006).

66.**B.E. Dobrescu and V.L. Pokrovsky**, "Production efficiency of Feshbach molecules in fermion systems", Phys. Lett. A 350 (1-2), 154-158 (2006).

67.**A. Altland, V. Gurarie, T. Kriecherbauer, and A. Polkovnikov**, "Nonadiabaticity and large fluctuations in a many-particle Landau-Zener problem", Phys. Rev. A **79**, 042703, 1-22 (2009).

68.**A.P. Itin and P. Törmä**, "Non-adiabaticity of a many-particle Landau-Zener problem: forward and backward sweeps", e-print arXiv:0901.4778, 1-4.

69.**A.P. Itin and P. Törmä**, "Dynamics of a many-particle Landau-Zener model: Inverse sweep", Phys. Rev. A **79**, 055602, 1-3 (2009).

70.**A. Ishkhanyan, G.P. Chernikov, and H. Nakamura**, "Rabi dynamics of coupled atomic and molecular Bose-Einstein condensates", Phys. Rev. A **70**, 053611, 1-9 (2004).

71.**A. Ishkhanyan and H. Nakamura**, "Strong-coupling limit in cold-molecule formation via photoassociation or Feshbach resonance through Nikitin exponential resonance crossing", Phys. Rev. A **74**, 063414, 1-9 (2006).

72.**L.D. Landau**, Phys. Z. Sowjetunion **2**, 46 (1932); C. Zener, Proc. R. Soc. London, Ser. A **137**, 696-703 (1932).

73.**R.S. Sokhoyan, B.T. Joulakian and A.M. Ishkhanyan**, "Strong nonlinearity regimes of two-mode photoassociation of atomic Bose-condensates", J. Contemp. Physics (Armenian Ac. Sci.), **41** (3), 23-28 (2006).

74.**A. Ishkhanyan, R. Sokhoyan, B. Joulakian, and K.-A. Suominen**, "Rosen–Zener model in cold molecule formation", Opt. Commun. **282**, 218-226 (2009).

75.**R.S. Sokhoyan**, "Demkov-Kunike model in cold molecule formation: the fast resonance sweep regime of the strong interaction limit", J. Contemp. Physics (Armenian Academy of Sciences) **45** (2), pp 51-57 (2010).

76.**A. Ishkhanyan, R. Sokhoyan, K.-A. Suominen, C. Leroy, and H.-R. Jauslin**, "Quadratic-nonlinear Landau-Zener Transition for Association of an Atomic Bose-Einstein Condensate with Inter-Particle Elastic Interactions Included", Eur. Phys. J. D 56 (3), 421-429 (2010).

77.**N. Sahakyan, H. Azizbekyan, R. Sokhoyan, C. Leroy, Y. Pashayan-Leroy, and A. Ishkhanyan**, "Landau-Zener transition for association of an atomic Bose-Einstein condensate with inter-particle elastic interactions included", Proc. of Conf. Laser Physics-2008, Ashtarak-2, pp. 29-33 (2009).

78.**R. Sokhoyan, C. Leroy, H.-R. Jauslin, and A. Ishkhanyan**, "Influence of the inter-particle elastic scattering on the quadratic-nonlinear Landau-Zener transition in photo- and magneto-association of ultracold atoms", Book of Abstracts of Intern. Advanced Research Workshop "MPOP-2009", p. 50, Yerevan (2009).

79.**P.D. Drummond and K.V. Kheruntsyan**, "Coherent molecular bound states of bosons and fermions near a Feshbach resonance", Phys. Rev. A **70**, 033609, 1-4 (2004).

80.**R.A. Duine and H.T.C. Stoof**, "Many-Body Aspects of Coherent Atom-Molecule Oscillations", Phys. Rev. Lett. **91**, 150405, 1-4 (2003).

81.**N. Sahakyan, H. Azizbekyan, H. Ishkhanyan, R. Sokhoyan, and A. Ishkhanyan**, "Weak coupling regime of the Landau-Zener transition for association of an atomic Bose-Einstein condensate", Laser Physics **20** (1), 291 (2010).

82.**B.W. Shore**, *Theory of Coherent Atomic Excitation* (Wiley, New York, 1990).

83.**A. Ishkhanyan**, "The integrability of the two-state problem in terms of confluent hypergeometric functions", J. Phys. A: Math. Gen. **30**, 1203-1208 (1997).

84.**I.I. Rabi**, Phys. Rev. **51**, 652-654 (1937).

85.**M. Abramowitz and I.A. Stegun**, *Handbook of Mathematical Functions* (Dover, New York, 1965).

86.**Yu.N. Demkov and M. Kunike**, Vest. Leningr. Univ. Fiz. Khim, 16, 39 (1969); **K.-A. Suominen and B.M. Garraway**, "Population transfer in a level-crossing model with two time scales", Phys. Rev. A **45**, 374-386 (1992).

87.**N. Rosen and C. Zener**, Phys. Rev. **40**, 502-507 (1932).

88.**A. Ishkhanyan**, "New analytically integrable models of the two-state problem", Opt. Commun. **176**, 155-161 (2000).

89.**E.E. Nikitin**, Adv. Chem. Phys. **5**, 135 (1970).

90.**E.E. Nikitin and S.Ya. Umanskii**, *Theory of Slow Atomic Collisions* (Springer, Berlin, 1984).

91.**E. Hodby, S.T. Thompson, C.A. Regal, M. Greiner, A.C. Wilson, D.S. Jin, E.A. Cornell, and C.E. Wieman**, "Production Efficiency of Ultracold Feshbach Molecules in Bosonic and Fermionic Systems", Phys. Rev. Lett. **94**, 120402, 1-4 (2005).

92.**V.I. Arnold**, *Mathematical methods of classical mechanics*, (SpringerVerlag, Berlin, 1989).

93.**A.V. Timofeev**, Sov. Phys. JETP **48**, 656-659 (1978).

94.**J. Tennyson, J.R. Cary, D.F. Escande**, Phys. Rev. Lett. **56** (20), 2117-2120 (1986); **J.R. Cary, D.F. Escande, and J. Tennyson**, "Adiabatic-invariant change due to separatrix crossing", Phys. Rev. A **34**, 4256-4275 (1986).

95.**A.I. Neishtadt**, Sov. J. Plasma Phys. **12**, 568-573 (1986); A.I. Neishtadt, PMM USSR **51**, 586-592 (1987).

96.**B.V. Chirikov and V.V. Vecheslavov**, JETP **90** (3), 562-569 (2000).

97.**S. Chow and T. Young**, Nonlin. Anal. **56**, 1047-1070 (2004).

98.**G.M. Zaslavsky**, *Physics of Chaos in Hamiltonian Dynamics* (Imperial College Press, London, 1998); **V.I. Arnold, V.V. Kozlov, and A.I. Neishtadt**, *Mathematical aspects of classical and celestial mechanics* (Third Edition, Springer, Berlin, 2006).

99.**A.P. Itin and S. Watanabe**, "Universality in nonadiabatic behavior of classical actions in nonlinear models of Bose-Einstein condensates", Phys. Rev. E **76**, 026218, 1-16 (2007).

100. **A.P. Itin, A.A. Vasiliev, G. Krishna, and S. Watanabe**, "Change in the adiabatic invariant in a nonlinear two-mode model of Feshbach resonance passage", Physica D **232**, 108-115 (2007).

101.**F. Strocchi**, "Complex Coordinates and Quantum Mechanics", Rev. Mod. Phys. **38**, 36-40 (1966).

102.**R. Sokhoyan, H. Azizbekyan, C. Leroy, and A. Ishkhanyan**, "Demkov–Kunike Model for Cold Atom Association: Weak Interaction Regime", J. Contemp. Phys. (Armenian Ac. Sci.) **44**(6), 272-277 (2009).

103.**J. Kevorkian and J.D. Cole**, *Perturbation Methods in Applied Mathematics* (Springer-Verlag, Heidelberg, 1985).

104.**R.H. Dicke**, "Coherence in Spontaneous Radiation Processes", Phys. Rev. **93**, 99-110 (1954).

105.**F.G. Tricomi**, *Integral Equations* (Dover Publications, New York, 1985); T.A. Burton, *Volterra Integral and Differential Equations* (Academic Press, New York, 1983).

106.**V.A. Yurovsky and A. Ben-Reuven**, "Formation of molecules from a Cs Bose-Einstein condensate", Phys. Rev. A **72**, 053618, 1-9 (2005).

107.**A.H. Nayfeh**, *Perturbation Methods* (Wiley-Interscience, New York, 1985); **J. Kevorkian and J.D. Cole**, *Multiple Scale and Singular Perturbation Methods* (Springer-Verlag, New York, 1996).

108.**M. Mackie, R. Kowalski, and J. Javanainen**, "Bose-Stimulated Raman Adiabatic Passage in Photoassociation", Phys. Rev. Lett. **84**, 3803-3806 (2000).

109. **M. Mackie, A. Collin, and J. Javanainen**, "Comment on "Stimulated Raman adiabatic passage from an atomic to a molecular Bose-Einstein condensate"", Phys. Rev. A **71**, 017601, 1-2 (2005).

110.**P.D. Drummond, K.V. Kheruntsyan, D.J. Heinzen, and R.H. Wynar**, "Stimulated Raman adiabatic passage from an atomic to a molecular Bose-Einstein condensate", Phys. Rev. A **65**, 063619, 1-14 (2002).

111.**J. Liu, L.-B. Fu, B. Liu, and B. Wu**, "Role of particle interactions in the Feshbach conversion of fermionic atoms to bosonic molecules", New J. Phys. **10**, 123018, 1-12 (2008).

112.**I.M. Gelfand and S.V. Fomin**, *Calculus of Variations* (Dover, New York, 2000).

Title: Formation of Molecules in Ultracold Atomic Gases via Quasi-Resonant Fields

Abstract: we study the nonlinear mean-field dynamics of diatomic molecule formation at coherent photo- and magneto-association of ultracold atoms focusing on the case when the system is initially in the all-atomic state. We show that in the limit of strongly nonlinear interaction between an ultra-cold atomic-molecular system and a quasi-resonant electromagnetic field, the molecule formation process, depending on the characteristics of the associating field, may evolve according two different scenarios, namely, weak- and strong-oscillatory regimes. In the first case the number of molecules increases without pronounced oscillations of atom-molecule populations, while in the second case high-amplitude Rabi-type oscillations arise. Assuming an arbitrary external field configuration, we construct analytical solutions to describe the system's temporal dynamics in the both interaction regimes. Further, we investigate the influence of inter-particle elastic scattering on the dynamics of coherent molecule formation subject to an external field configuration of the resonance-crossing Landau-Zener model. We derive an approximate solution which for the first time describes the whole temporal dynamics of the molecule formation in this general case.

Key words: Feshbach resonance, photoassociation, magneto-association, ultracold molecules, BEC of molecules.

Titre : Formation de molécules dans des gaz atomiques ultra froids par des champs quasi résonnants.

Résumé : Nous étudions la dynamique non linéaire en champ moyen de la formation de molécules diatomiques par photo-association ou magnéto-association d'atomes ultra froids pour un système entièrement atomique dans l'état initial. Nous montrons que dans la limite d'une forte interaction non linéaire entre un système atome-molécule ultra froid et un champ électromagnétique quasi résonnant, le processus de formation du condensat moléculaire peut évoluer suivant deux scénarios en fonction des caractéristiques du champ : régime faiblement oscillatoire ou régime fortement oscillatoire. Dans le cas du régime faiblement oscillatoire, le nombre de molécules augmente sans oscillations prononcées des populations atomiques et moléculaires alors que de fortes oscillations de Rabi apparaissent dans le second cas. Nous présentons des solutions analytiques décrivant la dynamique temporelle du système dans ces deux cas. Nous étudions ensuite l'influence de la diffusion élastique entre particules sur la dynamique de formation cohérente de molécules sous l'action d'un champ extérieur représenté par le modèle de Landau-Zener. Nous déterminons une solution approchée qui décrit bien toute la dynamique temporelle de formation moléculaire dans ce cas général.

Mots clefs : résonance de Feshbach, photo-association, magnéto-association, molécules ultra froides, CBE moléculaire.